



AALBORG UNIVERSITY

Master Thesis

MOBILE COMMUNICATIONS 2011

## **Can you fix the iPhone?**

**A study about the human body influence on the performance of antennas and ways to parameterize this influence**

Under the supervision of: Dr. Mauro PELOSI  
& Prof. Gert. F. Pedersen

Research conducted by and report written by:

Marc CORNUEJOLS, Guillaume VIGNAL and Arnaud ZEENDER

## Abstract

In response to a lack of research in the domain of studies concerning the impact of the human body on the performance of an antenna, this thesis explores this impact. It also tries to determine a criterion concerning the robustness of the antenna with regard of this impact. However it is ultimately shown that there is no real criterion, or rather an infinity of them and that the robustness can only be found experimentally.

## Signatures

<b>Marc Cornuéjols</b>	
<b>Guillaume Vignal</b>	
<b>Arnaud Zeender</b>	

## Table of Contents

LIST OF FIGURES.....	5
LIST OF TABLES .....	11
LIST OF SYMBOLS AND ABBREVIATIONS.....	12
INTRODUCTION.....	14
CHAPTER ONE: TOOLS OF MEASUREMENT AND SIMULATION.....	16
I – Introduction .....	16
II – Power Dissipated.....	17
1) Calculation methods of power dissipation.....	17
2) Total power dissipation.....	19
3) Power dissipation along an axis .....	19
III – Three Dimensional Correlations.....	20
1) Cross-correlation definition and explanation .....	20
2) Interpretation of results.....	23
IV – S11 Parameter .....	24
V – Imaginary Part.....	25
VI – Smith Chart.....	26
VI – Finding the appropriate brick .....	31
CHAPTER TWO: SIDE EXPERIMENTS .....	33
I – Conductivity, permittivity and permeability variations.....	33
II – Narrowband PIFA study .....	38
III – Impact of the permittivity of the substrate on a thin substrate-layered PIFA antenna .....	40
IV – Defining the composition of the human hand.....	43
CHAPTER THREE: SIMULATION PARADIGM AND ALTERATION.....	47
I – Introduction .....	47
II – Slicer .....	47
III – Difference in power calculation.....	48
IV – Changes brought to AAU3 .....	49
CHAPTER FOUR: COMPARISON OF REFERENCE ANTENNAS .....	50
I – Introduction .....	50
II – Dipole.....	51

III – Monopole .....	56
IV – PIFA.....	61
V – Slotted PIFA.....	66
VI – Narrowband PIFA .....	71
VII – PIFA with substrate .....	76
VIII – IFA.....	81
IX – Loop.....	86
X – Folded loop.....	91
CHAPTER FIVE: PARAMETERISATION AND ROBUSTNESS CRITERION .....	96
I – Percentage of power dissipated .....	96
II – 3D Correlation of E-fields.....	97
III – General shape evaluation.....	97
IV – Variation of the resonant frequency and the associated S11 parameter .	103
V – Evolution of the Efficiency.....	104
VI – Global view of the rankings .....	105
CONCLUSION.....	106
References.....	107

# LIST OF FIGURES

Fig. 1 User sensitive part of the iPhone 4 antenna _____	P14
Fig. 2 Example sets A and B_____	P21
Fig. 3 First cross-correlation coefficient computation on overlapping cells _____	P22
Fig. 4 Second cross-correlation coefficient computation_____	P22
Fig. 5 Fourth cross-correlation coefficient computation _____	P22
Fig. 6 A two port network representing a transmission line_____	P24
Fig. 7 A S11 plot as a function of frequency_____	P25
Fig. 8 Imaginary part of a dipole resonating at 1GHz_____	P26
Fig. 9 Smith Chart_____	P27
Fig. 10 Impedance circles_____	P28
Fig. 11 Imaginary parts_____	P28
Fig. 12 Impedance axes_____	P29
Fig. 13 Total impedance_____	P30
Fig. 14 Reflection coefficient at the transmission line_____	P30
Fig. 15 Wavelength scale_____	P31
Fig. 16 An AAU3 human hand design_____	P32
Fig. 17 The simplified human hand model_____	P32
Fig. 18 Scheme of the variations experiment, a PIFA antenna facing a brick_____	P34
Fig. 19 Relative power dissipation according to the variation of sigma_____	P35

Fig. 20 Relative power dissipation according to the variations of epsilon_____	P36
Fig. 21 Relative power dissipation according to the variation of mu____	P36
Fig. 22 Power dissipation along the x-axis with a permeability of 42.5_	P37
Fig. 23 Power dissipation along the x-axis with a permeability of 1.5__	P37
Fig. 24 PIFA antennas separated by 1, 2, 5 and 10mm from the ground plane_____	P38
Fig. 25 Reflection coefficient for PIFA antennas elevated by 1, 2, 5 and 10mm_____	P39
Fig. 26 Thin-layered substrate PIFA antenna_____	P40
Fig. 27 Performance variation for substrate PIFA antennas with different permittivity for the substrate_____	P42
Fig. 28 Comparative experiments_____	P43
Fig. 29 1 <sup>st</sup> layer representing a fat layer, 2 <sup>nd</sup> layer representing a Tissue-Equivalent Liquid (TEL)_____	P44
Fig. 30 1 <sup>st</sup> layer representing a muscle, 2 <sup>nd</sup> layer representing a bone_	P45
Fig. 31 1 <sup>st</sup> layer and 2 <sup>nd</sup> layer representing a TEL_____	P45
Fig. 32 Paper results_____	P46
Fig. 33 Regular field graph_____	P48
Fig. 34 Slicer_____	P48
Fig. 35 A free space dipole antenna design_____	P51
Fig. 36 A brick close by the dipole_____	P51
Fig. 37 Free space S11 for a dipole antenna_____	P52
Fig. 38 Brick S11 for a dipole antenna_____	P52
Fig. 39 Imaginary part of a free space dipole_____	P53
Fig. 40 Brick imaginary part of a dipole_____	P53
Fig. 41 Smith Chart of a free space dipole_____	P54

Fig. 42 Brick Smith Chart of a dipole_____	P54
Fig. 43 Power dissipated along axis X for a dipole_____	P55
Fig. 44 The free space design of a monopole_____	P56
Fig. 45 The brick design of a monopole_____	P56
Fig. 46 S11 of a monopole in free space_____	P57
Fig. 47 Brick S11 of a monopole_____	P58
Fig. 48 Imaginary part of a free space monopole_____	P58
Fig. 49 Brick imaginary part of a monopole_____	P58
Fig. 50 Smith Chart for a free space monopole_____	P59
Fig. 51 Brick Smith Chart for a monopole_____	P59
Fig. 52 Power dissipated along x for a monopole_____	P60
Fig. 53 The free space design of a PIFA_____	P61
Fig. 54 The brick design of a PIFA_____	P61
Fig. 55 S11 of a PIFA in free space_____	P62
Fig. 56 Brick S11 of a PIFA_____	P62
Fig. 57 Imaginary part of a free space PIFA_____	P63
Fig. 58 Brick imaginary part of a PIFA_____	P63
Fig. 59 Smith Chart for a free space PIFA_____	P64
Fig. 60 Brick Smith Chart for a PIFA_____	P64
Fig. 61 Power dissipation along x for a PIFA_____	P65
Fig. 62 The free space design of a slotted PIFA_____	P66
Fig. 63 The brick design of a slotted PIFA_____	P66
Fig. 64 S11 of a slotted PIFA in free space_____	P67
Fig. 65 Brick S11 of a slotted PIFA _____	P67
Fig. 66 Imaginary part of a free space slotted PIFA_____	P68
Fig. 67 Brick imaginary part of a slotted PIFA_____	P68

Fig. 68 Smith Chart for a free space slotted PIFA_____	P69
Fig. 69 Brick Smith Chart for a slotted PIFA_____	P69
Fig. 70 Power dissipation along x for a slotted PIFA_____	P70
Fig. 71 The free space design of a narrowband PIFA antenna_____	P71
Fig. 72 The brick design of a narrowband PIFA antenna_____	P71
Fig. 73 S11 of a narrowband PIFA antenna in free space_____	P72
Fig. 74 Brick S11 of a narrowband PIFA antenna_____	P72
Fig. 75 Imaginary part of a free space narrowband PIFA antenna_____	P73
Fig. 76 Brick imaginary part of a narrowband PIFA antenna_____	P73
Fig. 77 Smith Chart for a free space narrowband PIFA antenna_____	P74
Fig. 78 Brick Smith Chart for a narrowband PIFA antenna_____	P74
Fig. 79 Power dissipation along x for a narrowband PIFA_____	P75
Fig. 80 The free space design of a PIFA with substrate_____	P76
Fig. 81 The brick design of a PIFA with substrate_____	P76
Fig. 82 S11 of a PIFA with substrate in free space_____	P77
Fig. 83 Brick S11 of a PIFA with substrate_____	P77
Fig. 84 Imaginary part of a free space PIFA with substrate_____	P78
Fig. 85 Brick imaginary part of a PIFA with substrate_____	P78
Fig. 86 Smith Chart for a free space PIFA with substrate_____	P79
Fig. 87 Brick Smith Chart for a PIFA with substrate_____	P79
Fig. 88 Power dissipation along x for a PIFA with substrate_____	P80
Fig. 89 The free space design of an IFA_____	P81
Fig. 90 The brick design of an IFA_____	P81
Fig. 91 S11 of an IFA in free space_____	P82
Fig. 92 Brick S11 of an IFA_____	P82
Fig. 93 Imaginary part of a free space IFA_____	P83

Fig. 94 Brick imaginary part of an IFA_____	P83
Fig. 95 Smith Chart for a free space IFA_____	P84
Fig. 96 Brick Smith Chart for an IFA_____	P84
Fig. 97 Power dissipation along x for an IFA_____	P85
Fig. 98 The free space design of a loop_____	P86
Fig. 99 The brick design of a loop_____	P86
Fig. 100 S11 of a loop in free space_____	P87
Fig. 101 Brick S11 of a loop_____	P87
Fig. 102 Imaginary part of a free space loop_____	P88
Fig. 103 Brick imaginary part of a loop_____	P88
Fig. 104 Smith Chart for a free space loop_____	P89
Fig. 105 Brick Smith Chart for a loop_____	P89
Fig. 106 Power dissipation along x for a loop antenna_____	P90
Fig. 107 The free space design of a folded loop_____	P91
Fig. 108 The brick design of a folded loop_____	P91
Fig. 109 S11 of a folded loop in free space_____	P92
Fig. 110 Brick S11 of a folded loop_____	P92
Fig. 111 Imaginary part of a free space folded loop_____	P93
Fig. 112 Brick imaginary part of a folded loop_____	P93
Fig. 113 Smith Chart for a free space folded loop_____	P94
Fig. 114 Brick Smith Chart for a folded loop_____	P94
Fig. 115 Power dissipation along x for a folded loop antenna_____	P95
Fig. 116 Comparison of the S11 parameters for the dipole antenna____	P98
Fig. 117 Comparison of the S11 parameters for the folded loop antenna_____	P99
Fig. 118 Comparison of the S11 parameters for the IFA antenna____	P99

Fig. 119 Comparison of the S11 parameters for the loop antenna\_\_\_\_\_P100

Fig. 120 Comparison of the S11 parameters for the monopole

Antenna\_\_\_\_\_P100

Fig. 121 Comparison of the S11 parameters for the PIFA antenna\_\_\_\_\_P101

Fig. 122 Comparison of the S11 parameters for the narrowband PIFA  
antenna\_\_\_\_\_P101

Fig. 123 Comparison of the S11 parameters for the slotted PIFA

antenna\_\_\_\_\_P102

Fig. 124 Comparison of the S11 parameters for the PIFA with substrate

antenna\_\_\_\_\_P102

# LIST OF TABLES

Table 1 Results of the variations experiment_____	P35
Table 2 Impact of distance from the ground plane on PIFA antenna performance_____	P39
Table 3 Performance variation of a thin-layered substrate PIFA antenna with a change of permittivity of the substrate_____	P41
Table 4 Values of specific hand components_____	P42
Table 5 Error calculation between computation techniques_____	P49
Table 6 Power dissipated for the different antennas_____	P96
Table 7 3D-correlation coefficients_____	P97
Table 8 Cross-correlation coefficients of S11 curves_____	P98
Table 9 Visual ranking_____	P103
Table 10 Resonant frequencies for the different antennas_____	P103
Table 11 S11 variations_____	P104
Table 12 Antennas efficiencies_____	P104
Table 13 Antennas final rankings_____	P105

# LIST OF SYMBOLS AND ABBREVIATIONS

$W_i$ : The instantaneous Poynting vector

$E_i$ : The instantaneous Electric field

$H_i$ : The instantaneous Magnetic field

$P_i$ : The instantaneous total power

$s$ : A closed surface crossed by the electric and magnetic fields

$W_{av}$ : The average Poynting vector

$W_{rad}$ : The radiated Poynting vector

$P_{av}$ : The average power

$P_{rad}$ : The radiated power

$p$ : The dissipated power

$\sigma$ : The conductivity

$d_k$ : The defined space step for the FDTD analysis along the axis  $k$

$r_{xy}$ : The correlation coefficient

$x_i$ : The value of the variable  $x$  at a given point

$y_i$ : The value of the variable  $y$  at a given point

$\bar{x}$ : The mean of  $x$

$\bar{y}$ : The mean of  $y$

$s_x$ : The sample standard deviation of variables  $x$

$s_y$ : The sample standard deviation of variables  $y$

$\Gamma$ : The reflection coefficient.

$Z_0$ : The characteristic impedance of the transmission line

$Z_A$ : The impedance at the input of the antenna

$Z$ : The impedance of the antenna

$R$ : The real part of the impedance of the antenna

$X$ : The imaginary part of the impedance of the antenna

FDTD: Finite Difference Time Domain

Epsilon: Permittivity

Sigma: Conductivity

Mu: Permeability

PIFA: Planar Inverted F Antenna

IFA: Inverted F Antenna

# INTRODUCTION

Ever since the dawn of wireless communications, antennas have been crucial in the process of designing efficient wireless systems. Being both the transmitting and receiving appendices of the overall network, their performance has over the years been thoroughly investigated and numerous antenna designs have been thought and/or implemented.

When considering the case of mobile handset antennas, engineers must face additional challenges, size being the most important of them. Therefore, constructors have at their disposal quantity of simulators and a vast number of theoretical or experimental parameters to foresee the overall quality of a design.



Fig. 1 User sensitive part of the iPhone 4 antenna

Yet with all these means at their disposal, one of the most important failures still today is the case of the iPhone 4. Why did this unforeseen error happen, and could it have been avoided?

The particularity of the iPhone 4 antenna is that rather than being internal as in many mobile phones, it is actually situated on the outer boundary of the mobile phone. And yet, this design said to be one of the most efficient Apple had ever realized came out to be a near disaster.

The fact is that, as for almost any mobile phone antenna, its design had been thought in free space, and it was most likely tested in experimental free space. This is the reason of the failure of this antenna; it was not considering the impact of the hand when a user was holding the phone.

While this error of implementation could have been avoided via experimentation with actual user body interference, it mainly shows a lack of consideration from mobile phone companies for the said impact. However, this situation has forced manufacturers to deepen their knowledge about user interference and to focus more consequently on this issue.

In this context, this thesis acts as a study on the impact of the body of the user on antennas and tries to determine a simulation level parameter that could indicate whether or not an antenna is robust to this impact. The main idea around this study being to avoid antenna manufacturers from having to experiment blindly on the topic, benefiting from a trend idea given by the parameter.

Firstly, a rough description is given about the FDTD implementation software used to conduct this research. Then, the tools of measurement investigated and used are described, followed by other leads research has required but which had only intermediate or little impact on the choice of a robustness parameter.

Secondly, reference antennas are described and analyzed through all "lenses" described in the previous section. They are then all compared and ranked by robustness with regard of the human hand interference.

Thirdly, the choice of theoretical robustness criterion and how this choice has come to be is described.

For now, let us focus on the tools used to consider robustness.

# CHAPTER ONE: TOOLS OF MEASUREMENT AND SIMULATION

## I – Introduction

Before proceeding to the actual measurement tools set-up during our research, it seems important to detail the limits to the experiment and to the project we fixed as we started the project.

The first limit was that we chose only to consider the hand mitigation of the signal and not the head as well for simplification purposes. The second limit was that we decided to assimilate the hand to a brick having the same power dissipation as the hand had (our reference antenna for this task being a folded loop antenna). Thus this required some “side experiments” to determine the appropriate brick which are later detailed in this report. The third limit to the project was the definition of robustness itself, and in this was actually not an easy task as for different criterion, the ranking of antenna varied.

As for the simulation paradigm, we chose to use the FDTD simulator developed by Aalborg University and which our supervisor used while experimenting for his PhD [1]. Around this Matlab program, we developed several scripts bound for the analysis of our results which will be detailed later on.

Briefly, the Finite Difference Time Domain numerical computation method is a way to approximate electric and magnetic fields in space and time particularly efficient for the type of volumes we were considering. Details and basics about FDTD can be found in references [2].

Let us now explore the measurement tools we developed or used, by short means of theory and explanation on why they are relevant and how to use the results they produce.

## II – Power Dissipated

### 1) Calculation methods of power dissipation

There are two ways to calculate the dissipated power in a Finite Difference Time Domain simulation. The one used by the AAU3 software is based on calculations of the pointing vector. In this method, we consider the instantaneous pointing vector as:

$$W_i = E_i \times H_i$$

Where  $E_i$  is the instantaneous electric field and  $H_i$  the instantaneous magnetic field.

It has been shown in [3] that from the instantaneous pointing vector, the instantaneous total power can be achieved thanks to the following formula:

$$P_i = \oiint W_i d_s$$

Where  $s$  is a closed surface crossed by the electric and magnetic fields (usually a sphere located in the radiating near field).

However, what we are interested in is not the instantaneous aspect of the power but rather its average over time. It has also been shown in [3] that the instantaneous pointing vector can be derived into a sum of a harmonic part and a non harmonic part. So when time averaging, the harmonic part disappears, leaving only the average pointing vector (average power density) as:

$$W_{av} = \frac{1}{2} \text{Re}[E \times H^*]$$

Similarly to the instantaneous power equation, we can obtain the average power from this formula, which happens to also be the radiated power:

$$P_{rad} = P_{av} = \oiint W_{rad} d_s = \oiint W_{av} d_s = \frac{1}{2} \oiint \text{Re}[E \times H^*] d_s$$

With  $P_{av}$  as the average power,  $P_{rad}$  as the radiated power,  $W_{rad}$  as the average power radiated density, and  $s$  a closed surface. By subtraction of the radiated power from the input power, we can finally obtain the dissipated power.

However, for another set of scripts, we had to use another calculation method, which is to compute cell-by-cell dissipation using the E-field magnitude and the conductivity of the material considered. The formula for this dissipation is given by the following formula, for one cell:

$$p_i = \frac{1}{2} \sigma_i |E_i|^2$$

With the following parameters:

- $p$ : the dissipated power by unit of volume ( $\text{W}/\text{m}^3$ )
- $\sigma$ : the conductivity ( $\text{S}/\text{m}$ )
- $E$ : the E field in one cell ( $\text{V}/\text{m}$ )

For each cell, the power dissipated is given by:

$$P_i = p_i d_x d_y d_z$$

With the following parameters:

- $P$ : the dissipated power in one cell
- $d_k$ : the defined space step for the FDTD analysis along the axis  $k$  ( $x$ ,  $y$  or  $z$ )

The total dissipated power can be calculated by:

$$P = \int_{i=0}^N P_i d_i$$

With the following parameters:

- $N$  the number of dissipative cells

The resultant equation is thus:

$$P = \int_{i=0}^N \iiint \frac{1}{2} \sigma_i |E_i|^2 d_i d_x d_y d_z$$

In a typical scenario,  $dx$   $dy$  and  $dz$  should be similar. In the case of AAU3, a FDTD cell has equally sized cells along each dimension. This method is much more convenient as we can obtain a cell by cell approach to power dissipation. As far as the implementation in a Finite Difference Time Domain simulation is concerned, in our case we transform the E and H fields in spherical coordinates before making any computation.

Furthermore, since we only consider a near field simulation, we make use of the near to far field transformation technique.

## 2) Total power dissipation

By its nature, power dissipation is one of the key aspects to explore in order to determine the robustness of an antenna to the human body. While not really deterministic due to its lack of details, the total power dissipation does give us an indication about how much an antenna suffers from the presence of a hand close to it.

Therefore, antennas will be compared to the mean of the total power dissipated by all antennas and statistics will be shown at the end of chapter 3. The reference antennas will also be analyzed independently on this value of total power dissipation.

## 3) Power dissipation along an axis

A way to obtain a closer look at power dissipation in a brick is to look at it separately along each axis. The idea behind it being to sum all power dissipation obtained via the cell by cell power dissipation formula described above along two axis for one specific value of  $x, y$  or  $z$  and then proceed to increment this value.

From this, we can obtain another mean of classification. The one we will be mostly interested in is the axis intersecting both the ground plane and the brick (the  $x$  axis). Power dissipation along the two first centimeters along this axis will tell us how much the antenna suffers from the brick and more importantly, how fast. This power dissipation will be measured both as a cell by cell graph and as a regrouped by centimeter graph which provides a greater visibility in terms of relative power dissipation.

### III – Three Dimensional Correlations

#### 1) Cross-correlation definition and explanation

Correlation can be defined as a measure of coherence between two variables. This means that variations within these variables are measured to grasp how much they behave accordingly. [4]

For one-dimensional variables and since in our case we consider equally sized variable arrays (as the size of the domain is kept a constant), this would mean using Pearson's product-moment equation [5]:

$$r_{xy} = \frac{\sum_{i=1}^n (x_i - \bar{x})(y_i - \bar{y})}{(n - 1)s_x s_y} = \frac{\sum_{i=1}^n (x_i - \bar{x})(y_i - \bar{y})}{\sqrt{\sum_{i=1}^n (x_i - \bar{x})^2 \sum_{i=1}^n (y_i - \bar{y})^2}}$$

Where  $x_i$  represents the value of the variable  $x$  at a given point, identically for  $y$ . In this equation,  $\bar{x}$  represents the mean of  $x$  and  $\bar{y}$  the mean of  $y$ .  $s_x$  and  $s_y$  are the sample standard deviation of variables  $x$  and  $y$ .

In our case, however, this formula is not sufficient as we consider that a given variable might also vary in space. Thus creating a need for pattern recognition which is provided by another correlation method: the cross correlation.

Cross-correlation is used in several domains like signal processing or medicine. The idea behind it is to apply a delay to one of the "signals" and comparing it to the other signal. This method of statistics is used to recognize tumors on radio scans of patients, for example.

While this method normally applies to different signals, trying to recognize a smaller one with a bigger one, it also applies for our case as the radiation pattern might vary between two measurements (with and without the brick, for example or in the case of different size of domains). The idea being to measure how much the electromagnetic fields vary accordingly when confronted with a slight change in the environment, the introduction of the human hand.

The idea of three dimension cross correlation can be visualized as this: we have a signal A (the results in free space for the fields of an antenna in three dimensions) in a matrix of size  $m \times n \times o$  and a signal B (the result with the addition of a brick nearby the antenna) in a matrix of size  $i \times j \times k$ . Each cell of the A and B matrixes corresponds to a space-cell of the FDTD computation method whose size depends on the space step chosen.

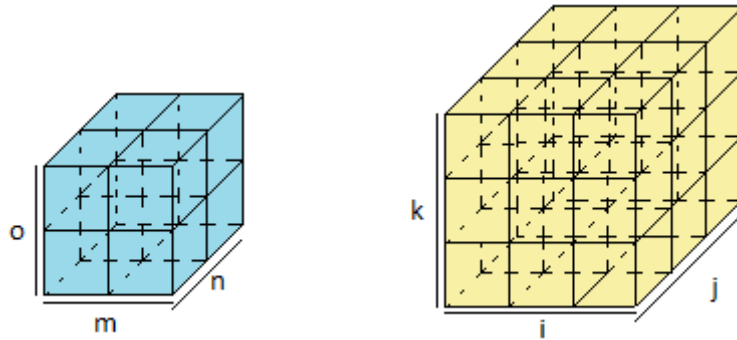


Fig. 2 Example sets A and B

The three dimension cross-correlation equation for discrete functions can be, analogously from one dimensional cross correlation, defined as:

$$(A * B)[x, y, z] = \sum_{p=-\infty}^{+\infty} \sum_{q=-\infty}^{+\infty} \sum_{r=-\infty}^{+\infty} A^*[p, q, r]B[p + x, q + y, r + z]$$

This means in fact that the set A will be superimposed over the set B at every possible location and a correlation coefficient will be derived from each of these particular locations. In our case, the result of this is a matrix of dimensions  $[m + i - 1, n + j - 1, o + z - 1]$  as all values where A and B do not overlap are of no interest. Figures 3 to 5 illustrate this process.

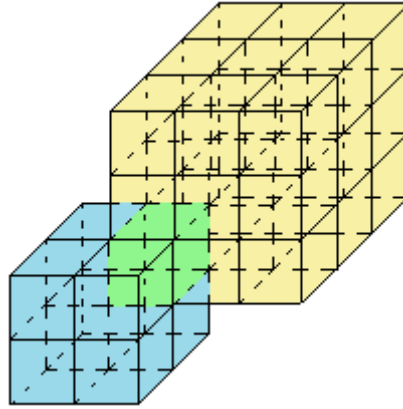


Fig. 3 First cross-correlation coefficient computation on overlapping cells

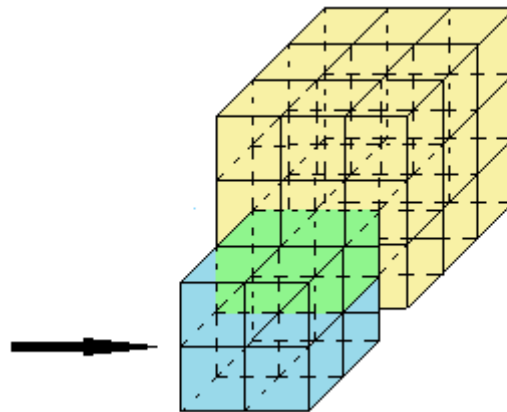


Fig. 4 Second cross-correlation coefficient computation

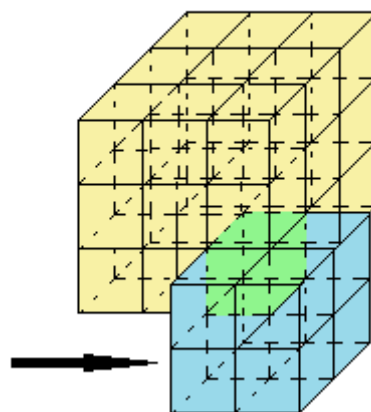


Fig. 5 Fourth cross-correlation coefficient computation

Then, by transposition on different rows and columns, all matching possibilities between set A and B are thus explored.

In our case, there are two possible scenarios for the use of correlation. Either as described above we simulate a reference antenna in free space in a small domain then simulate in a wider domain the same antenna with a brick in its vicinity. The aim of the cross-correlation in this case is to find a matching E-field pattern inside the wider domain.

The second possibility is a simpler correlation in the case where the size of the domains in free space and brick simulation are identical. In this case, to refer to Figures 3 to 5, we only consider the correlation coefficient at the exact spot where both variable matrixes perfectly match one another. This second method has given better results and is thus mainly used in the parts below.

## 2) Interpretation of results

As the correlation calculation results in a correlation coefficient, it is important to know how to interpret it. In the case of different-sized domains and "pattern" recognition, results have shown that very high correlation coefficients are attained when nearly null electromagnetic fields are correlated (on the edges for example, when only part of each set of result overlap).

A correlation coefficient ranks from -1 to +1, depending on the type of relationship correlating the two variables or, in our case, sets:

- A correlation coefficient of +1 indicates a positive relationship, meaning that when one variable increases or decreases, so does the other one.
- A correlation coefficient of -1 indicates a negative or opposite relationship, meaning that one set of data behaves oppositely to the other.
- A correlation coefficient of 0 means that there is no link between the two variables.
- In a general manner, if the absolute value of the correlation coefficient is above 0.7 it is considered as a high correlation between the variables, on the other hand absolute values lower than 0.3 indicate a low correlation.

However, correlation does not indicate causality. In our case, this means that even if an antenna has a very high correlation coefficient between free space and brick simulations, it does not mean that it is linked to the

free space simulation. It might however mean that the resistance to the brick is higher for this antenna.

Let us now proceed to another tool of measurement, the S11 parameter analysis.

## IV – S11 Parameter

To understand the concept of the S11 parameter, let us consider a transmission line represented by a two-port network where on one end lays the source and on the other the antenna itself (figure 6).

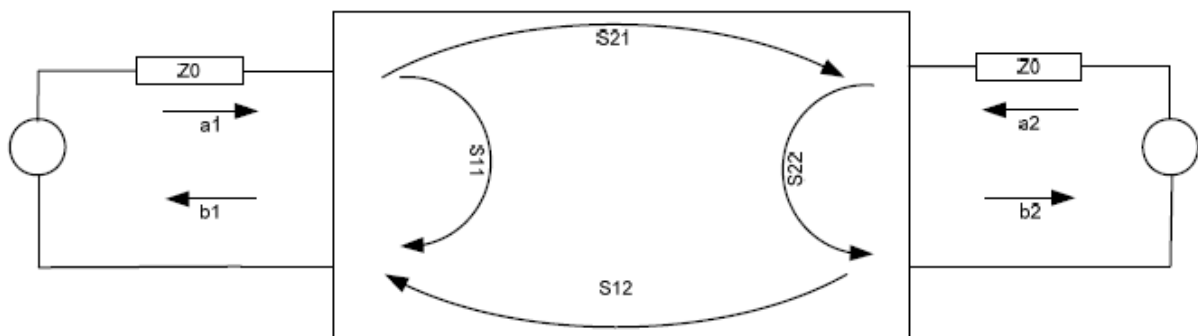


Fig. 6 A two port network representing a transmission line

The concept of the S11 parameter is simply to represent the reflection coefficient at the input of the transmission line. What we aim for, with this parameter, is for it to be the lowest possible at the resonance frequency of the antenna. Ideally, this would mean a value of 0 but in practice we often consider that a -10dB is sufficient [6].

The formula for the reflection coefficient is given by:

$$\Gamma = \frac{Z_0 - Z_A}{Z_0 + Z_A}$$

Where  $Z_0$  represents the impedance of the transmission line and  $Z_A$  represents the impedance at the input of the antenna. To get a perfect matching (a reflection coefficient with a value of 0), we need to have an identical value for  $Z_A$  and  $Z_0$ .

The reflection coefficient varies with frequency and can thus have a plot which looks like the one in figure 7.

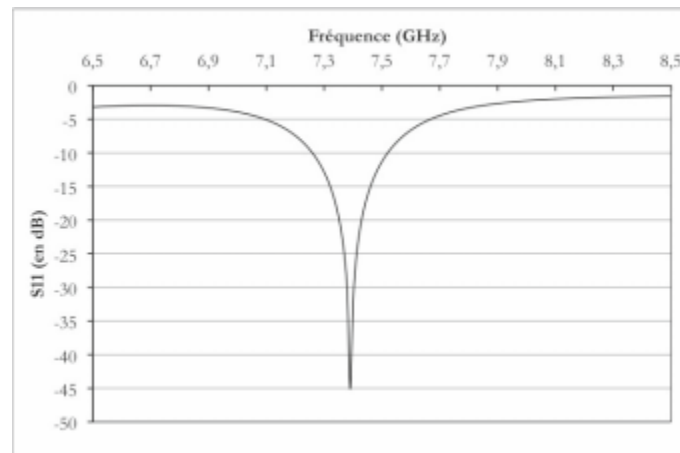


Fig. 7 A S11 plot as a function of frequency

From this graph, we can actually obtain much information. First, it is possible to get the bandwidth by looking at the -6dB values. In figure 7, for example, the bandwidth is about 0.55 GHz. Secondly, it is also possible to get the resonant frequency, which in the graph would be around 7.4 GHz.

The S11 graph is a key tool to see the impact of the hand on an antenna. Indeed, we are interested by the impact on the bandwidth, but also on the effect on the resonant frequency and “depth” of the S11 parameter.

## V – Imaginary Part

The impedance of an antenna is a complex number, given by the formula  $Z = R + jX$  where  $j$  is the square root of  $-1$ . This impedance has two components, a real and an imaginary part:

- The real part corresponds to the power radiated or absorbed within the antenna [7]
- The imaginary part corresponds to the power stored in the reactive near field of the antenna [7]

We consider there is a resonant frequency where the imaginary part of the impedance is equal to zero. The imaginary part graph has for purpose to see how the imaginary part varies with frequency.

Also, an impedance is said to be inductive when its imaginary part is negative and capacitive when otherwise [8].

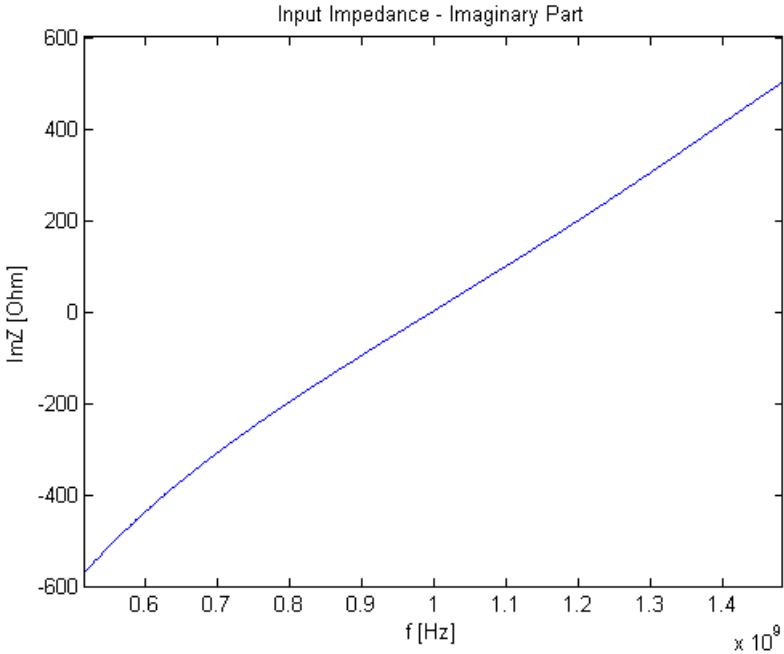


Fig. 8 Imaginary part of a dipole resonating at 1GHz

## VI – Smith Chart

The Smith chart is a graph which allows us to represent the impedance variation of a dipole in function of frequency.

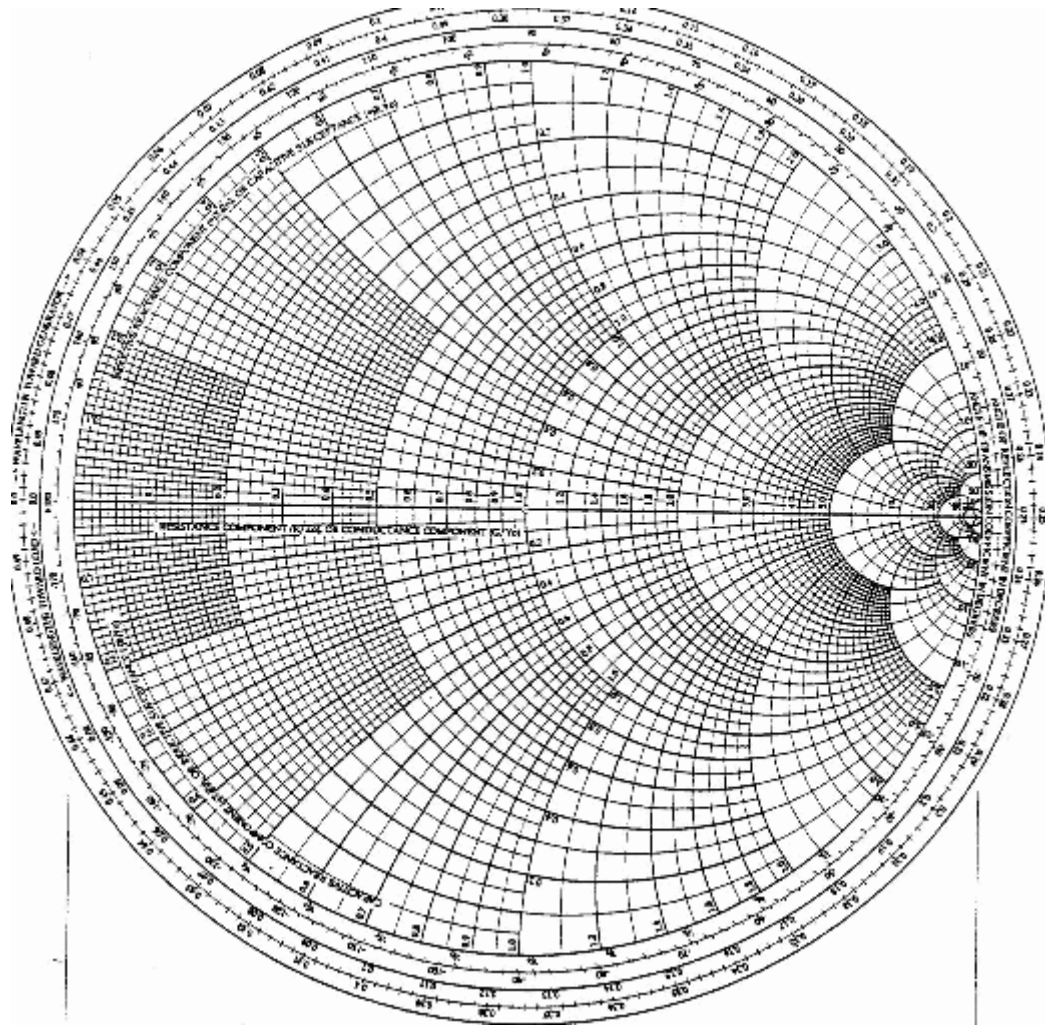


Fig. 9 Smith Chart

Any impedance,  $Z = R + jX$ , can be represented on the Smith Chart. To determine where an impedance is represented, you have to proceed in two steps.

Firstly, thanks to the real part of the impedance, you can determine on which constant resistance circle the impedance will be represented [11].

Indeed, each circle, in the Smith chart, are representing a constant resistance [9], as we can see on the next scheme:

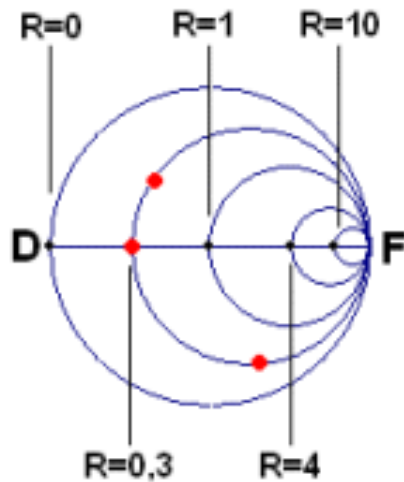


Fig. 10 Impedance circles

Each red point, on the previous scheme, has the same resistance ( $R=0.3$ ), but they do not have the same imaginary part [12].

The line between the point D and the point F represent all the impedances with an imaginary part equal to zero.

The point D represents an impedance equal to zero (short circuit). The point F represents an impedance with an infinite imaginary part (open line).

Secondly, thanks to the imaginary part, you can determine on which constant reactance circle the impedance will be represented.

These constant reactance circles are represented on the next scheme:

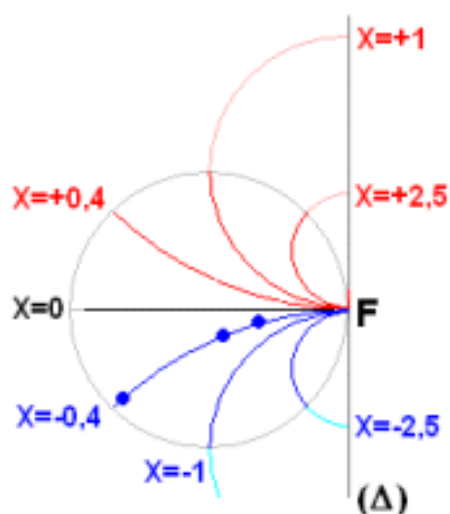


Fig. 11 Imaginary parts

Each blue points, on the previous scheme, has the same reactance ( $X=-0.4$ ), but they don't have the same real part.

All the inductive reactance ( $X>0$ ) are in red on the previous scheme, and the capacitive reactance ( $X<0$ ) are in blue.

We can notice that the circle corresponding to  $Z=0$ , in green on the next scheme, which is the normalized Smith Chart[10].

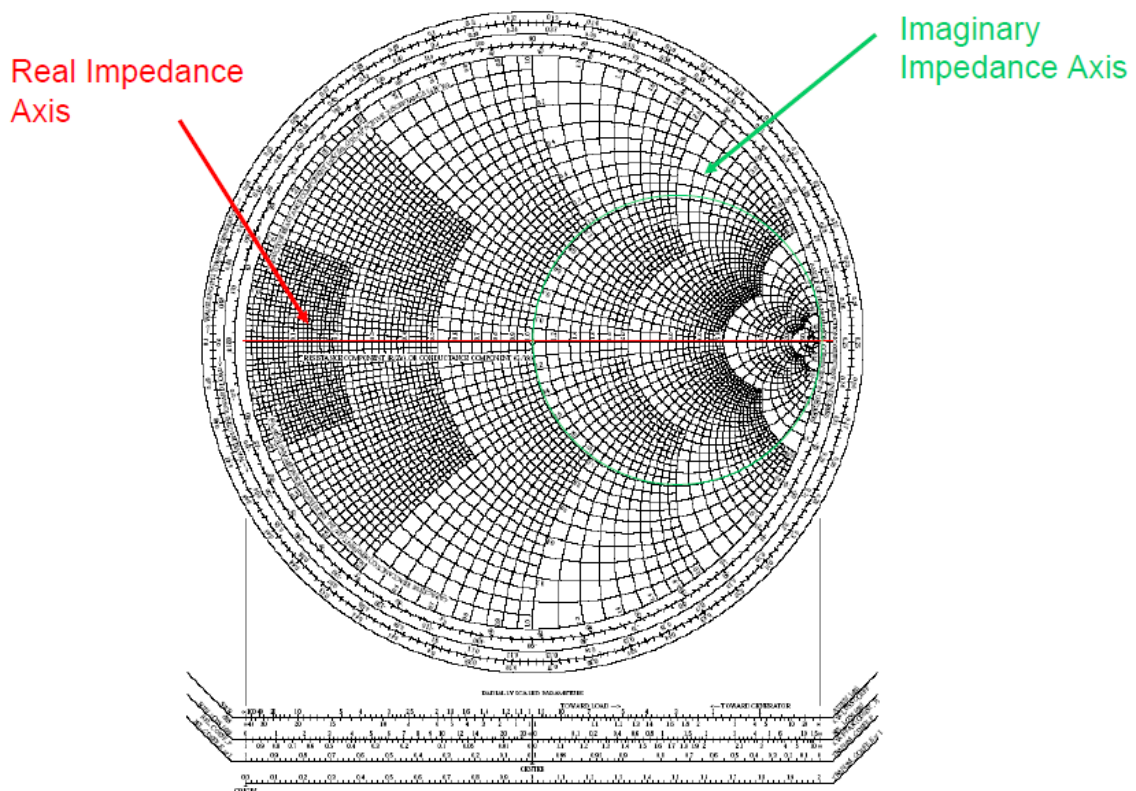


Fig. 12 Impedance axes

With this normalized Smith Chart, each part of the impedance must be divided by the characteristic impedance  $Z_0$  of the transmission line. The representation uses the normalized impedance.

For example, the representation of the normalized impedance  $Z=0.3+0.4j$ , is on the next graph:

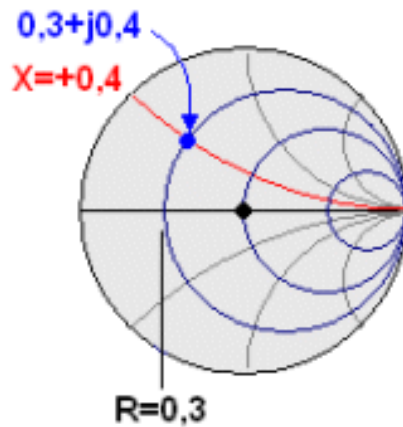


Fig. 13 Total impedance

The reflection coefficient is  $\Gamma = \frac{Z-Z_0}{Z+Z_0}$  with  $Z_0$  the characteristic impedance can be read on the Smith Chart. It's given by the line between the point representing the impedance, and the center of the Smith chart (  $R=1$  and  $X=0$ ). Indeed, the smith chart is the representation of the reflection coefficient in polar coordinates.

## Impedance

$$Z_L = 25 - j100 \Omega$$

$$z_L = Z_L / Z_0$$

$$z_L = 0.5 - j2 \Omega$$

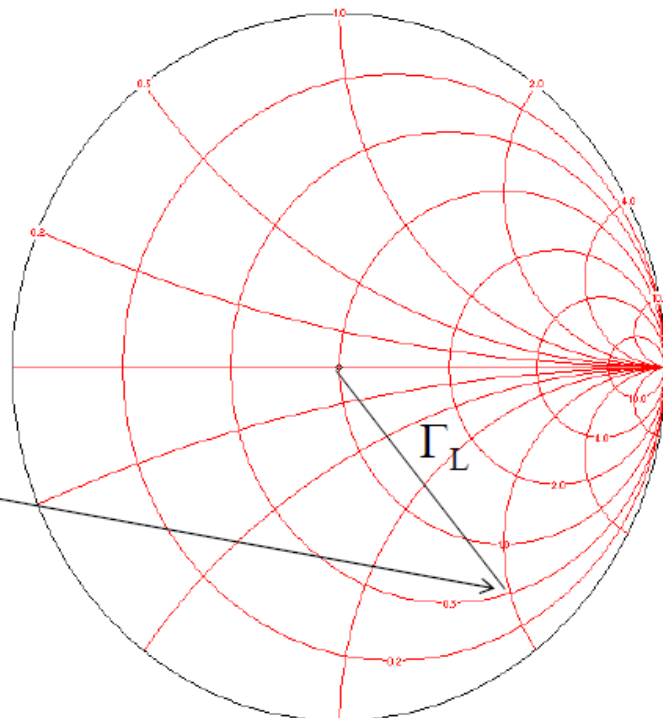


Fig. 14 Reflection coefficient at the transmission line

The scale around the smith chart represents the wavelength but also the angle of the reflection coefficient:

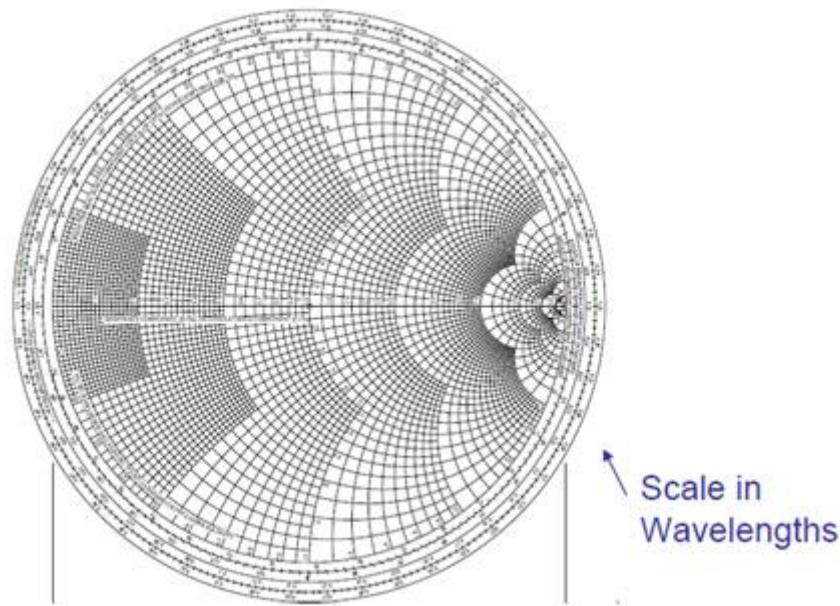


Fig 15. Wavelength scale

So, we are able, thanks to the Smith chart, to have the reflection coefficient in function of frequency. In conclusion, the smith chart can be used to solve matching problems.

## VI – Finding the appropriate brick

One of the most important aspects of this research was to define a reference brick that could be used by telecommunications engineers to simulate the impact of the human hand on the quality of their antenna design. In order to achieve this reference brick, a certain number of assertions had to be made:

- As the design was to be as simple as possible, we considered the hand as a single layer object, so we did not consider the bone, flesh or fat's particular impact on power dissipation. However, this was the topic of a side experiment described in the chapter below.
- We had acquired an AAU3-compatible design (figure 16) for the human hand from the PhD of Mauro Pelosi, our supervisor, which we tried so make simpler. [1]

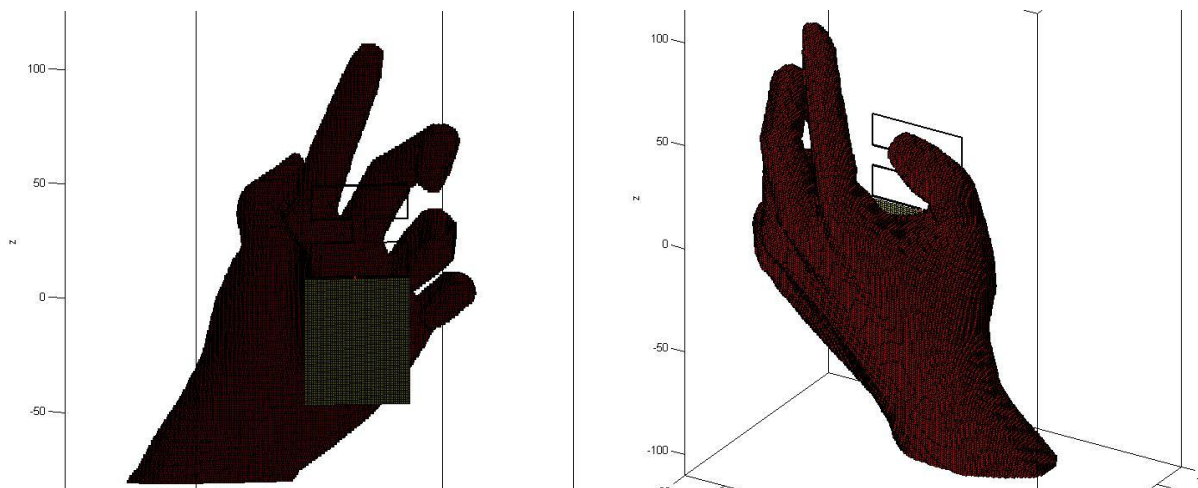


Fig. 16 An AAU3 human hand design

The key factor for the acceptance of the reference brick that would become our human hand proxy was that the total power dissipated was identical between the brick and the hand. This simplification has limits, of course, as the power dissipated calculated along the axes is of course a very rough estimation.

The hand being rather thin (from 1 to 3 centimeters at maximum), the brick should also not be cubic but rather thin. In the end, we did find a brick corresponding to these different criterions (show in fig 17) with parameters of permittivity=36.2, conductivity=0.79 and permeability=1.

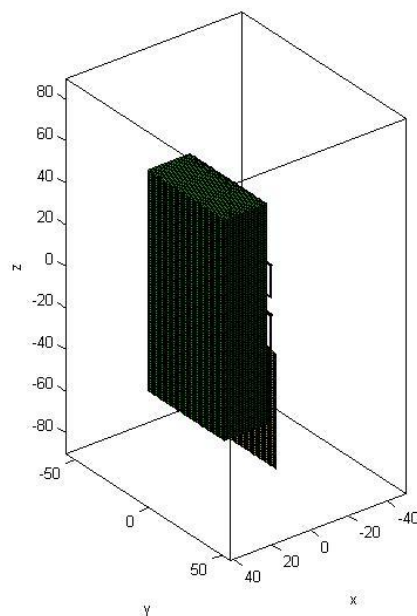


Fig. 17 The simplified human hand model

# CHAPTER TWO: SIDE EXPERIMENTS

Aside from the main experiment about the determination of a robustness criterion, we have pushed our research into several sub-areas related to the topic based on references we read to understand the topic or simply to determine as accurately as possible the way the tools described above would be used.

## I – Conductivity, permittivity and permeability variations

The human hand is composed of several layers (fat, skin, bone, flesh et cetera) which have distinct values for conductivity (the ability to conduct current), permittivity (the measure of resistance to electric field formation) and permeability (the degree of magnetization of a material in response to a magnetic field).

The purpose of this experiment was to determine the impact of these three parameters on the power dissipation of the fields within these modified mediums.

In order to do so, we consider a PIFA antenna and a brick of 40x250x250 millimeters at the distance of 30 millimeters from the antenna and we consider the rest of the medium to be free space. Figure 18 below shows the layout of the experiment.

As for results, we consider power dissipation along three separate axes as described in the power dissipation chapter. However, we were only interested by the x-axis power dissipation in the first three centimeters.

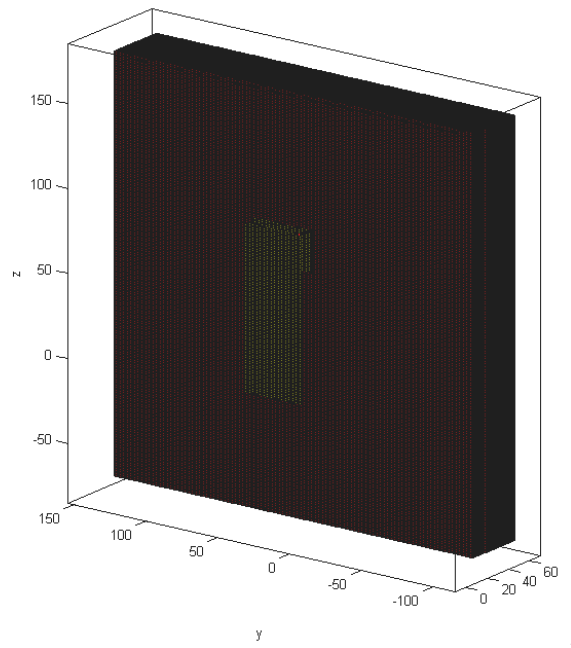


Fig. 18 Scheme of the variations experiment, a PIFA antenna facing a brick

In table 1, we compiled the results of this experiment. These results should be interpreted as following:

- Increasing the conductivity ( $\sigma$ ) decreases the total power dissipated by the brick, however, it also increases the percentage of the total power dissipated in the first three centimeters (Figure 19).
- Increasing the permeability ( $\mu$ ) decreases the total power dissipated and the power dissipated in the first three centimeters (Fig 20).
- Increasing the permittivity ( $\epsilon$ ) increases the total power dissipated as well as the power dissipated in the first three centimeters (Fig 21).

Sigma	Mu	Epsilon	Pdis C by C	Pdis < 3cm	% of total
0,85	1	42,5	8,34E-10	7,10E-10	85,11
1	1	42,5	8,52E-10	7,47E-10	87,68
2	1	42,5	8,05E-10	7,79E-10	96,75
3	1	42,5	7,11E-10	7,04E-10	98,92
4	1	42,5	6,34E-10	6,30E-10	99,44
1	1	1	1,04E-09	1,02E-09	97,80
1	1	1,5	1,05E-09	1,03E-09	97,71
1	1	2	1,06E-09	1,03E-09	97,61
1	1	10	1,11E-09	1,06E-09	95,65
1	1	20	1,05E-09	9,74E-10	92,71
1	1	30	9,04E-10	8,13E-10	90,00
1	2	42,5	1,10E-09	1,02E-09	93,05
1	4	42,5	1,48E-09	1,43E-09	96,74

Table 1 Results of the variations experiment

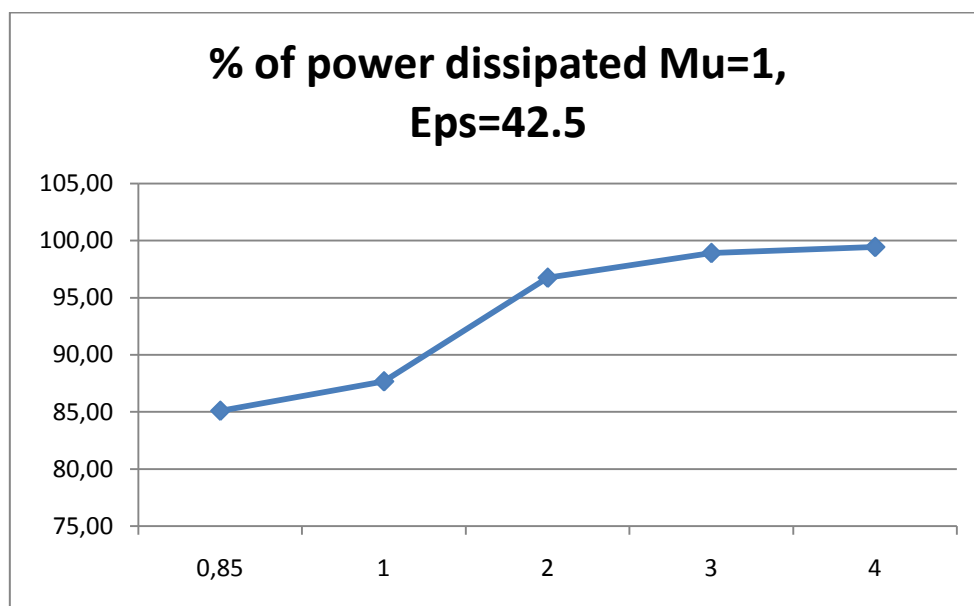


Fig. 19 Relative power dissipation according to the variation of sigma

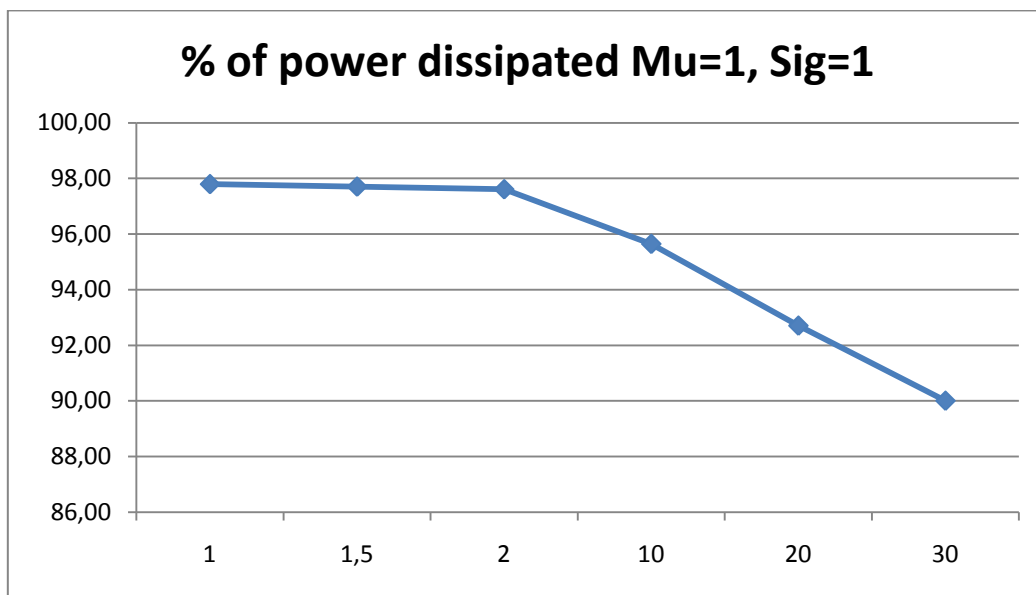


Fig. 20 Relative power dissipation according to the variations of epsilon

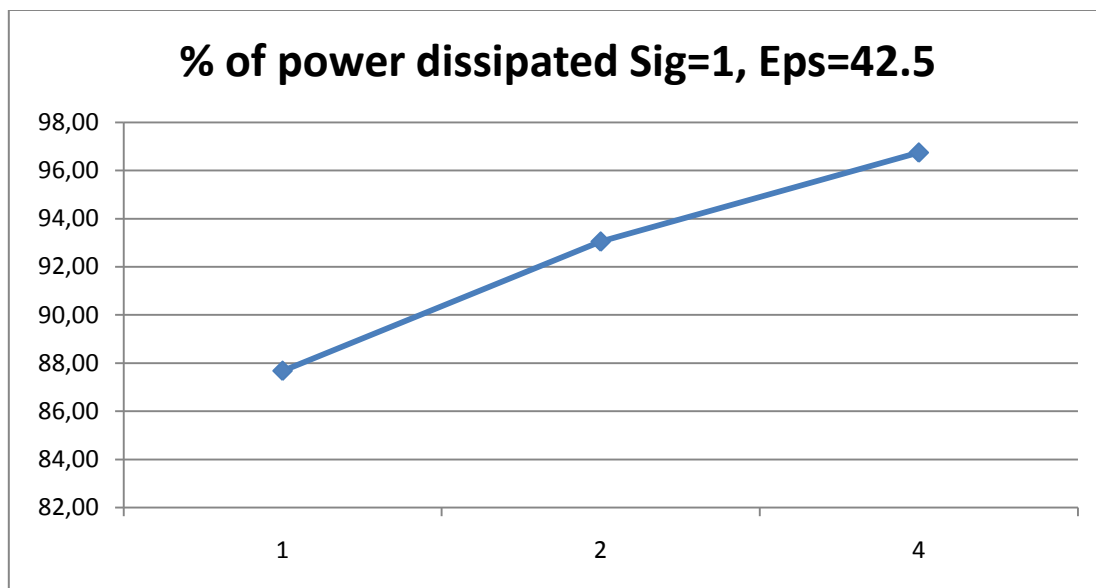


Fig. 21 Relative power dissipation according to the variation of mu

In the same manner, some results have shown that the repartition of power dissipation varies a great deal when varying parameters as shown in figures 22-23 below.

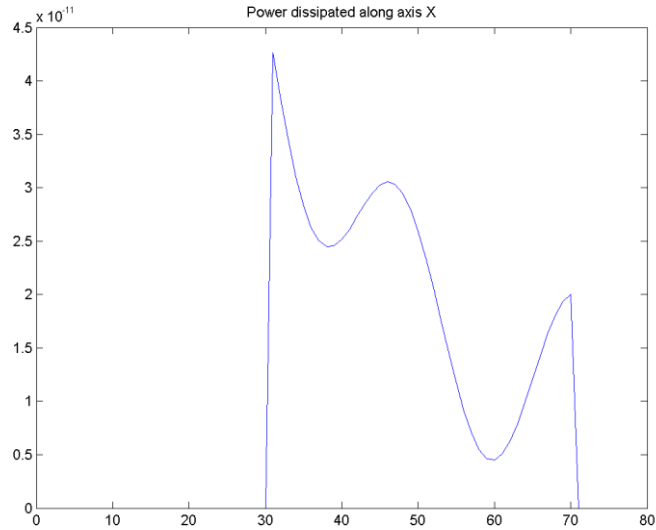


Fig. 22 Power dissipation along the x-axis with a permeability of 42.5

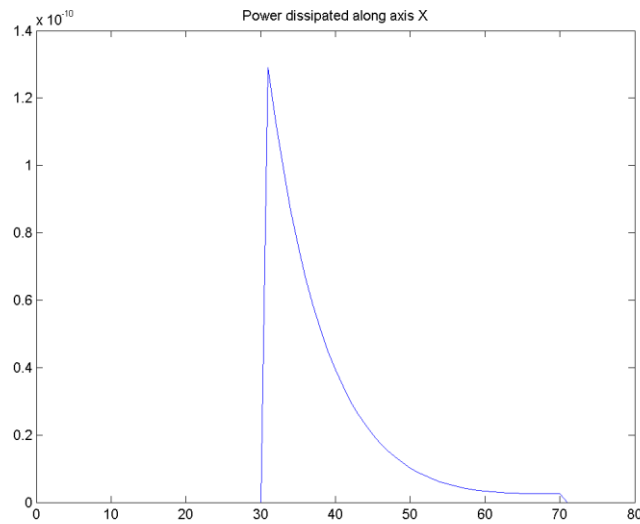


Fig. 23 Power dissipation along the x-axis with a permeability of 1.5

While in the end we considered the hand as a homogeneous brick with parameters of  $\mu = 1$ ,  $\sigma = 0.79$  and  $\epsilon = 36.2$ , this research has raised some interesting questions about the impact of these parameters on the agglomeration or not of the total power dissipation at one end of the brick.

## II – Narrowband PIFA study

One of the antennas we decided to include as our reference antennas was the narrowband PIFA antenna, for which we aimed to resonate at a frequency of 850MHz (UMTS V). We decided to look at the impact of bringing the antenna closer to the ground plane as a matter of reflection coefficient and bandwidth. Our reference PIFA antenna was separated from the ground plane by 10 millimeters, and this study used distances of 1, 2 and 5 millimeters to witness the impact of this distance.

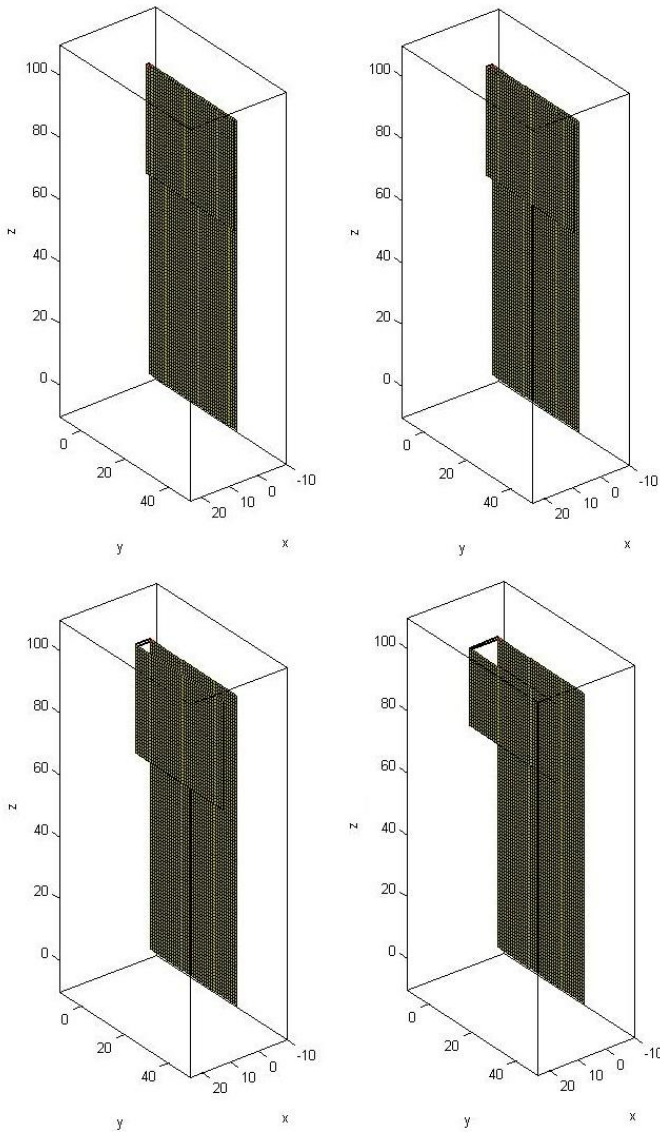


Fig. 24 PIFA antennas separated by 1, 2, 5 and 10mm from the ground plane

From this experiment, we obtained results shown in figure 25 and further expanded in table 2 below.

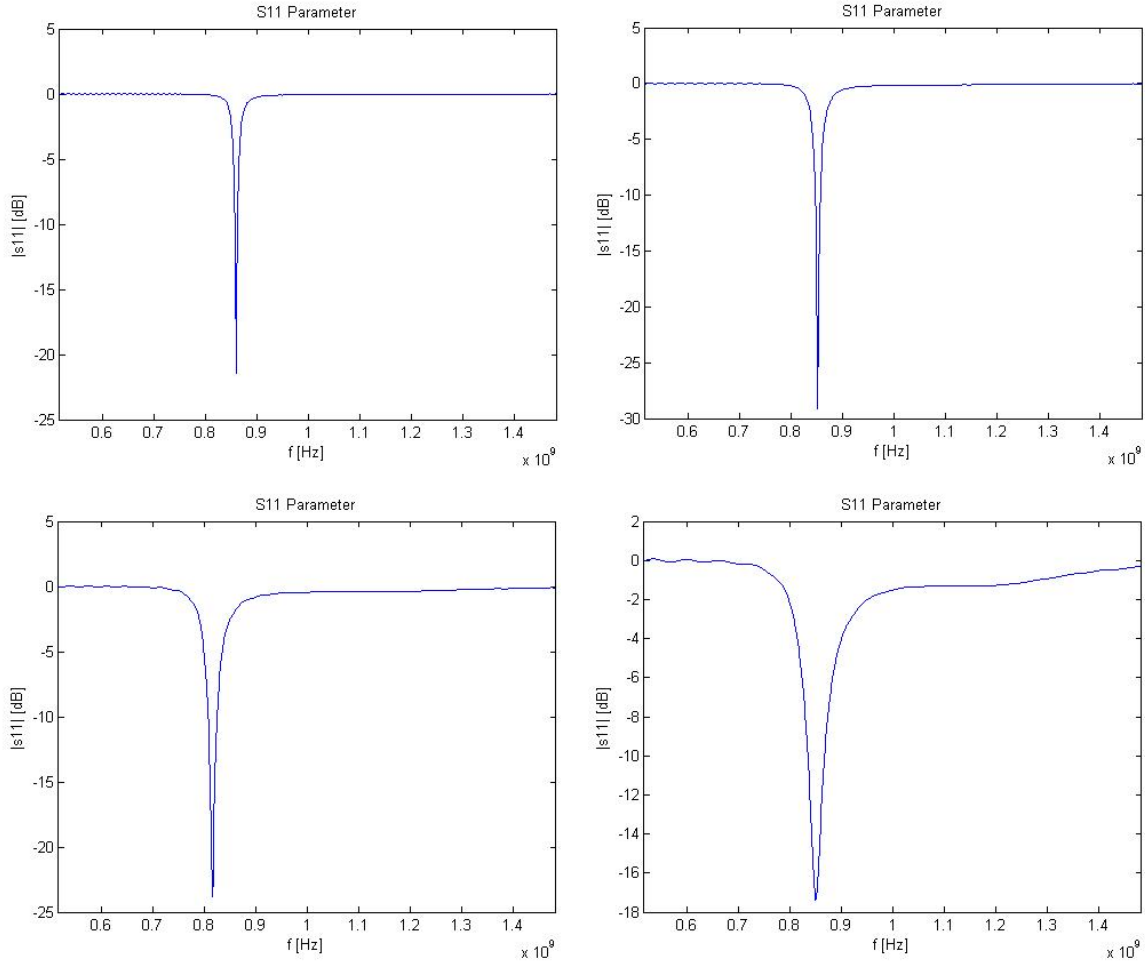


Fig. 25 Reflection coefficient for PIFA antennas elevated by 1, 2, 5 and 10mm

Distance from Ground plane	Bandwidth	Reflection coefficient
1	10 MHz	-22 dB
2	20 MHz	-29 dB
5	35 MHz	-24 dB
10	80 MHz	-17 dB

Table 2 Impact of distance from the ground plane on PIFA antenna performance

With elevation, the bandwidth of the antenna increases, but its reflection coefficient increases as well, making the antenna more vulnerable to

interference. For the robustness experiment, a 1mm PIFA narrowband antenna was used.

### III – Impact of the permittivity of the substrate on a thin substrate-layered PIFA antenna

One of the reference antennas considered was the PIFA with substrate, one of the first designs was a thin layer of substrate directly imposed on the PIFA antenna. As several substrates are available, a quick study was made on the impact of a change of permittivity of the substrate on the performance of the antenna. The antenna design can be seen in figure 26 below.

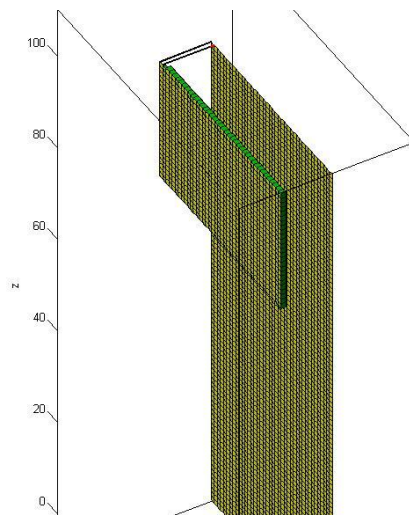


Fig. 26 Thin-layered substrate PIFA antenna

The considered values of permittivity were 1, 2, 2.3, 2.5, 2.7 and 3 F/m. Results of this experiment are shown in figure 27 below and expanded in table 3.

Permittivity	Resonance frequency	Bandwidth	Reflection coefficient
1	850 MHz	60 MHz	-17 dB
2	830 MHz	50 MHz	-20 dB
2.3	830 MHz	40 MHz	-22 dB
2.5	830 MHz	35 MHz	-23 dB
2.7	830 MHz	30 MHz	-23 dB
3	830 MHz	25 MHz	-23 dB

Table 3 Performance variation of a thin-layered substrate PIFA antenna with a change of permittivity of the substrate

The conclusion of this study is that when increasing the permittivity of the substrate, the reflection coefficient decreases to a minimum (in our case of -23 dB), the resonance frequency varies little and more importantly, the bandwidth decreases with the increase of permittivity. In the case of the substrate PIFA reference antenna used for robustness simulations, a permittivity of 1 F/m was chosen.

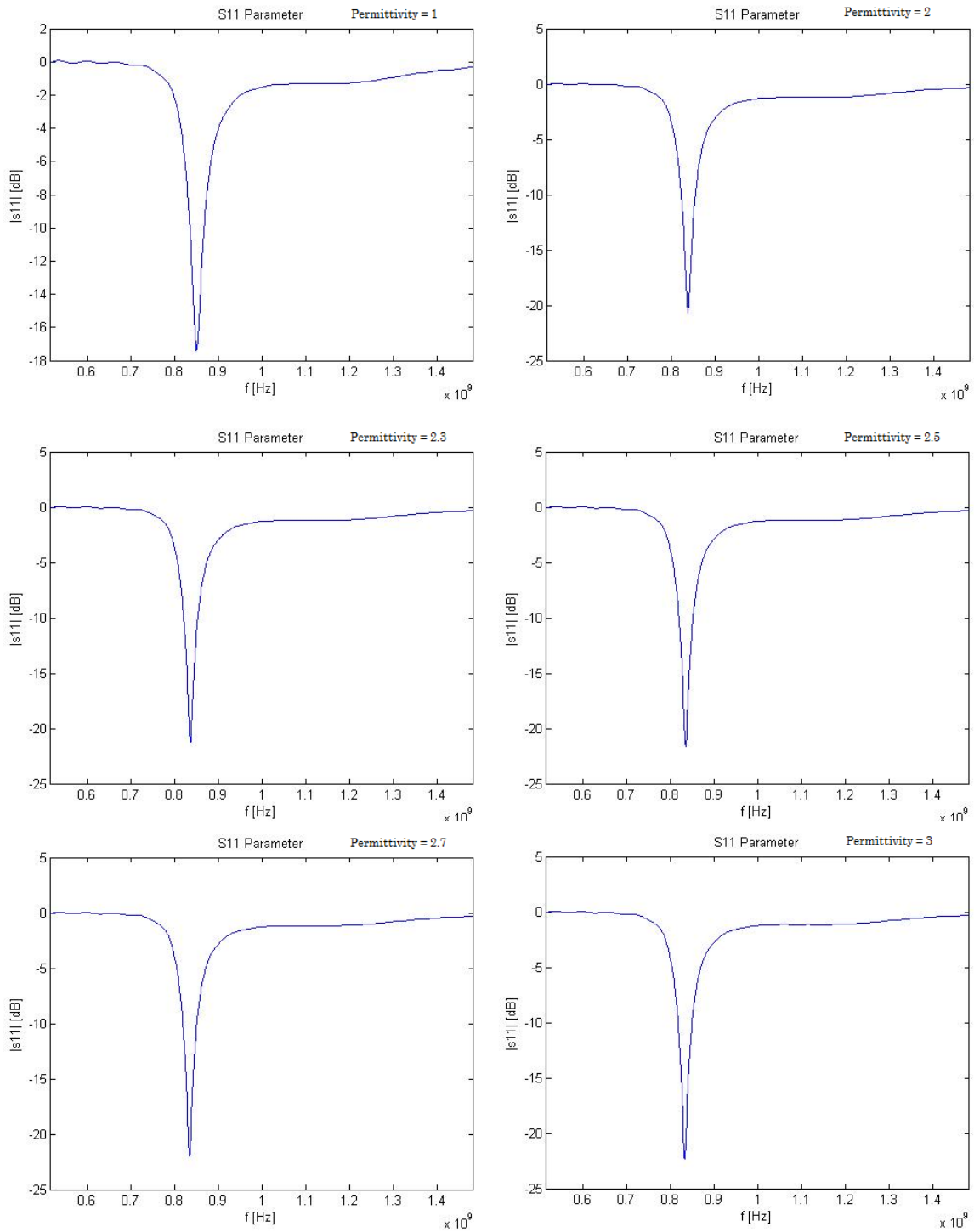


Fig. 27 Performance variation for substrate PIFA antennas with different permittivity for the substrate

## IV – Defining the composition of the human hand

In order to determine the best brick to test our antennas, we decided to reproduce some experiments from an article published in Microwave and optical technology letters [13]. The goal was to compare the results obtained with AAU3. We designed different bricks to respect the initial experiments parameters.

We put two bricks with different permittivity and conductivities with the distances used in the article's experiments.

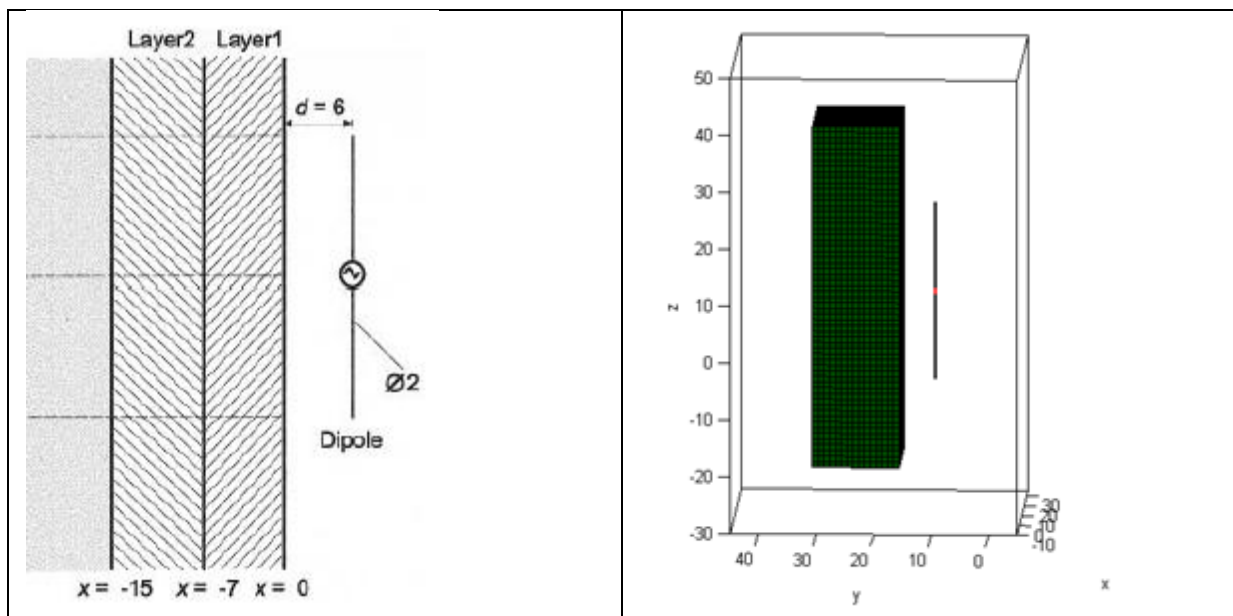


Fig. 28 Comparative experiments

The experiments were performed with a dipole antenna resonating at 900MHz. We studied 3 cases:

- 1<sup>st</sup> layer representing a fat layer, 2<sup>nd</sup> layer representing a Tissue-Equivalent Liquid (TEL)
- 1<sup>st</sup> layer representing a muscle, 2<sup>nd</sup> layer representing a bone
- 1<sup>st</sup> layer and 2<sup>nd</sup> layer representing a TEL

Material	permittivity	conductivity
Tissue-Equivalent Liquid (TEL)	42.50	0.850
Muscle	55.95	0.969
Bone	16.62	0.242
Fat	5.00	0.025

Table 4 Values of specific hand components

What we were concerned in these simulations was the E field magnitude. In figures below, the results are presented

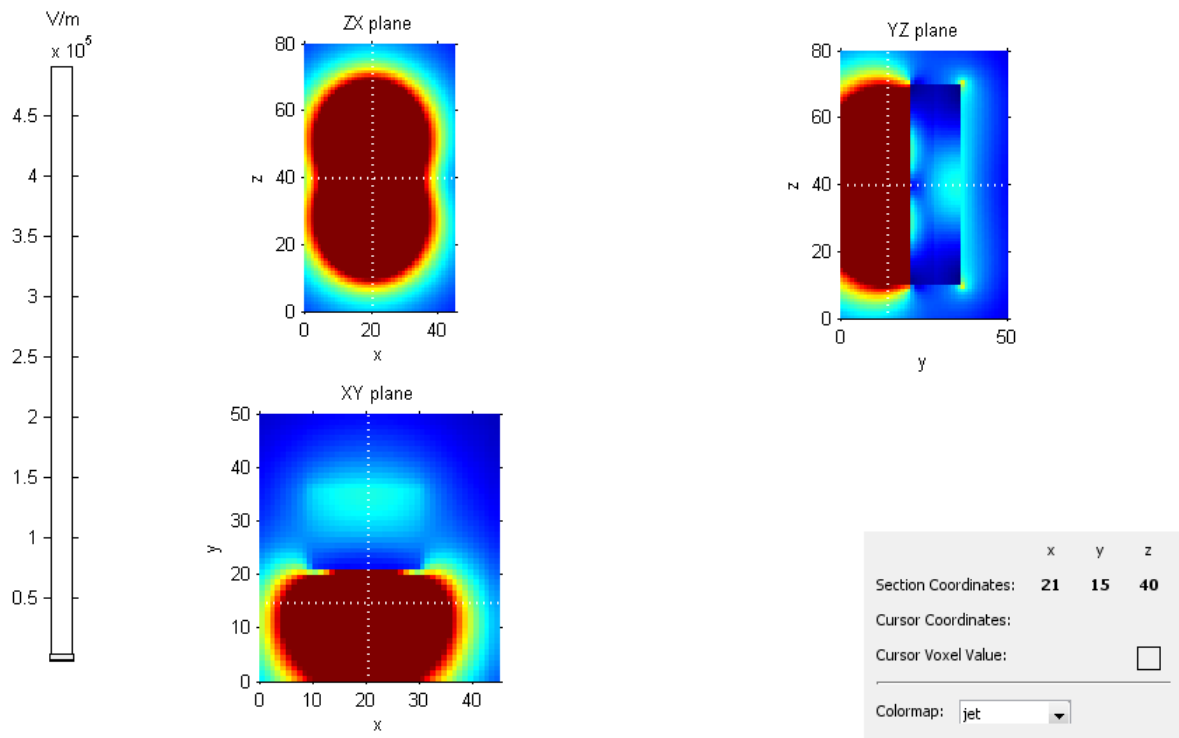


Fig. 29 1<sup>st</sup> layer representing a fat layer, 2<sup>nd</sup> layer representing a Tissue-Equivalent Liquid (TEL)

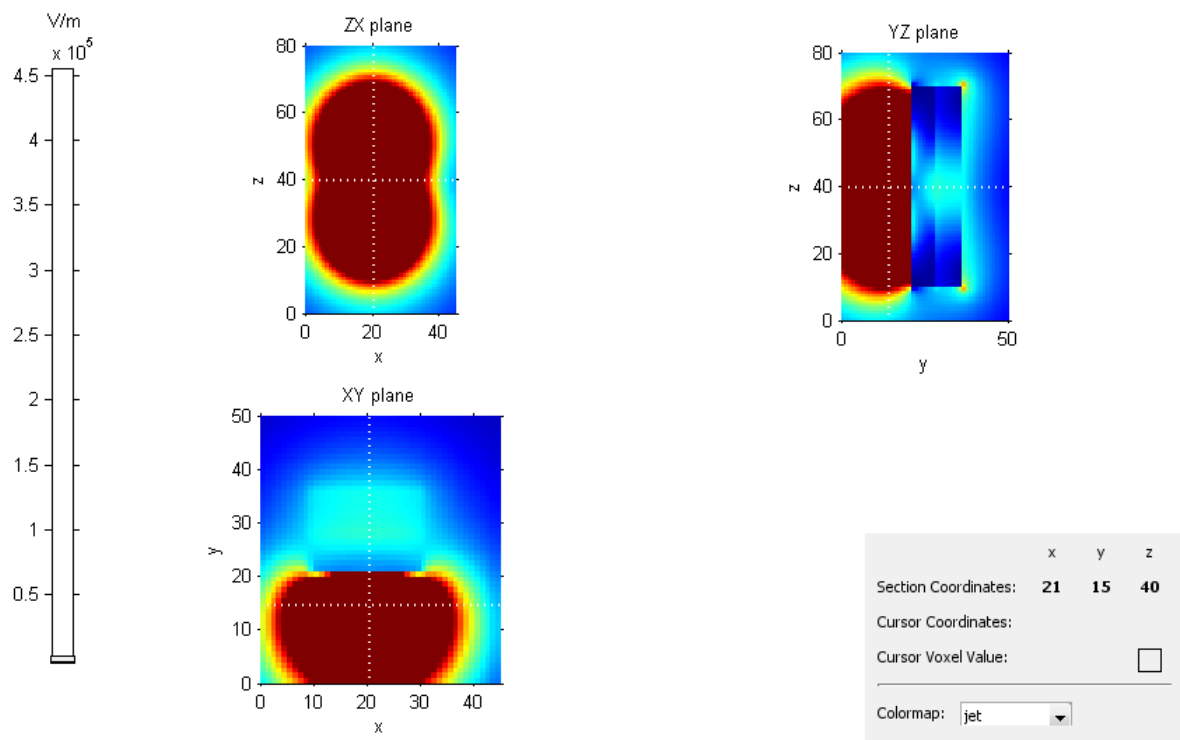


Fig. 30 1<sup>st</sup> layer representing a muscle, 2<sup>nd</sup> layer representing a bone

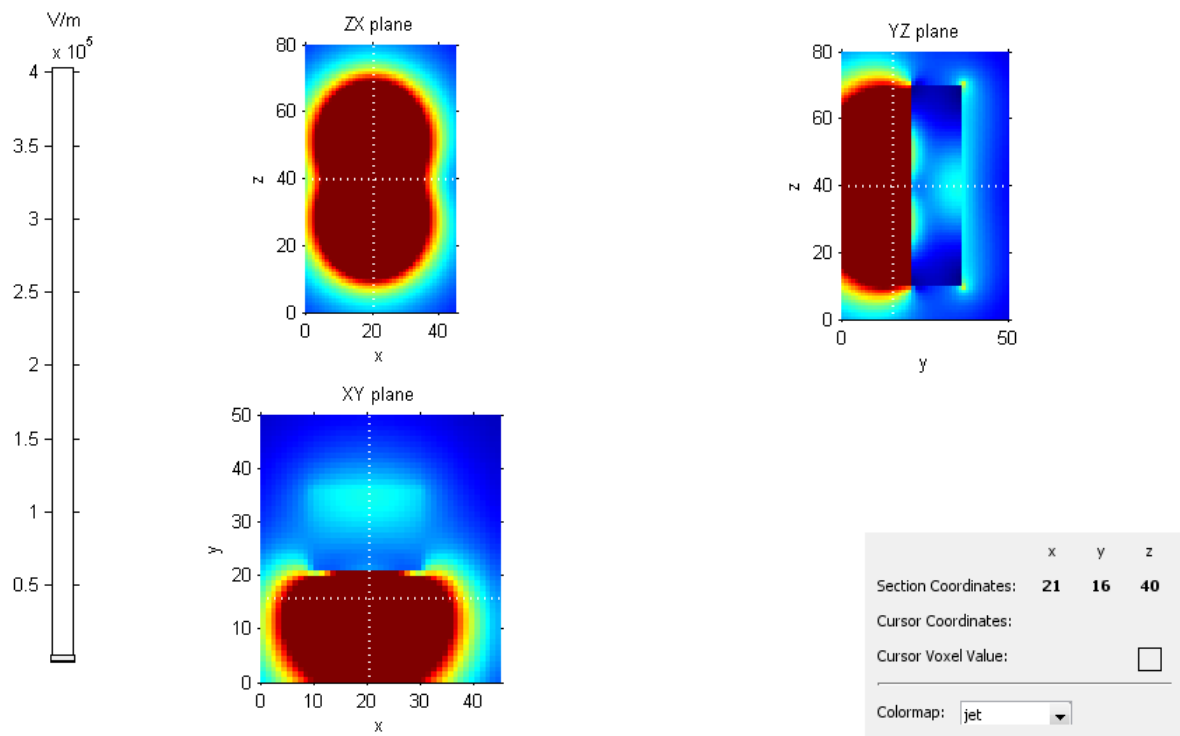


Fig. 31 1<sup>st</sup> layer and 2<sup>nd</sup> layer representing a TEL

With the different tools of AAU3, we were able to have some precise measures for the E field. Unfortunately, we were not able to compare precisely our results with those of the article [14]. For example, our comparison graph for the 3<sup>rd</sup> case is shown in figure 32 below.

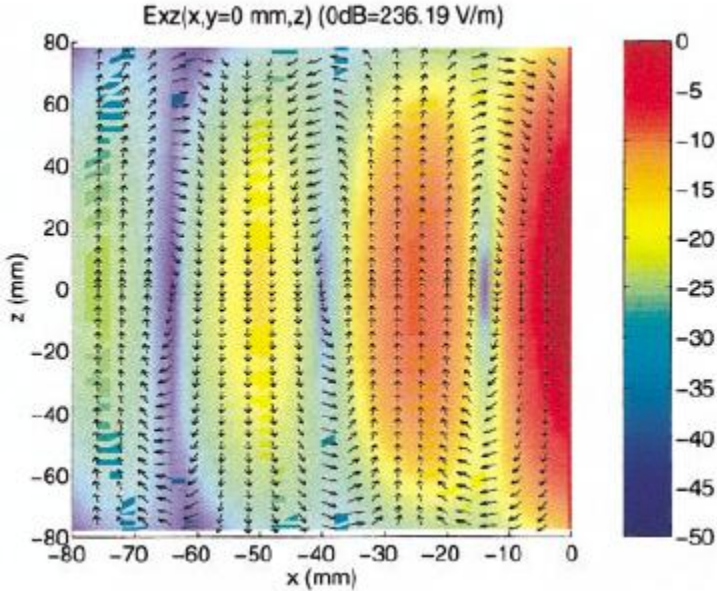


Fig. 32 Paper results

While recreating the results of this paper has revealed itself of no use for our own problem, it was still a pertinent insight on the importance of the nature of the hand and the composition of its simulated alter ego.

# CHAPTER THREE: SIMULATION PARADIGM AND ALTERATION

## I – Introduction

As described in the introduction, we used for this project a Finite Difference Time Domain approach to the computation of fields near our antennas. This FDTD analysis was made possible via the AAU3 software, a Matlab based software allowing us to design antennas and simulate their theoretical fields and such in a very customizable manner [15]. Furthermore, this software allowed us to design objects with specific parameters (like the hand or just a brick) to be put close to the antenna.

While this program has been at the center of our simulation environment, it turns out a few changes needed to be made to the code in order for us to obtain the best possible results. Notably, this is what made us to a slicer to visualize three dimensional fields more clearly than what AAU3 offered, but not only. Indeed, with the use of two separate power dissipation calculation techniques, results have shown that there is a difference between the power dissipated results of these two methods. Eventually, the changes brought to the software will be described.

## II – Slicer

The AAU3 program being able to compute electromagnetic fields in three dimensions, it seems obvious that a pertinent graphic approach to the results be set in place. However, the basic AAU3 software did not possess a convenient way to visualize these fields (figure 33), as having to set a cursor on three different graphs to see a result was not very satisfying. So, in order to have a more graphic result, we programmed a script which

shows along an axis a “slice” of the three dimensional results matrix. That way, the fields were much easier to witness (figure 34).

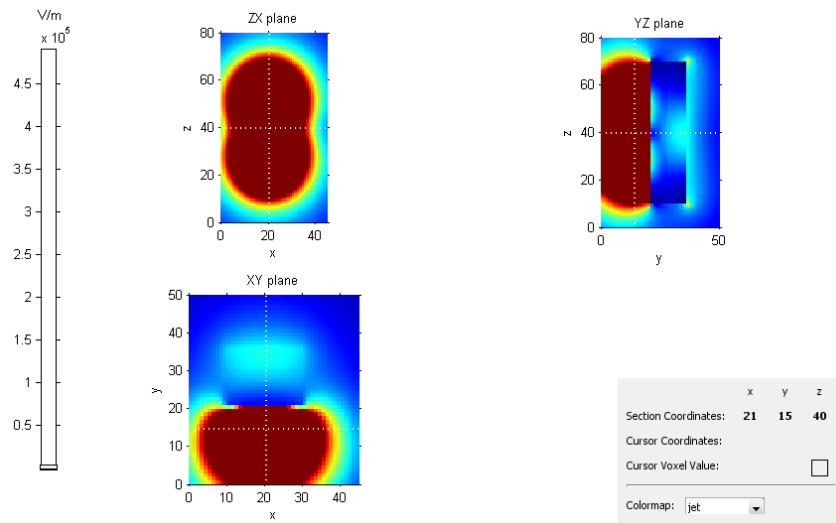


Fig. 33 Regular field graph

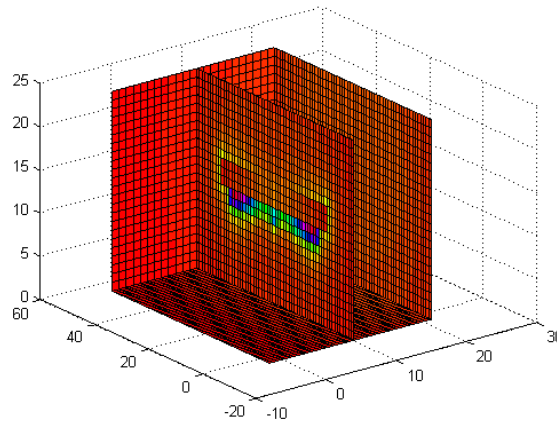


Fig. 34 Slicer

### III – Difference in power calculation

As described in chapter two, there are two methods of calculation for the total power dissipated. One approach, used by the AAU3 software, is via the computation of the pointing vector. The other is a more down-to-earth method, the summation of the power dissipation of each cell.

While using both techniques in our simulations, we realized that the results were not identical, which led to some questioning about whether

one or the other technique was not correctly implemented. However, it turned out that both were correct, so we did some research to see if this error could be predicted. Using the same simulation as the “Conductivity, permittivity and permeability variations” side experiment, we obtained the results in table 4 below.

Sigma	Mu	Epsilon	Pdis C by C	Pdis AAU3	%Err
0,85	1	42,5	8,34E-10	8,53E-10	2,24
1	1	42,5	8,52E-10	8,71E-10	2,22
2	1	42,5	8,05E-10	8,27E-10	2,65
3	1	42,5	7,11E-10	7,36E-10	3,33
4	1	42,5	6,34E-10	6,59E-10	3,82
1	1	1	1,04E-09	1,07E-09	2,74
1	1	1,5	1,05E-09	1,08E-09	2,72
1	1	2	1,06E-09	1,09E-09	2,69
1	1	10	1,11E-09	1,14E-09	2,44
1	1	20	1,05E-09	1,07E-09	2,18
1	1	30	9,04E-10	9,24E-10	2,21
1	2	42,5	1,10E-09	1,12E-09	2,26
1	4	42,5	1,48E-09	1,52E-09	2,68

Table 5 Error calculation between computation techniques

While the error is always small, it seems as though the smaller the total power dissipation was, the higher the error was. This made us think that there might be a “static” error overcome with large numbers. However, we could not prove this hypothesis.

## IV – Changes brought to AAU3

The main alteration we had to bring to AAU3 concerned the exportation of parameters and files. As such, we have made the exportation of results systematic and computation of fields and such automatic as well. Finally, we developed some scripts to compute the power dissipation or even show it right after computation by AAU3.

# CHAPTER FOUR: COMPARISON OF REFERENCE ANTENNAS

## I – Introduction

Now that we have defined the different lenses under which the antennas will be analyzed, let us introduce the simulation results and an interpretation on each of these results. Every antenna will first be compared to itself in free space, but with a brick close-by. Then, in the next chapter, all antennas will be compared to one another.

In this chapter, antennas will be described by a certain number of graphs or data:

- Actual graph of the antenna
- S11 graph
- Imaginary part graph
- Smith chart
- 3D correlation coefficient
- Power dissipated along axes
- Total power dissipated
- Antenna efficiency

## II – Dipole

The actual design of the antenna:

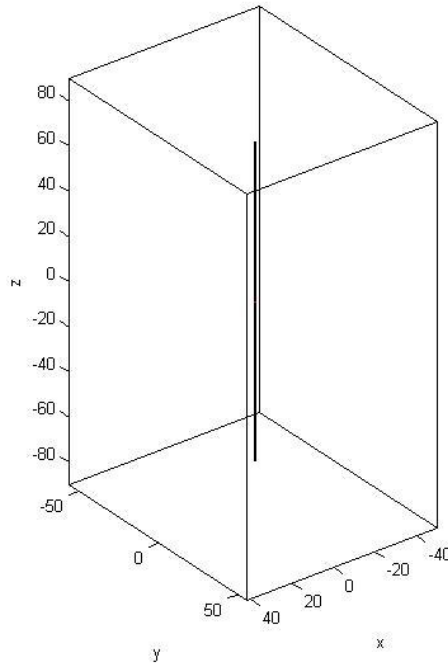


Fig. 35 A free space dipole antenna design

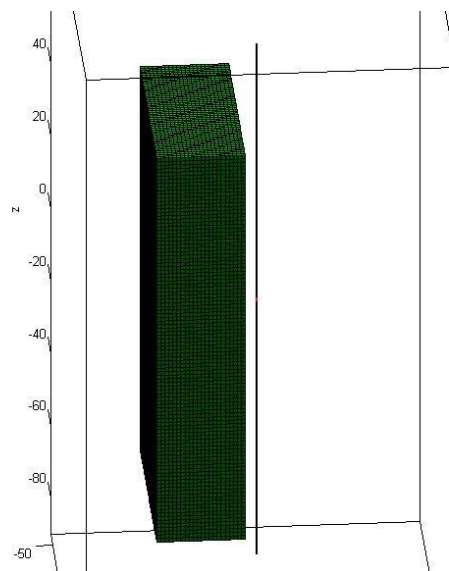


Fig. 36 A brick close by the dipole

The comparative S11 graphs:

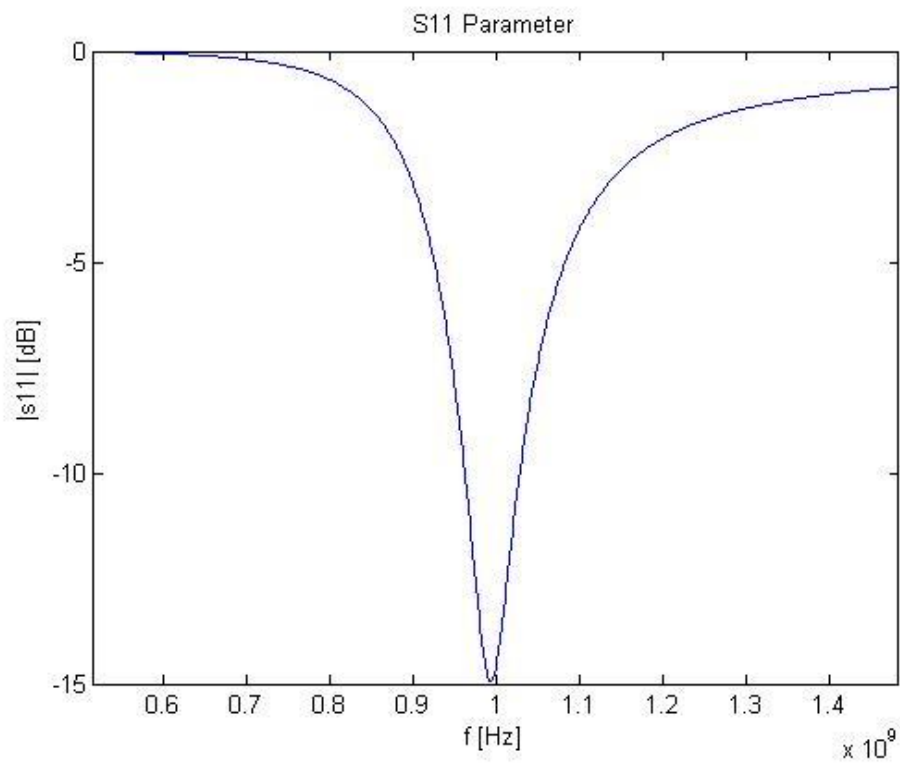


Fig. 37 Free space S11 for a dipole antenna

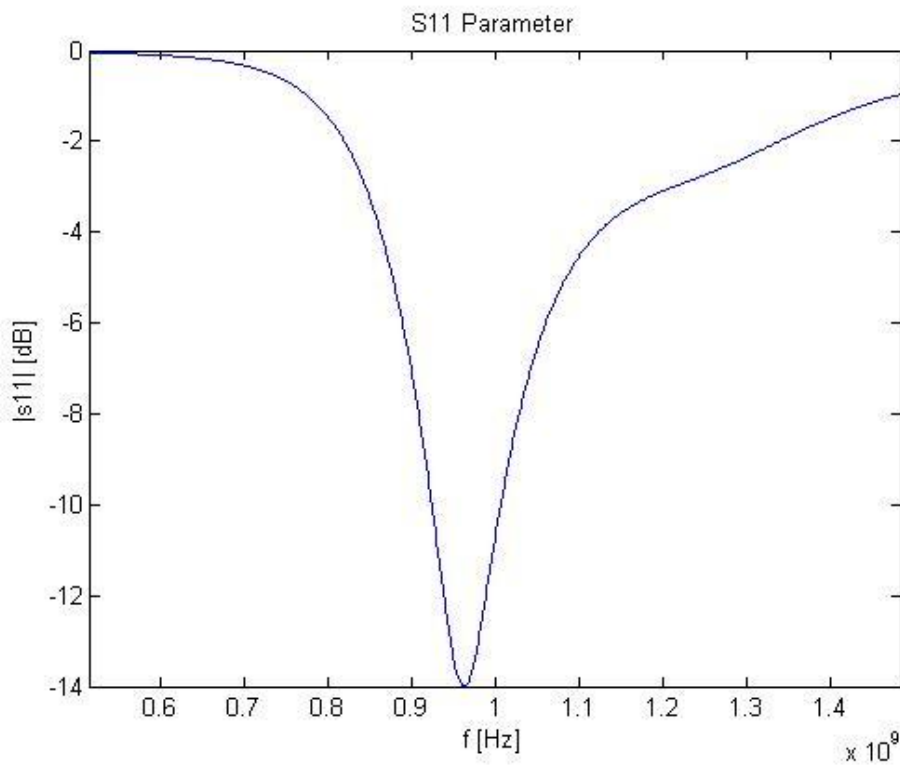


Fig. 38 Brick S11 for a dipole antenna

Imaginary parts of the dipole:

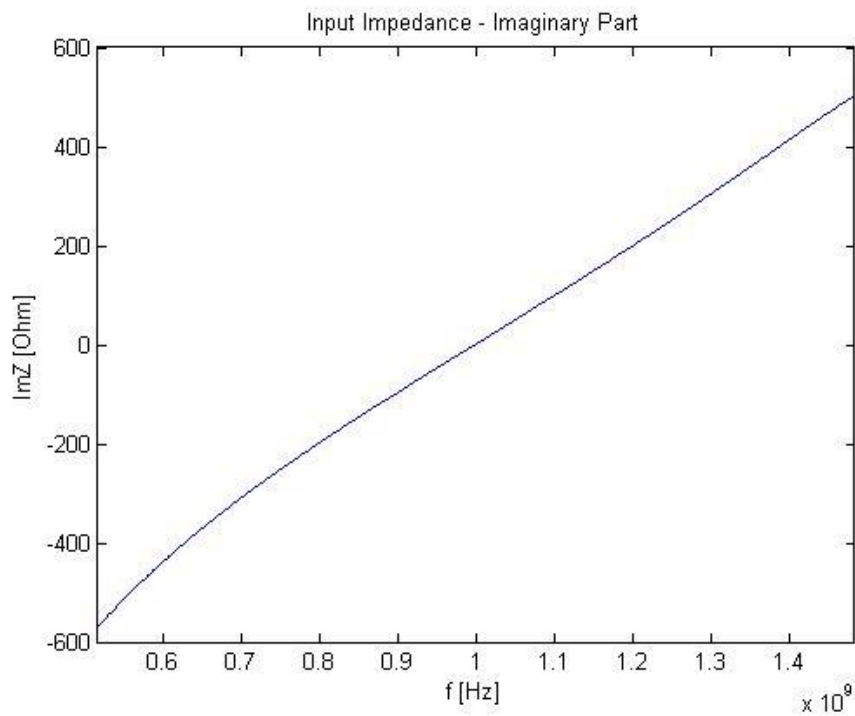


Fig. 39 Imaginary part of a free space dipole

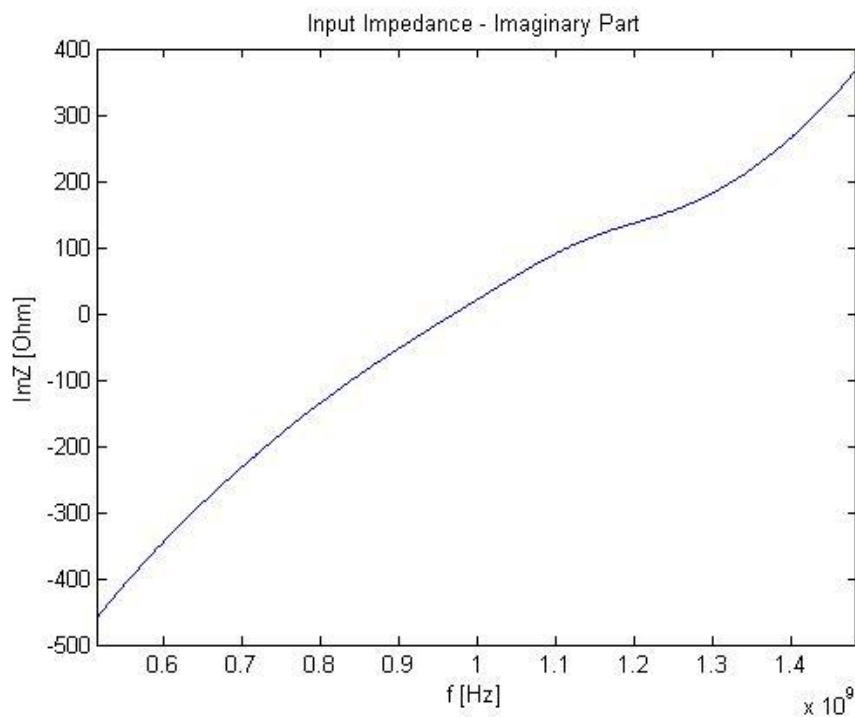


Fig. 40 Brick imaginary part of a dipole

Smith charts:

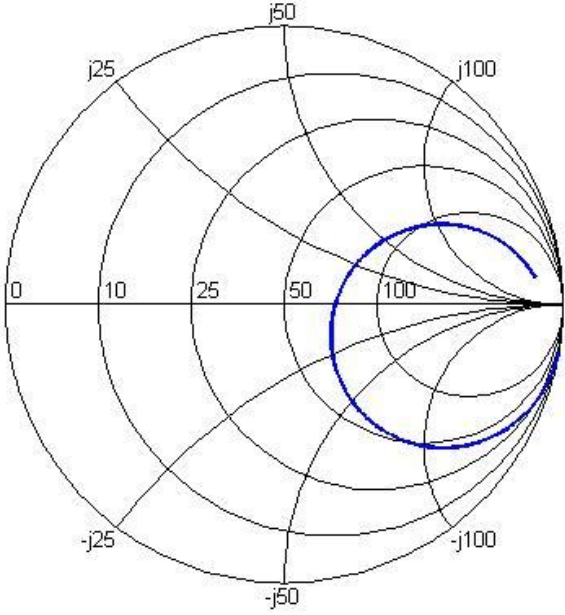


Fig. 41 Smith Chart of a free space dipole

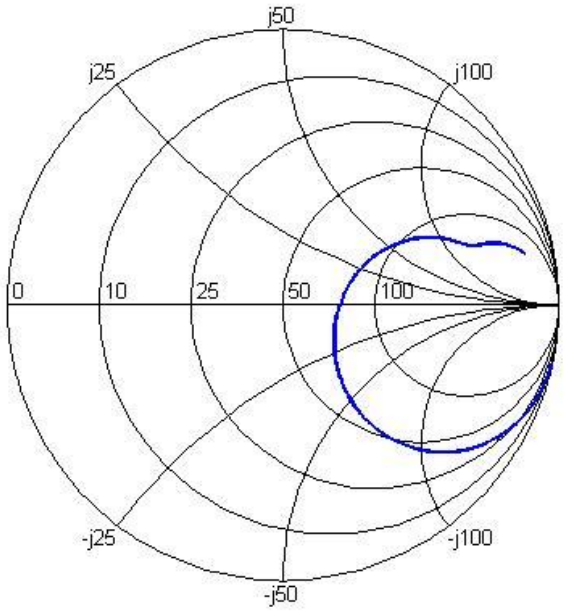


Fig. 42 Brick Smith Chart of a dipole

### Power dissipation along x:

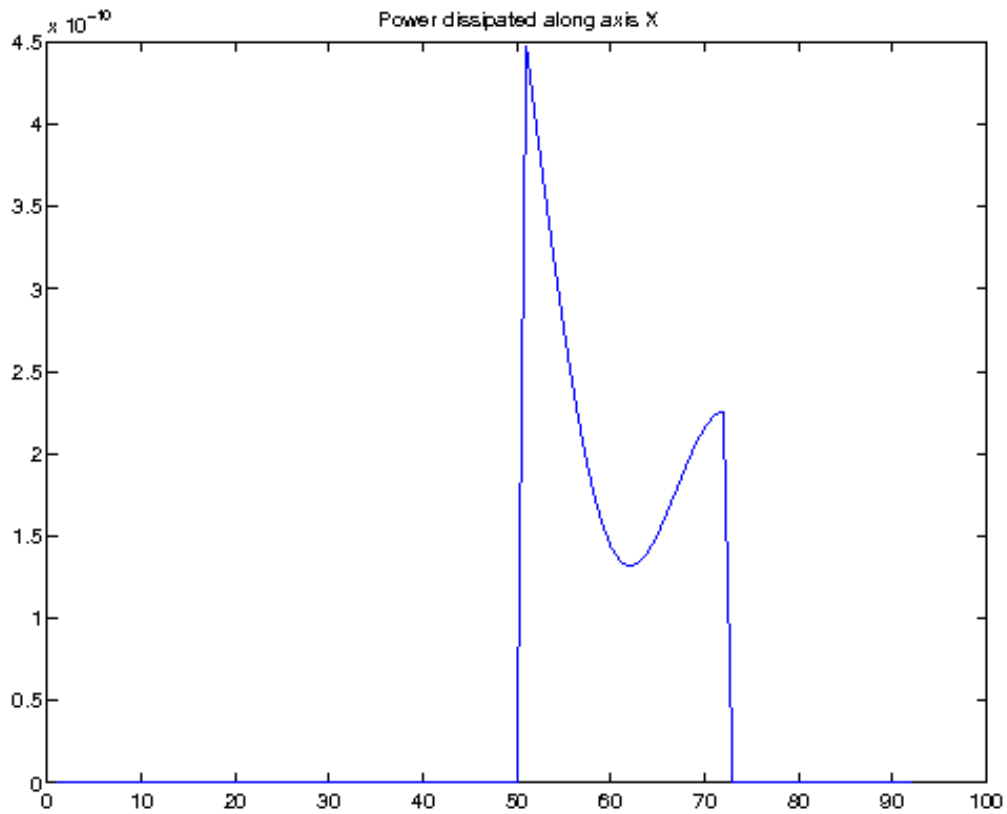


Fig. 43 Power dissipated along axis X for a dipole

### Numerical indicators:

- 3D Correlation coefficient	9.3818471e-01
- Total power dissipated	4.8250443e-09
- Power dissipated in the first 1.1cm	2.9959556e-09
- In percentage of total power dissipated	62.091774%
- Antenna efficiency without brick	0.98655
- Antenna efficiency with brick	0.32928

### III – Monopole

The actual design of the antenna:

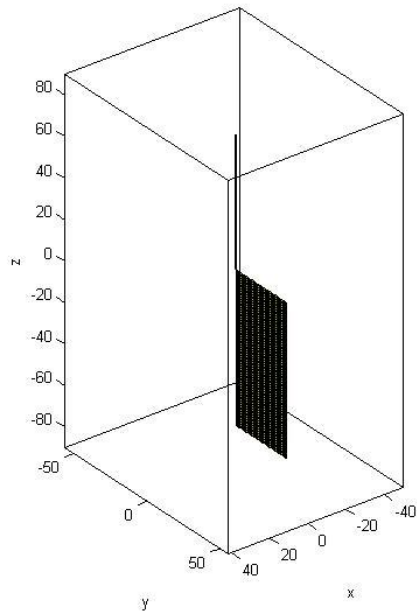


Fig. 44 The free space design of a monopole

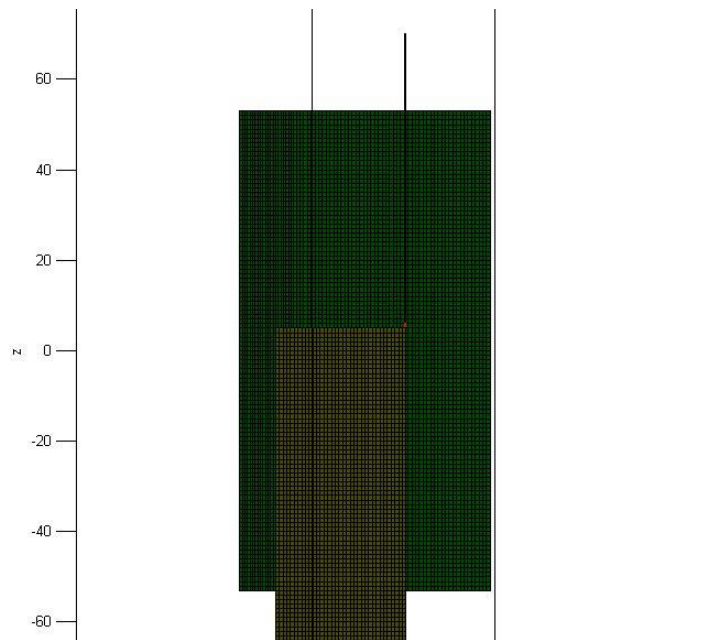


Fig. 45 The brick design of a monopole

The comparative S11 graphs:

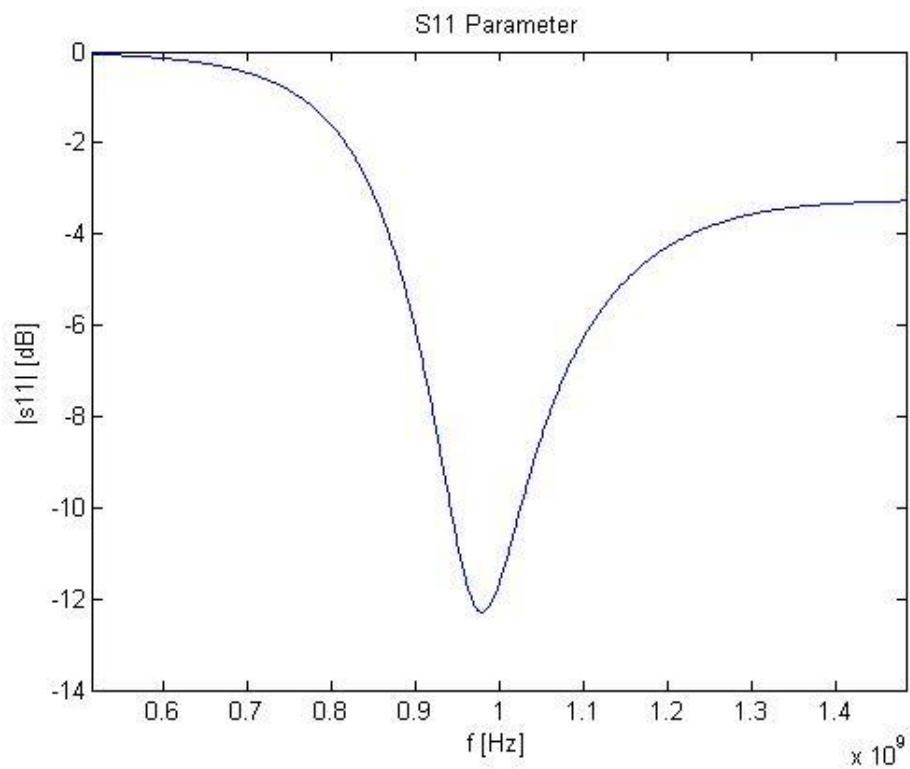


Fig. 46 S11 of a monopole in free space

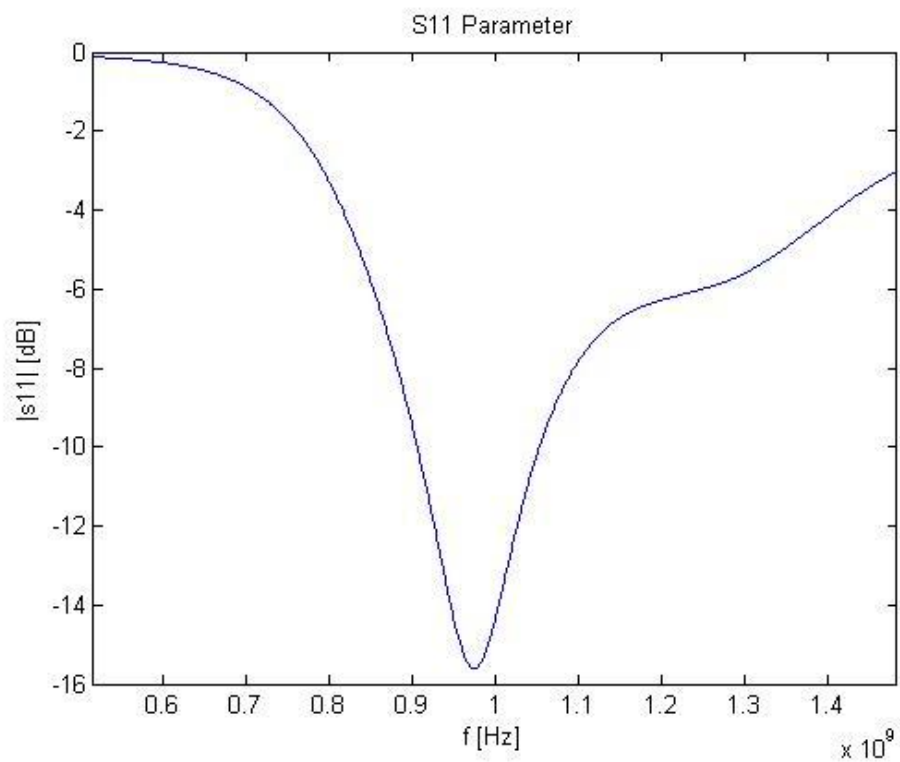


Fig. 47 Brick S11 of a monopole

Imaginary parts of the monopole:

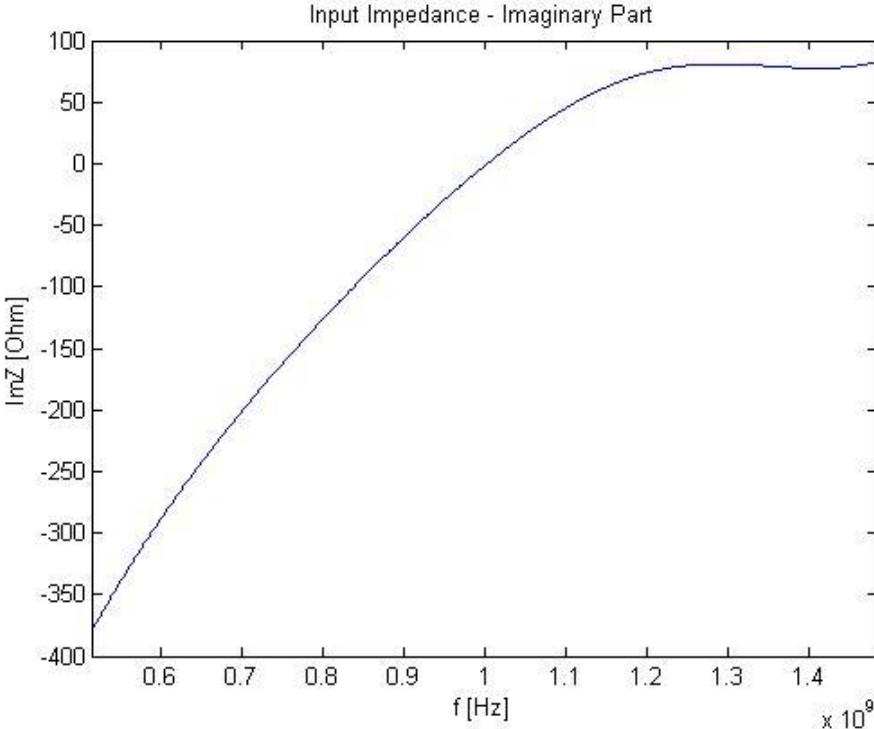


Fig. 48 Imaginary part of a free space monopole

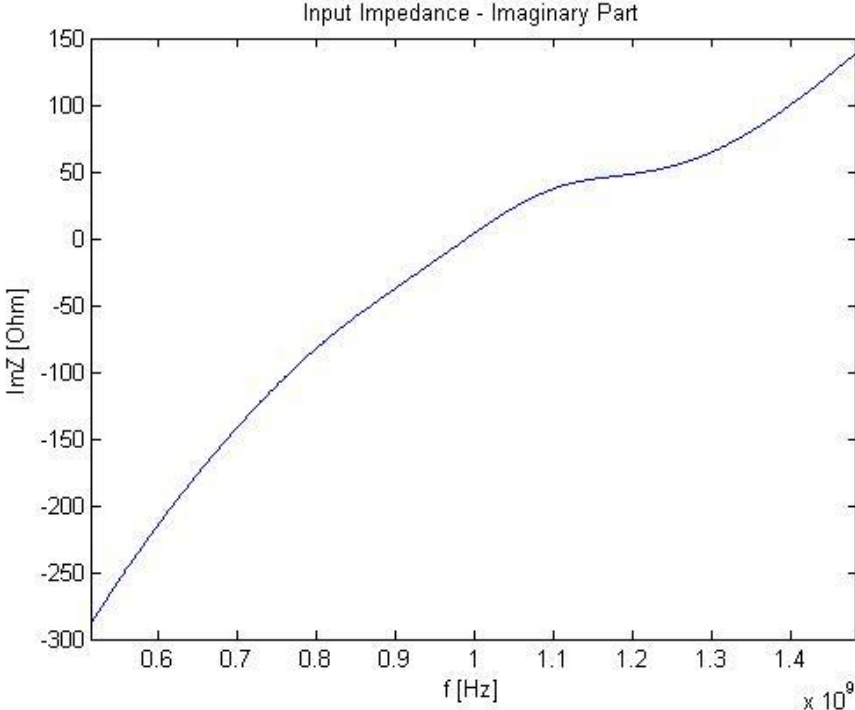


Fig. 49 Brick imaginary part of a monopole

Smith Charts:

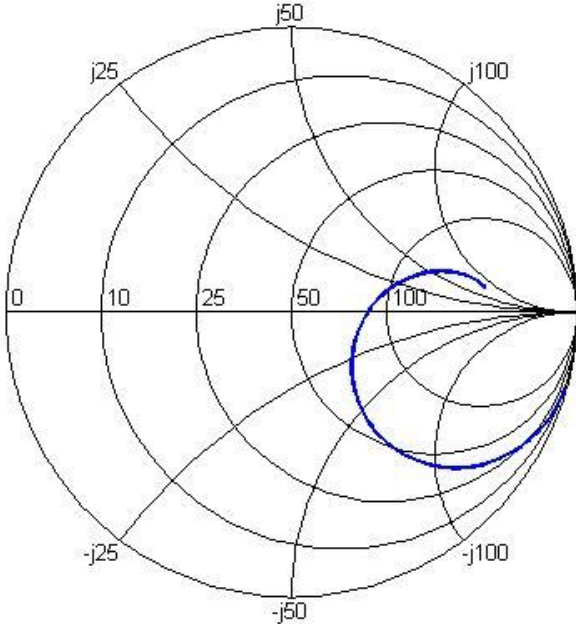


Fig. 50 Smith Chart for a free space monopole

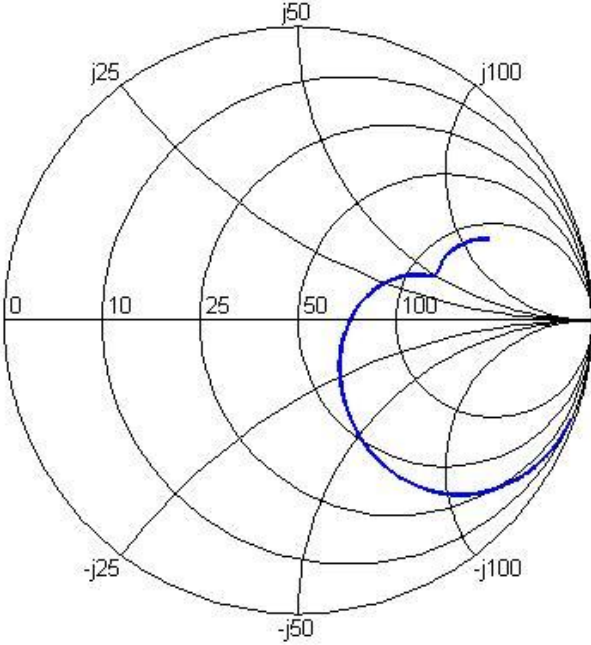


Fig. 51 Brick Smith Chart for a monopole

Power dissipation along x:

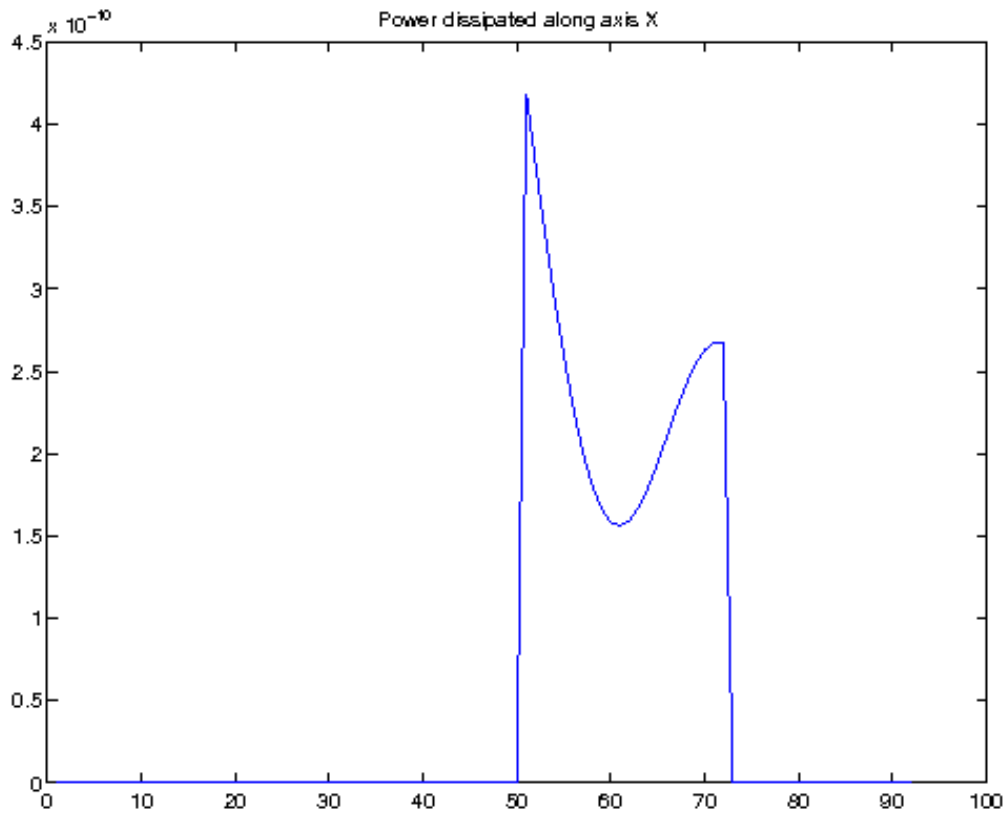


Fig. 52 Power dissipated along x for a monopole

Numerical indicators:

- |   |               |
|---|---------------|
| - 3D Correlation coefficient              | 8.8779460e-01 |
| - Total power dissipated                  | 5.2063101e-09 |
| - Power dissipated in the first 1.1cm     | 2.9341756e-09 |
| - In percentage of total power dissipated | 56.358065%    |
| - Antenna efficiency without brick        | 0.98757       |
| - Antenna efficiency with brick           | 0.31217       |

## IV – PIFA

The actual design of the antenna:

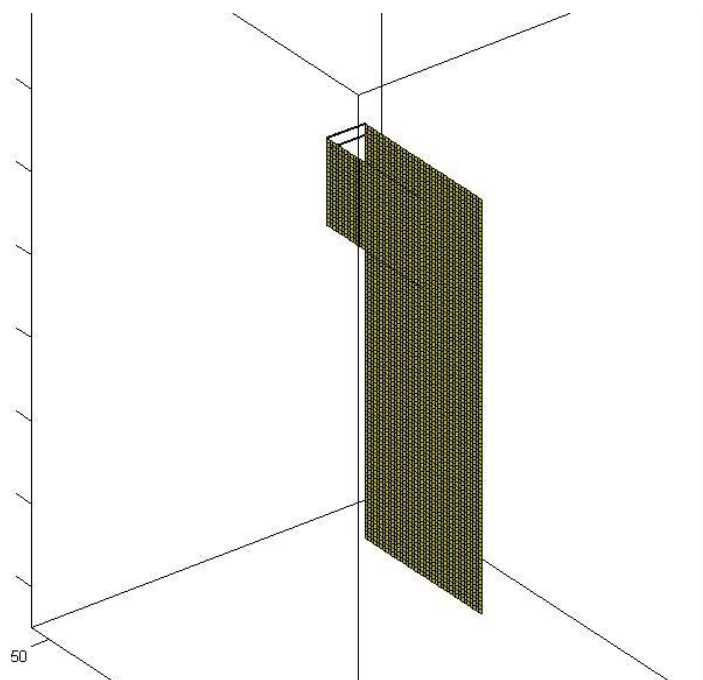


Fig. 53 The free space design of a PIFA

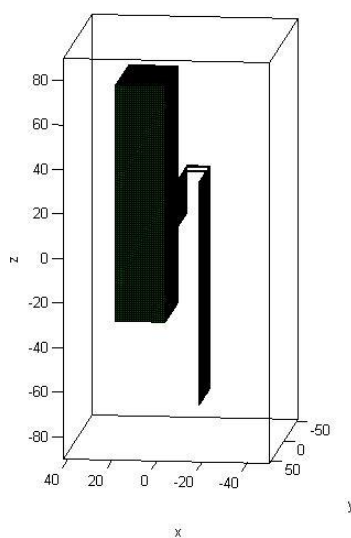


Fig. 54 The brick design of a PIFA

The comparative S11 graphs:

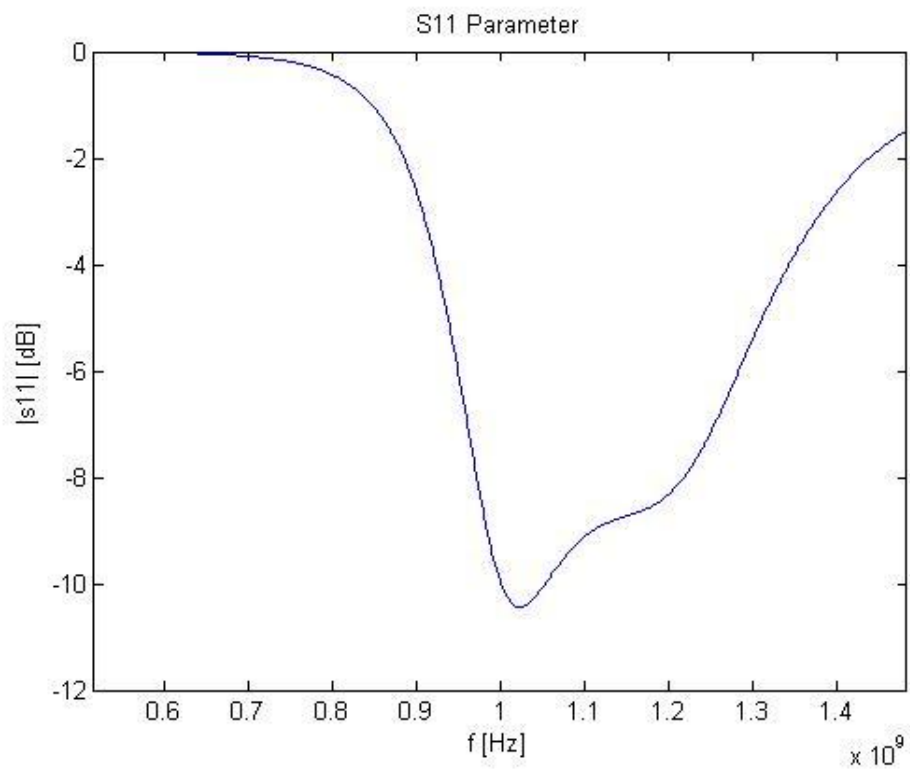


Fig. 55 S11 of a PIFA in free space

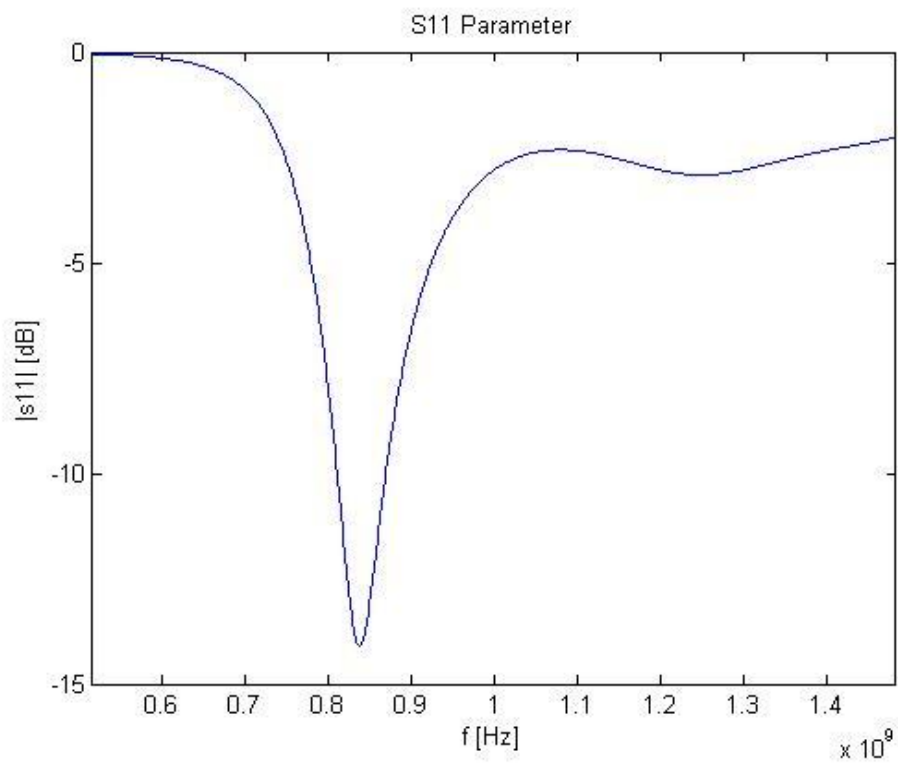


Fig. 56 Brick S11 of a PIFA

Imaginary parts of the PIFA:

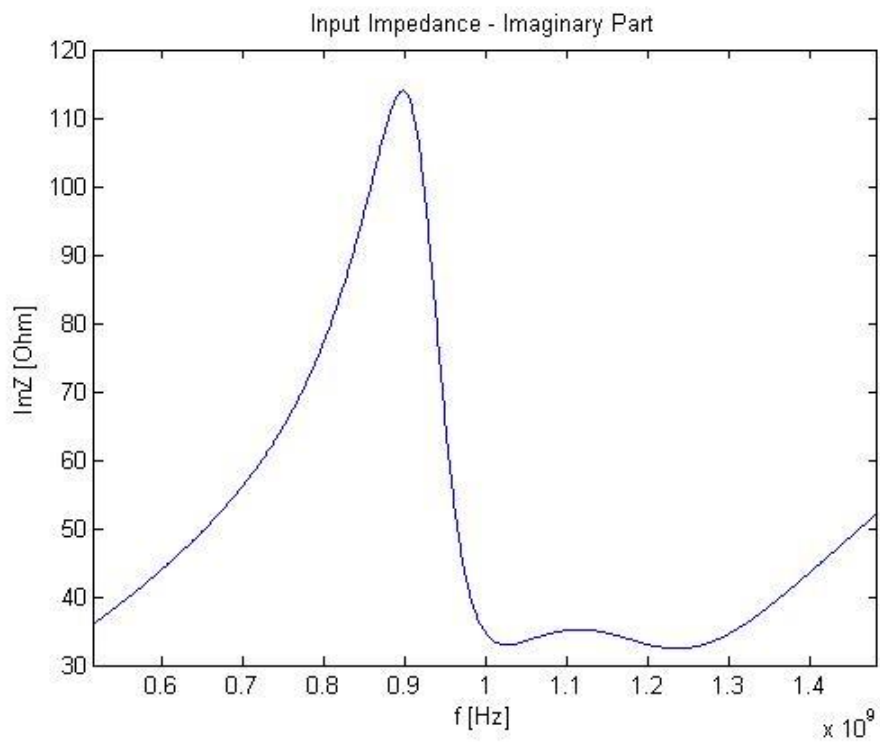


Fig. 57 Imaginary part of a free space PIFA

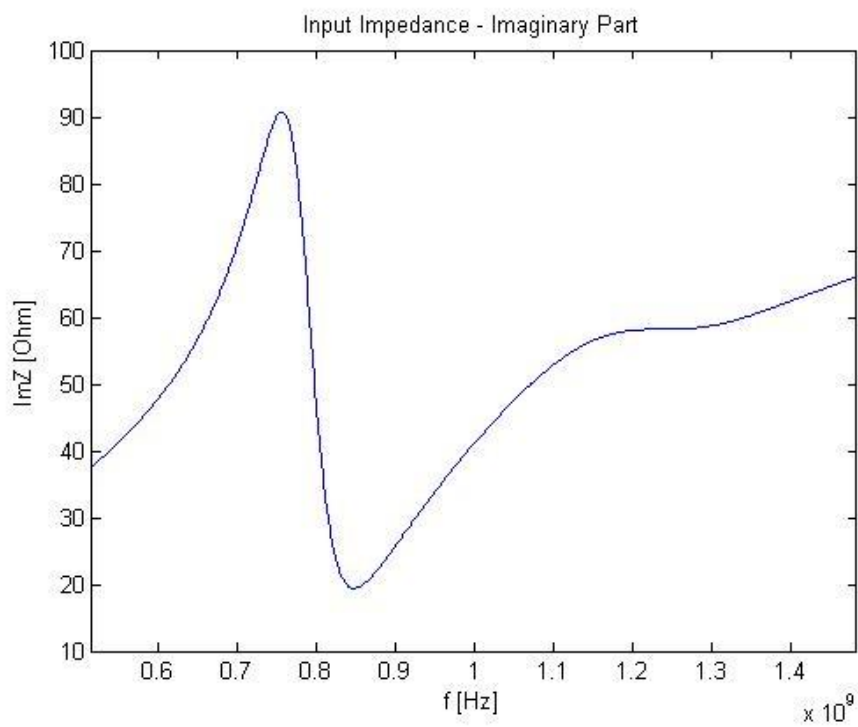


Fig. 58 Brick imaginary part of a PIFA

Smith Charts:

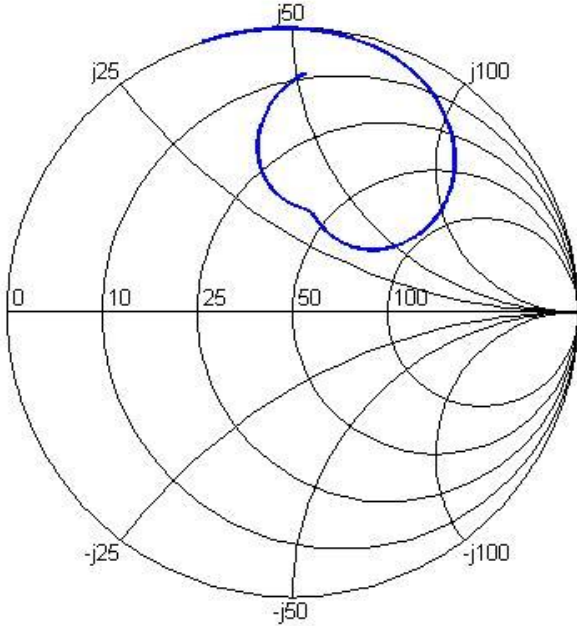


Fig. 59 Smith Chart for a free space PIFA

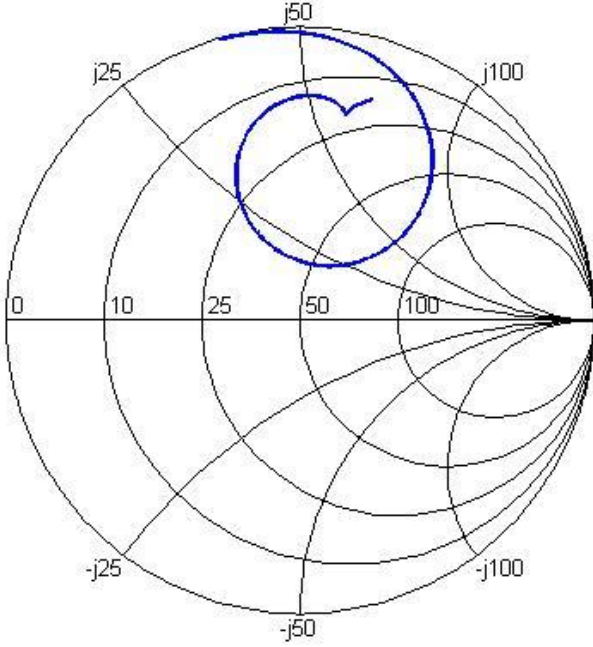


Fig. 60 Brick Smith Chart for a PIFA

Power dissipation along x:

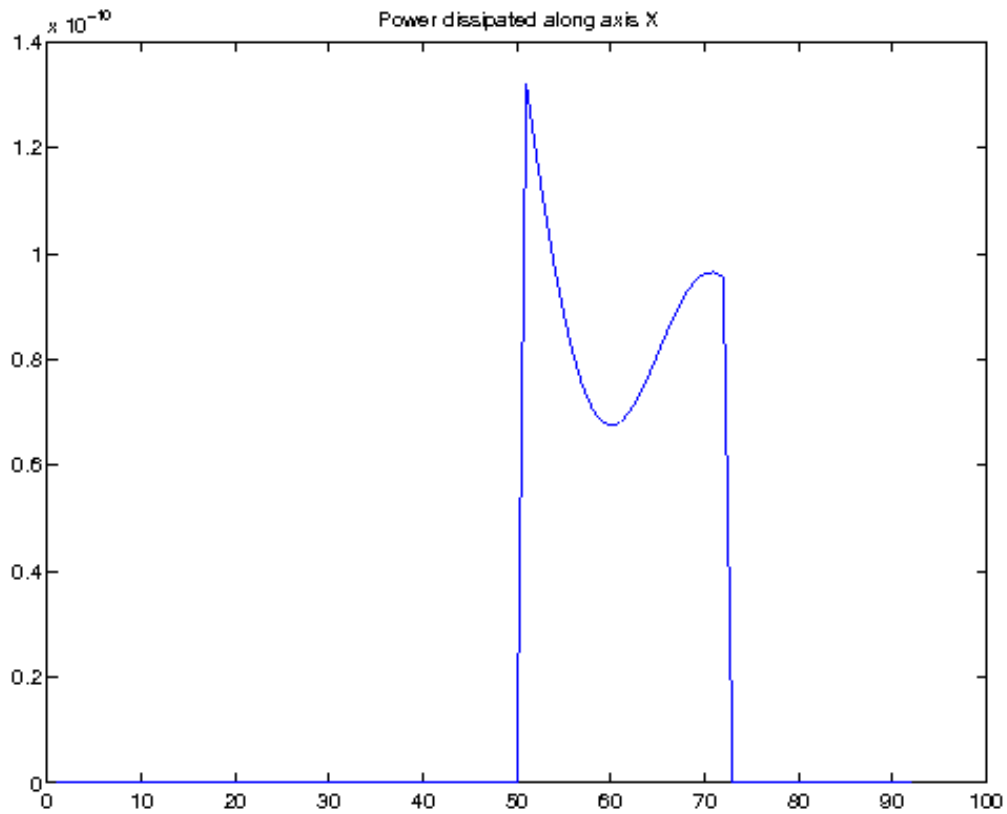


Fig. 61 Power dissipation along x for a PIFA

Numerical indicators:

- |   |               |
|---|---------------|
| - 3D Correlation coefficient              | 7.7953279e-01 |
| - Total power dissipated                  | 1.9273124e-09 |
| - Power dissipated in the first 1.1cm     | 1.0463317e-09 |
| - In percentage of total power dissipated | 54.289677%    |
| - Antenna efficiency without brick        | 0.99398       |
| - Antenna efficiency with brick           | 0.48337       |

# V – Slotted PIFA

The actual design of the antenna:

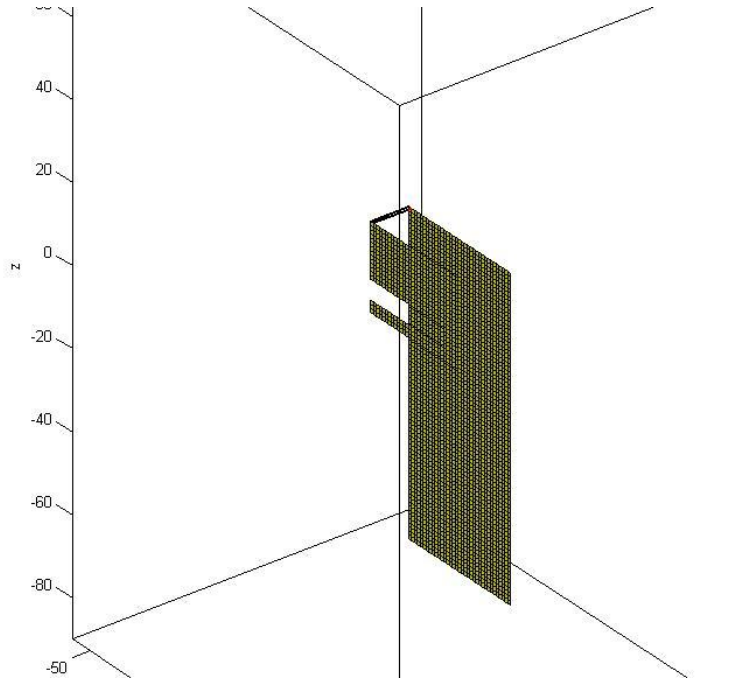


Fig. 62 The free space design of a slotted PIFA

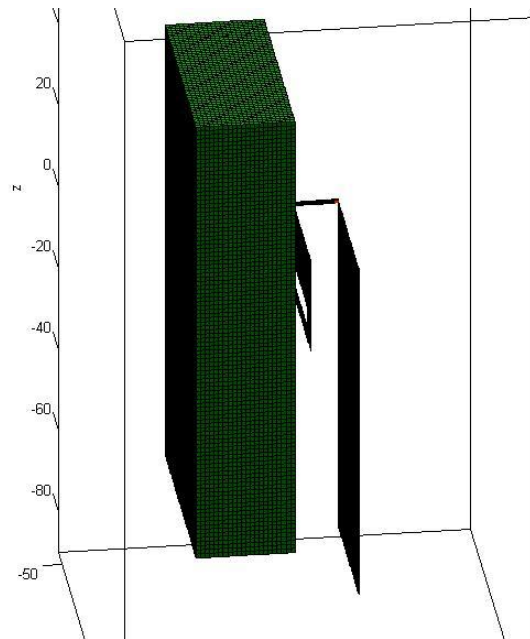


Fig. 63 The brick design of a slotted PIFA

The comparative S11 graphs:

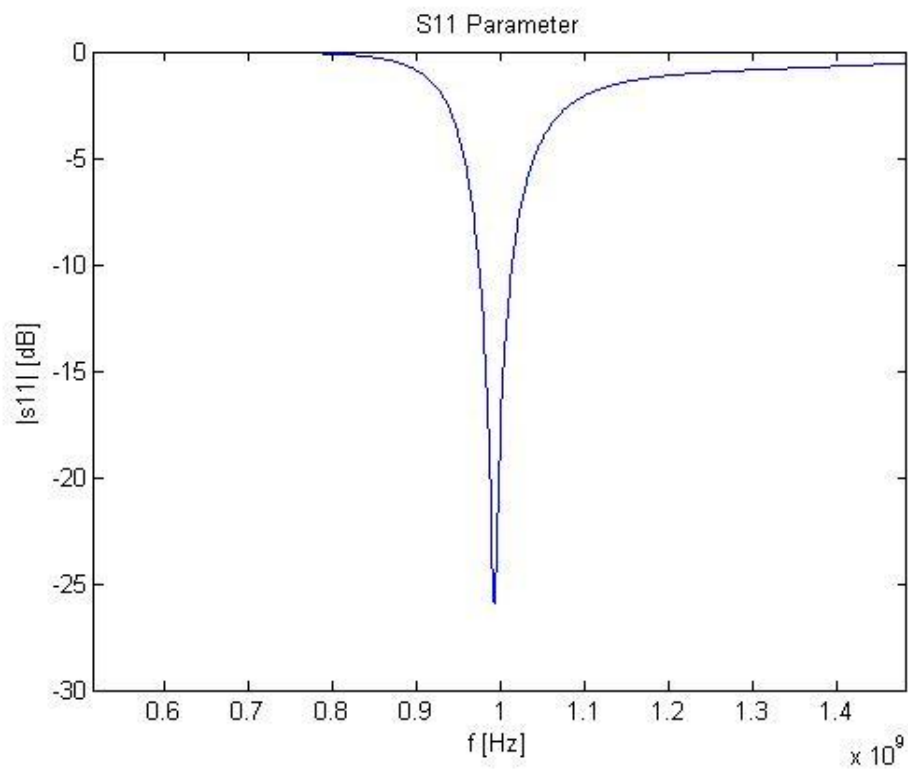


Fig. 64 S11 of a slotted PIFA in free space

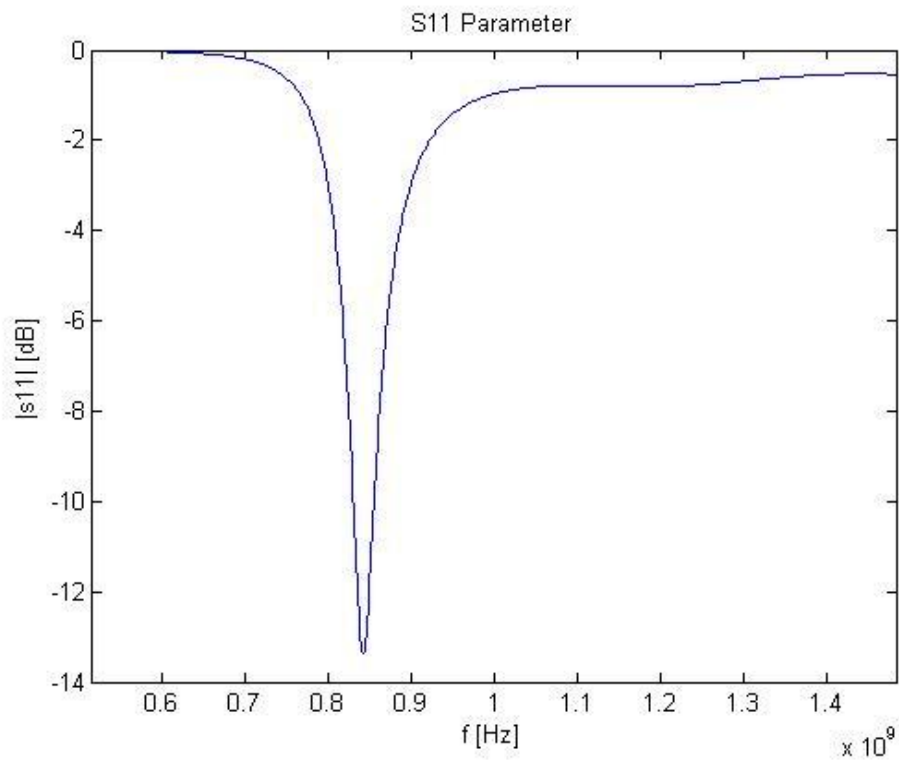


Fig. 65 Brick S11 of a slotted PIFA

Imaginary parts of the slotted PIFA:

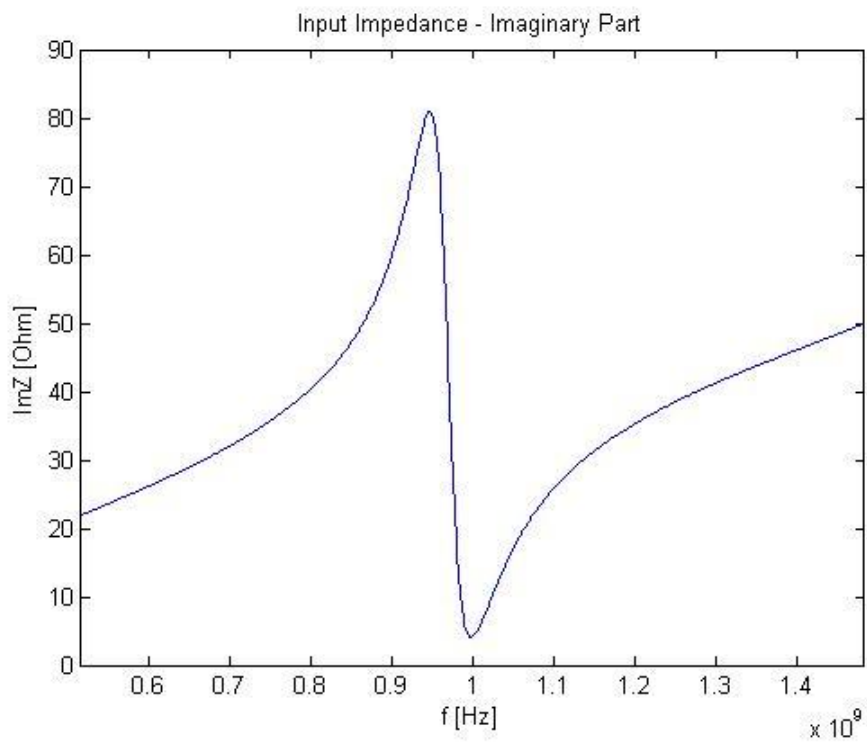


Fig. 66 Imaginary part of a free space slotted PIFA

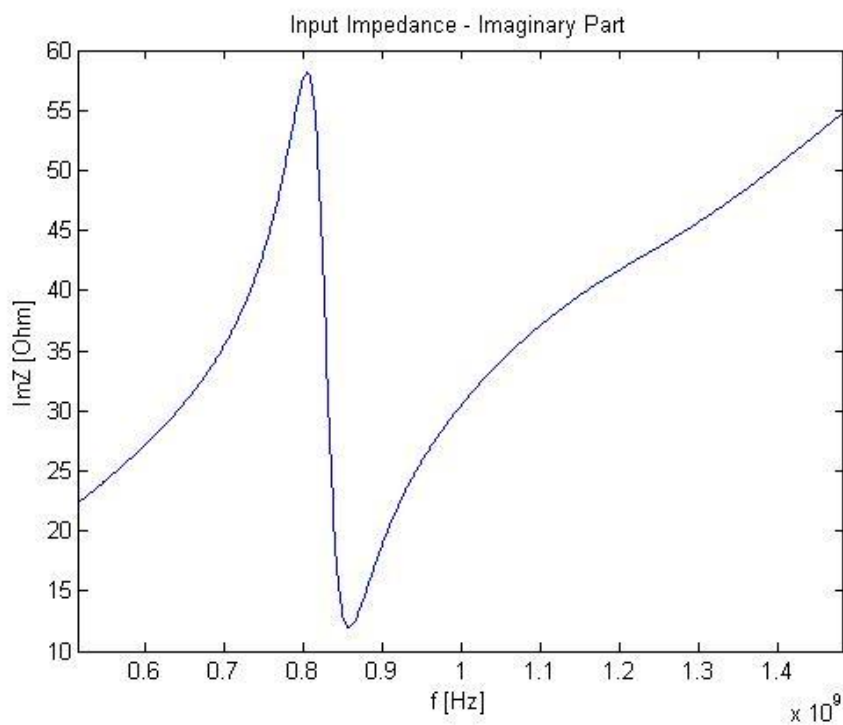


Fig. 67 Brick imaginary part of a slotted PIFA

Smith Charts:

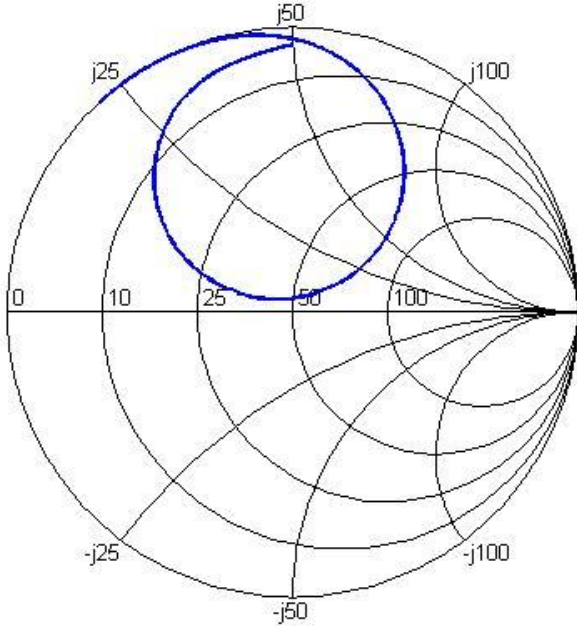


Fig. 68 Smith Chart for a free space slotted PIFA

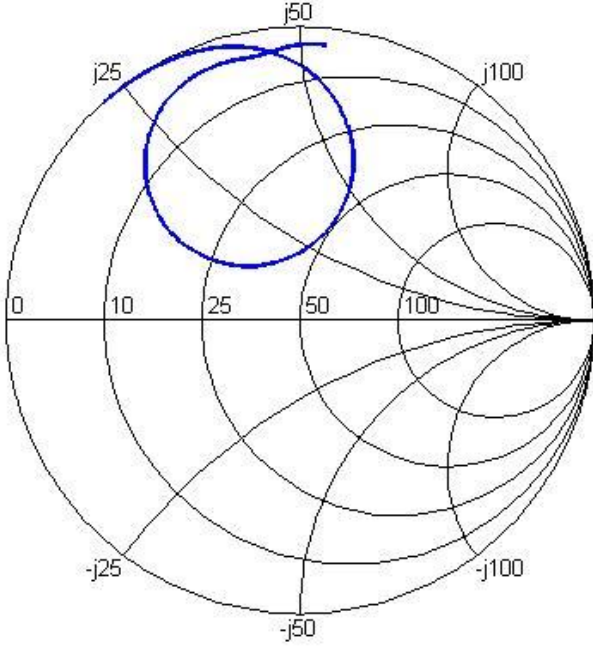


Fig. 69 Brick Smith Chart for a slotted PIFA

### Power dissipation along x:

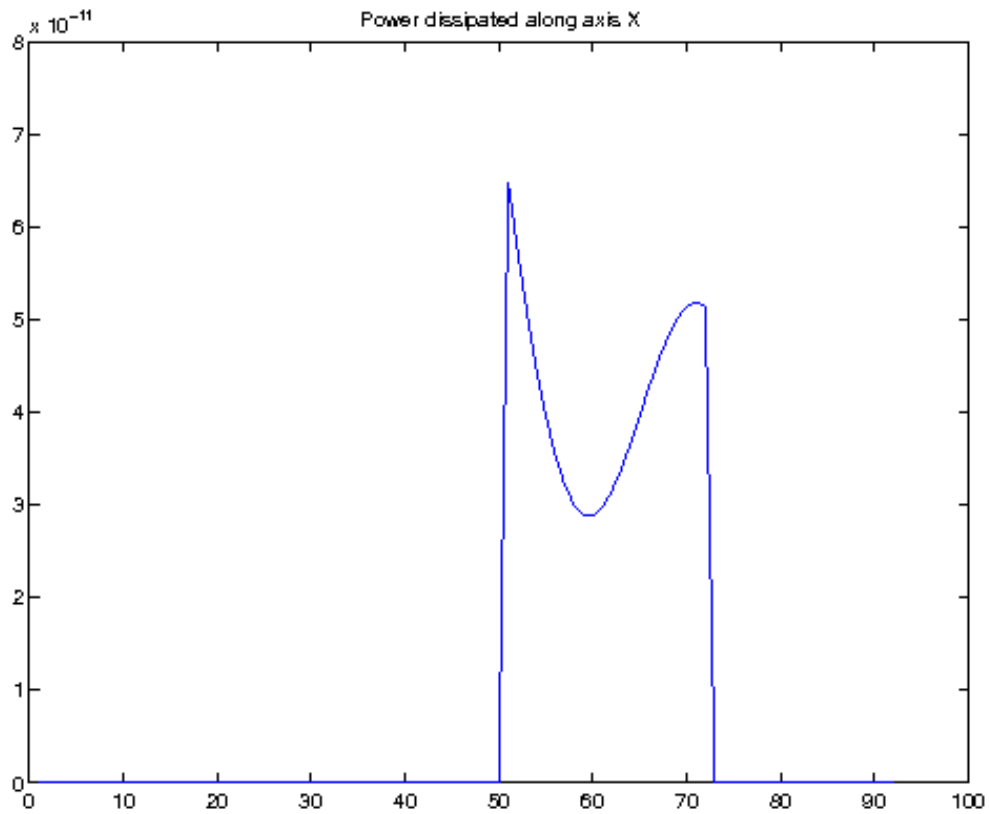


Fig. 70 Power dissipation along x for a slotted PIFA

### Numerical indicators:

- 3D Correlation coefficient	8.2940498e-01
- Total power dissipated	9.2544406e-10
- Power dissipated in the first 1.1cm	4.7393127e-10
- In percentage of total power dissipated	51.211228%
- Antenna efficiency without brick	0.98656
- Antenna efficiency with brick	0.39744

## VI – Narrowband PIFA

The actual design of the antenna:

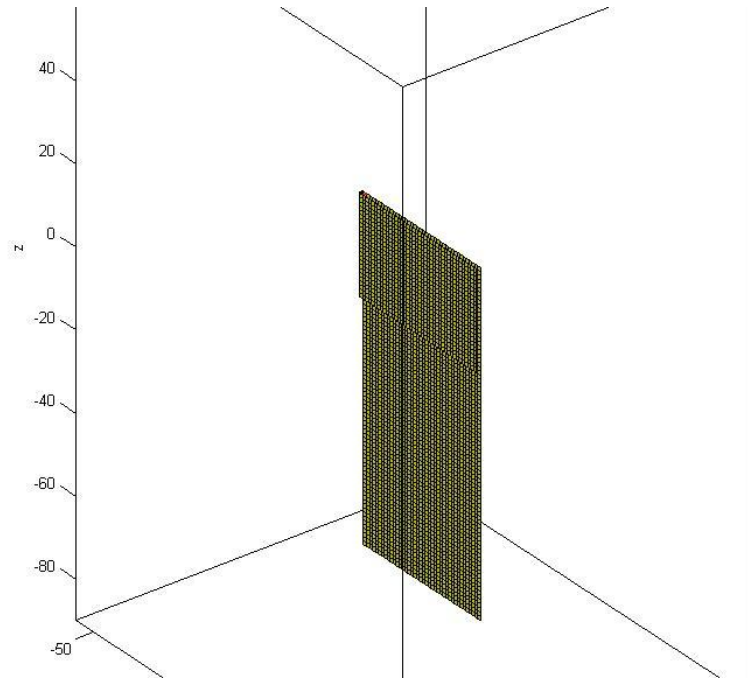


Fig. 71 The free space design of a narrowband PIFA antenna

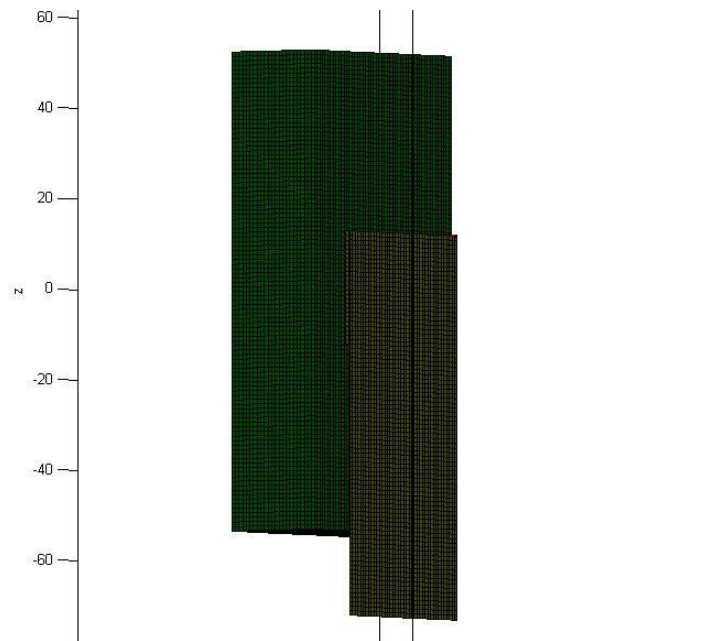


Fig. 72 The brick design of a narrowband PIFA antenna

The comparative S11 graphs:

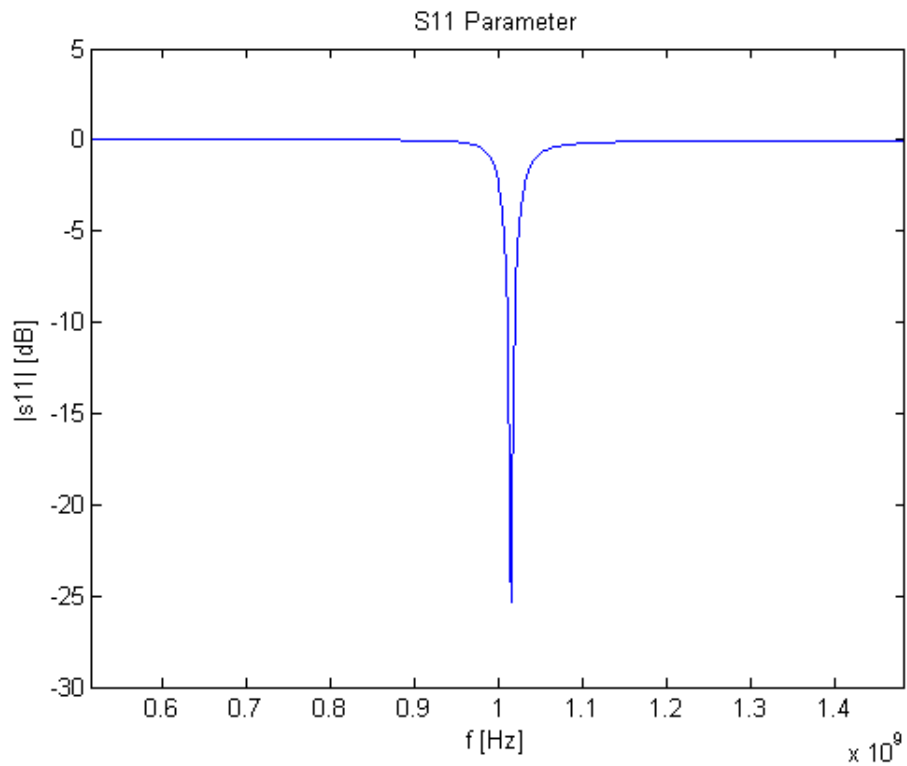


Fig. 73 S11 of a narrowband PIFA antenna in free space

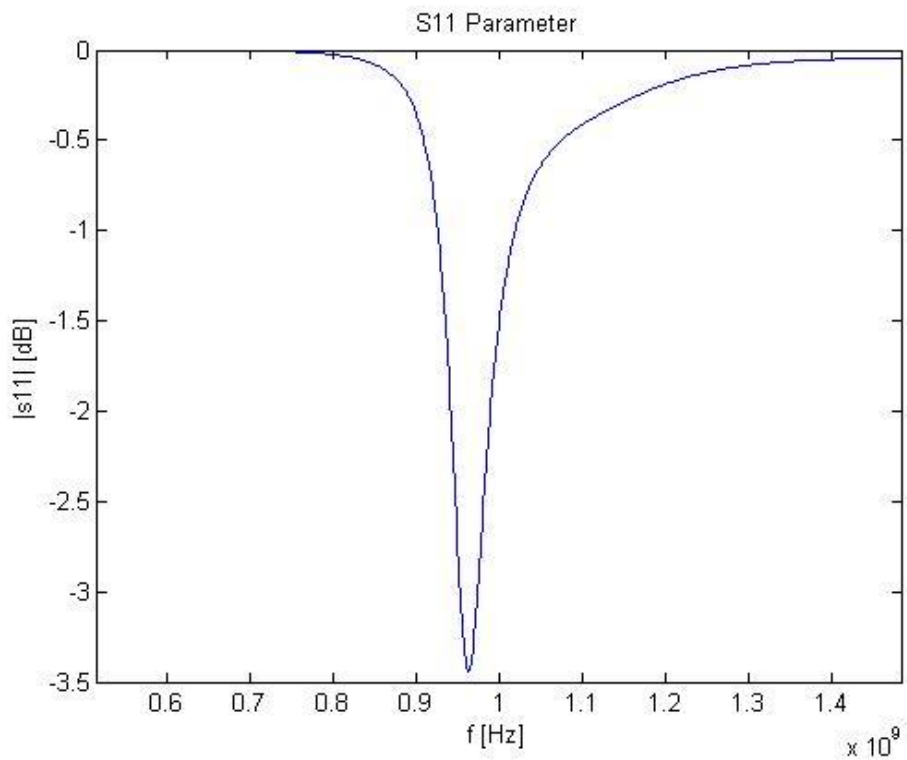


Fig. 74 Brick S11 of a narrowband PIFA antenna

Imaginary parts of the narrowband PIFA antenna:

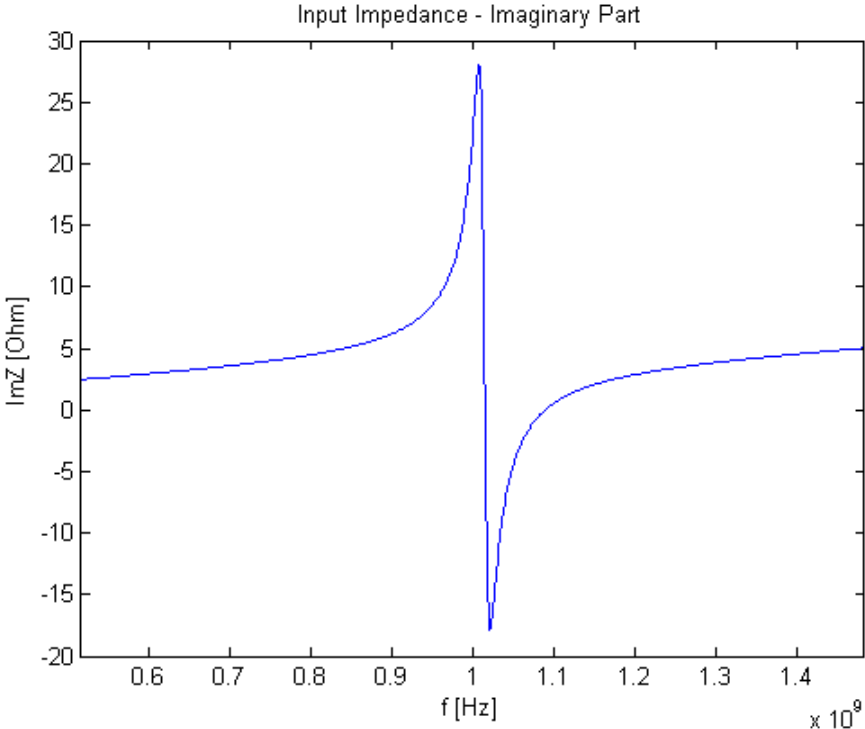


Fig. 75 Imaginary part of a free space narrowband PIFA antenna

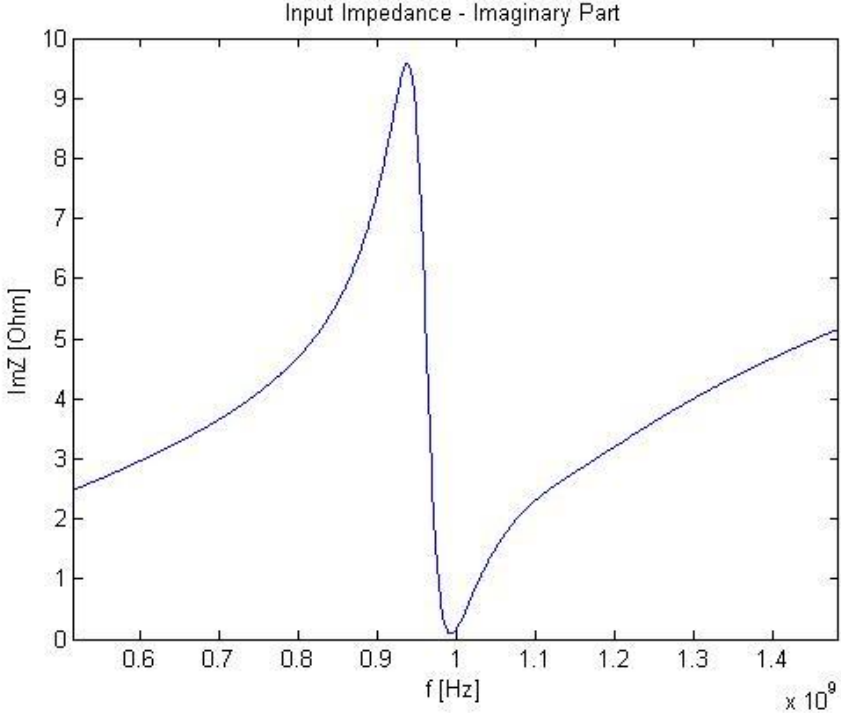


Fig. 76 Brick imaginary part of a narrowband PIFA antenna

Smith Charts:

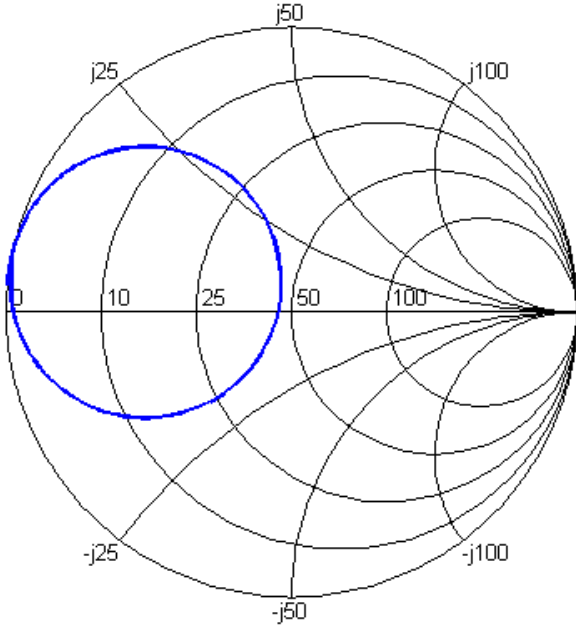


Fig. 77 Smith Chart for a free space narrowband PIFA antenna

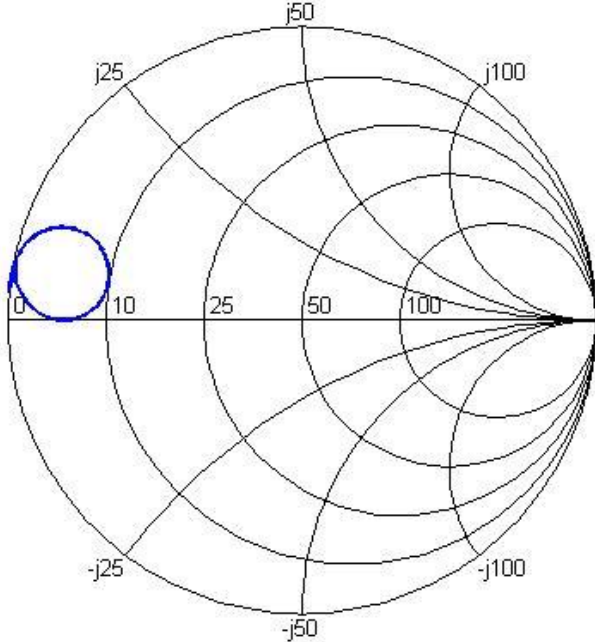


Fig. 78 Brick Smith Chart for a narrowband PIFA antenna

Power dissipation along x:

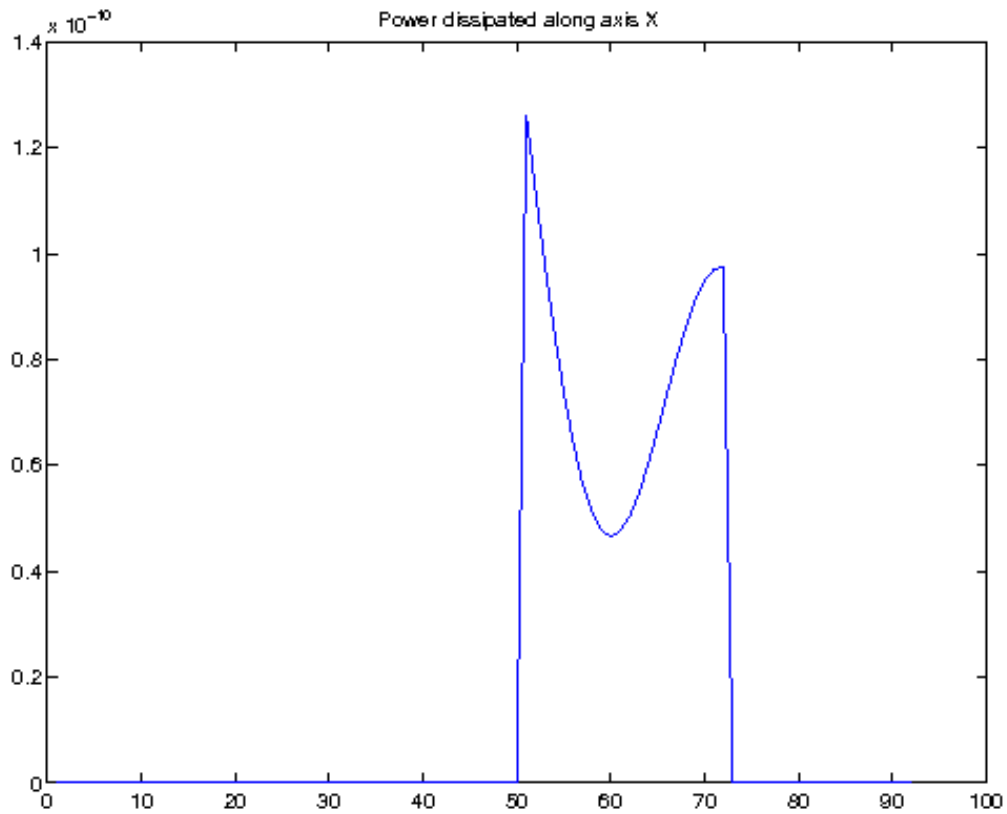


Fig. 79 Power dissipation along x for a narrowband PIFA

Numerical indicators:

- |   |               |
|---|---------------|
| - 3D Correlation coefficient              | 9.3440412e-01 |
| - Total power dissipated                  | 1.6607819e-09 |
| - Power dissipated in the first 1.1cm     | 8.5868733e-10 |
| - In percentage of total power dissipated | 51.703797%    |
| - Antenna efficiency without brick        | 0.99329       |
| - Antenna efficiency with brick           | 0.27208       |

## VII – PIFA with substrate

The actual design of the antenna:

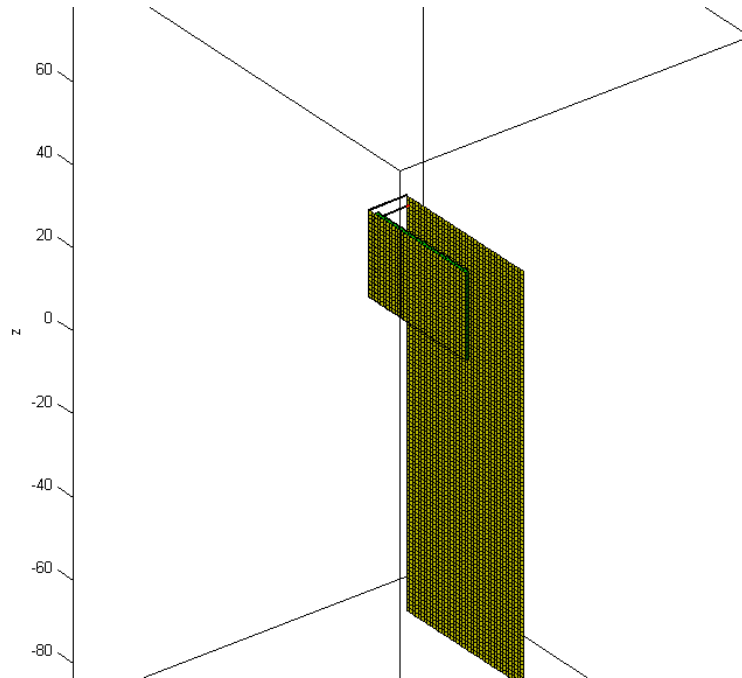


Fig. 80 The free space design of a PIFA with substrate

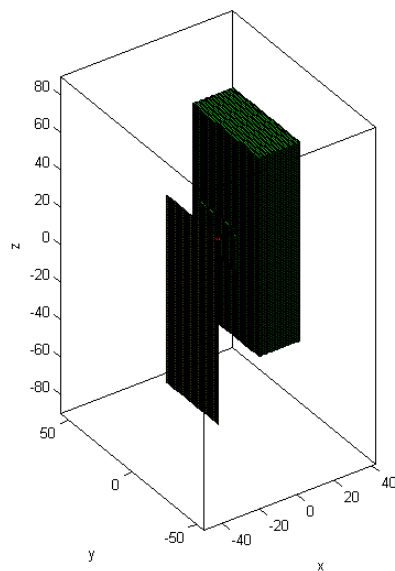


Fig. 81 The brick design of a PIFA with substrate

The comparative S11 graphs:

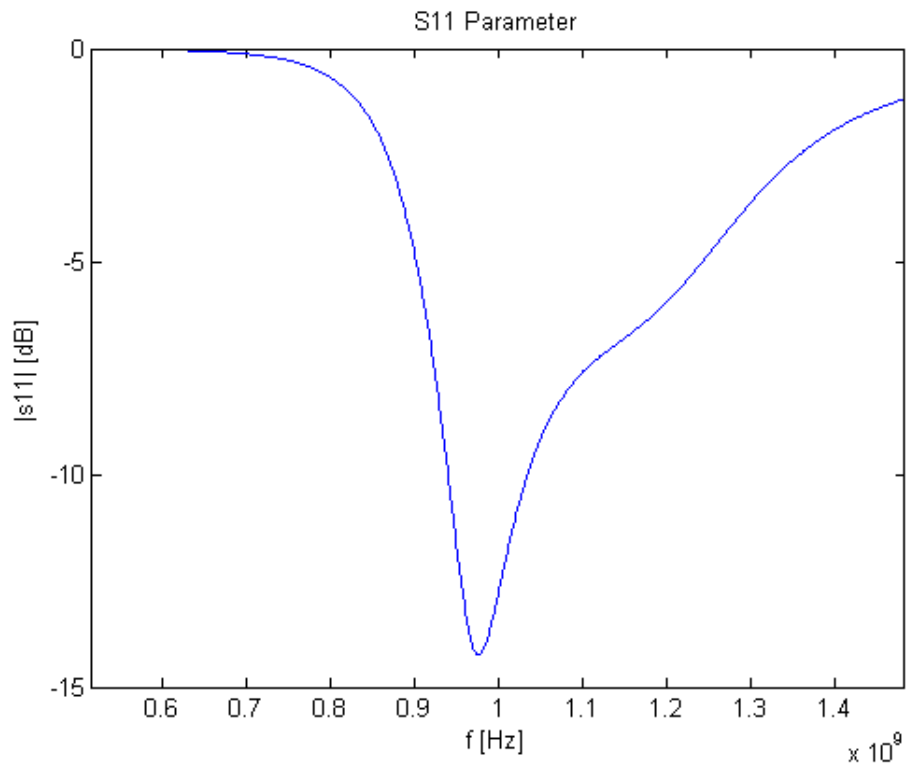


Fig. 82 S11 of a PIFA with substrate in free space

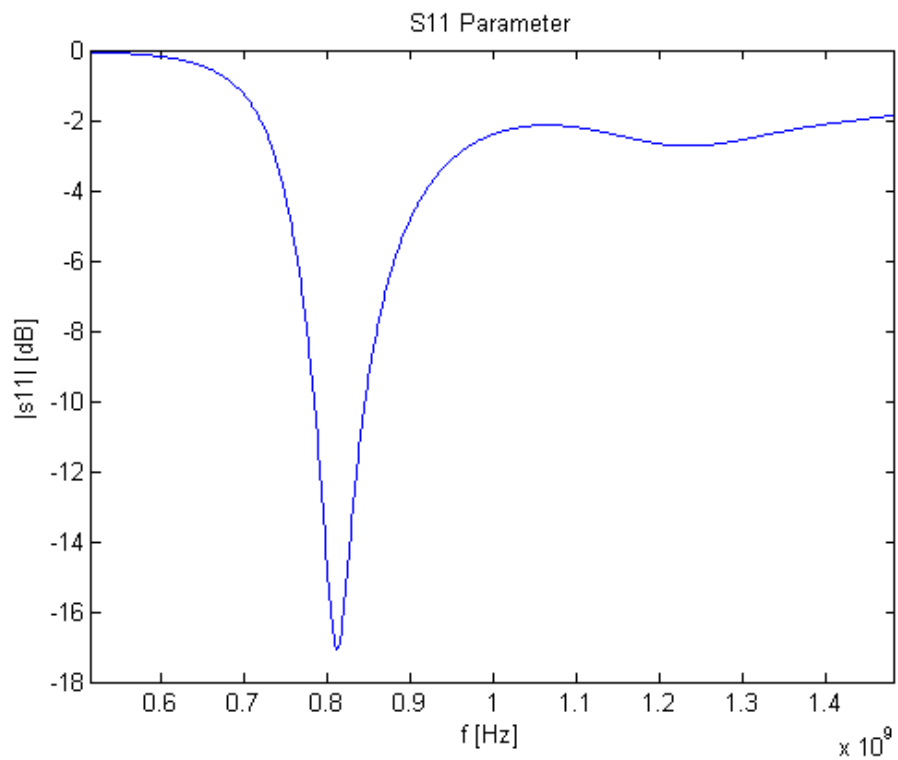


Fig. 83 Brick S11 of a PIFA with substrate

Imaginary parts of the PIFA with substrate:

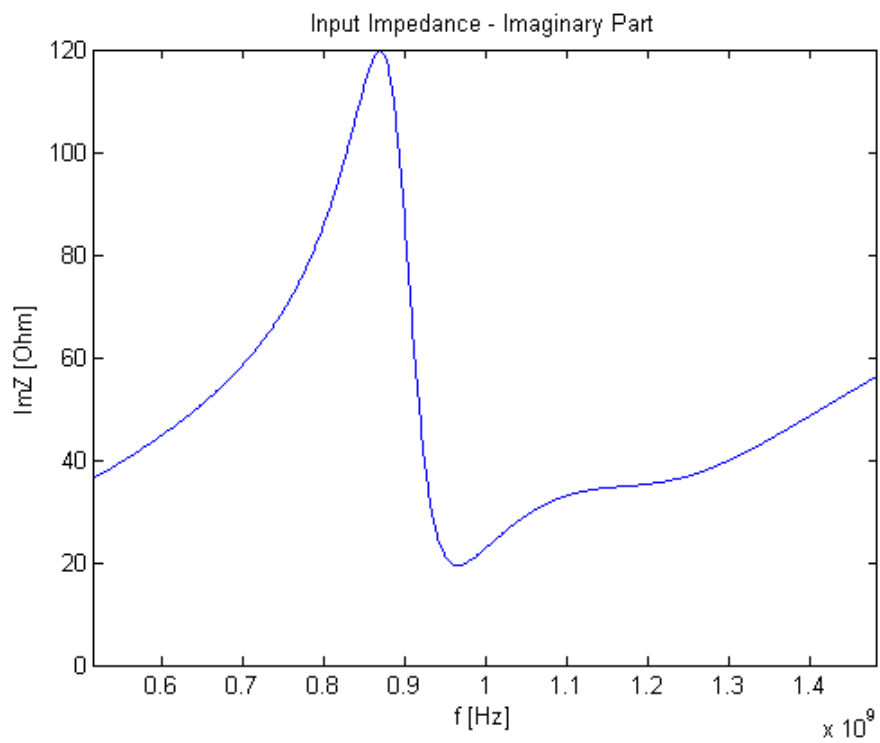


Fig. 84 Imaginary part of a free space PIFA with substrate

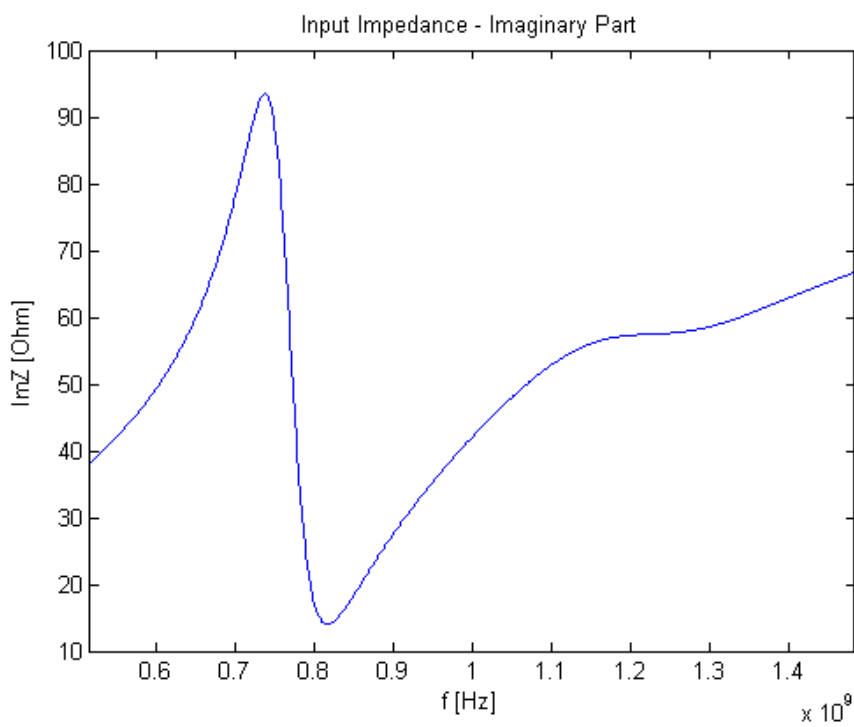


Fig. 85 Brick imaginary part of a PIFA with substrate

Smith Charts:

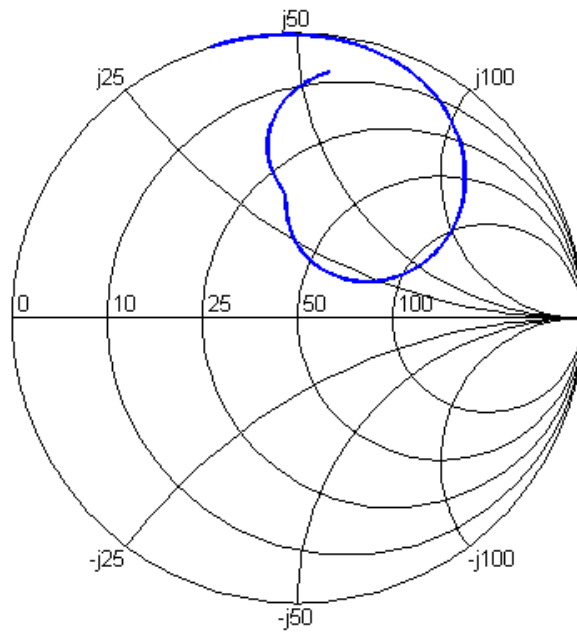


Fig. 86 Smith Chart for a free space PIFA with substrate

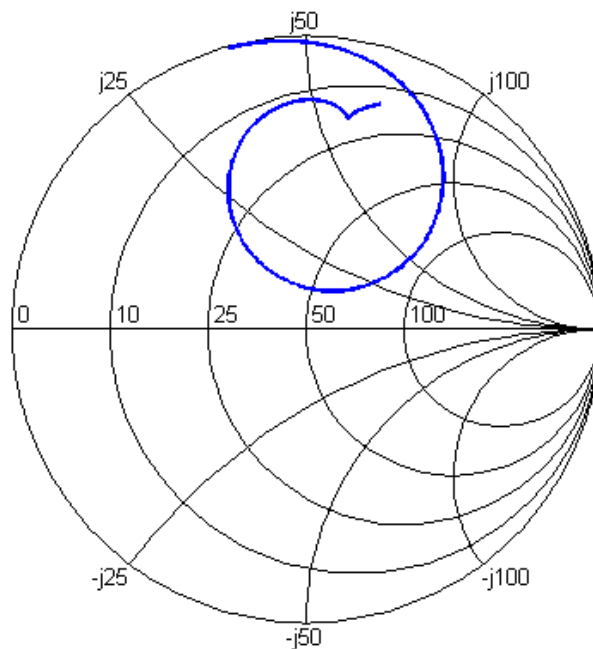


Fig. 87 Brick Smith Chart for a PIFA with substrate

Power dissipation along x:

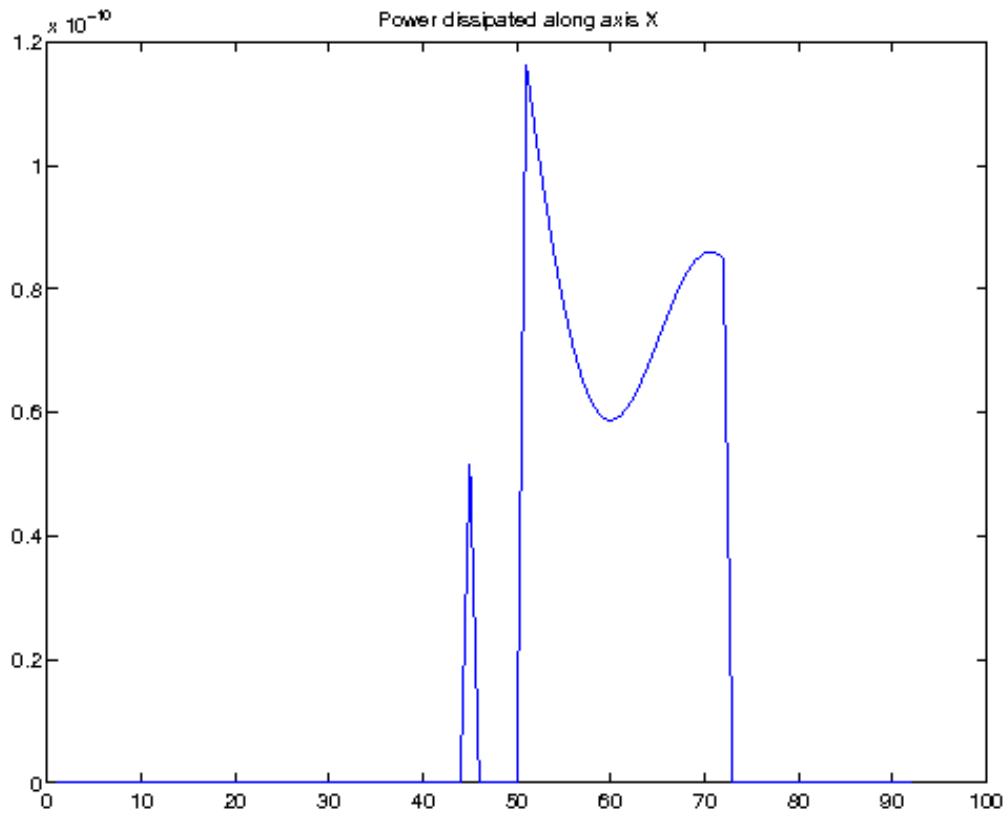


Fig. 88 Power dissipation along x for a PIFA with substrate

Numerical indicators:

- 3D Correlation coefficient	7.8212312e-01
- Total power dissipated	1.7478407e-09
- Power dissipated in the first 1.1cm	9.1430834e-10
- In percentage of total power dissipated	52.310736%
- Antenna efficiency without brick	0.95965
- Antenna efficiency with brick	0.4699

## VIII – IFA

The actual design of the antenna:

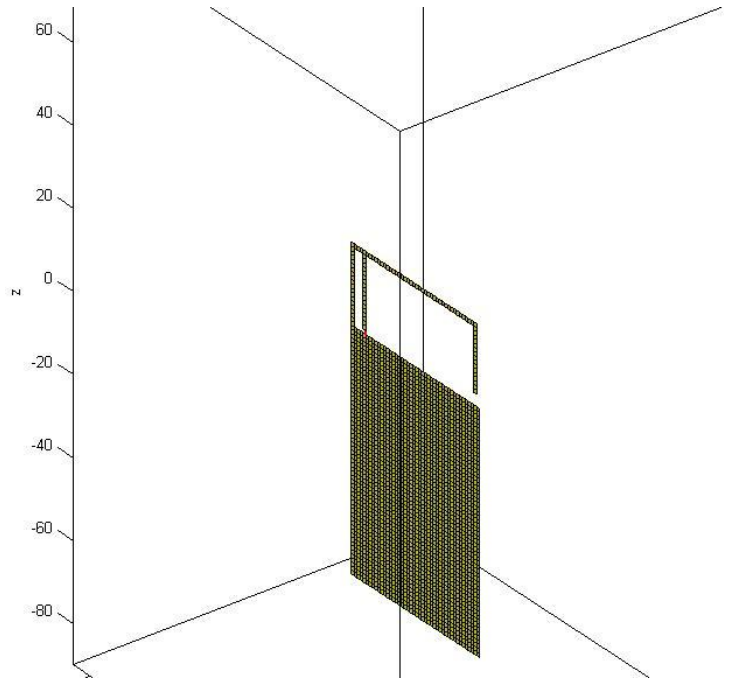


Fig. 89 The free space design of an IFA

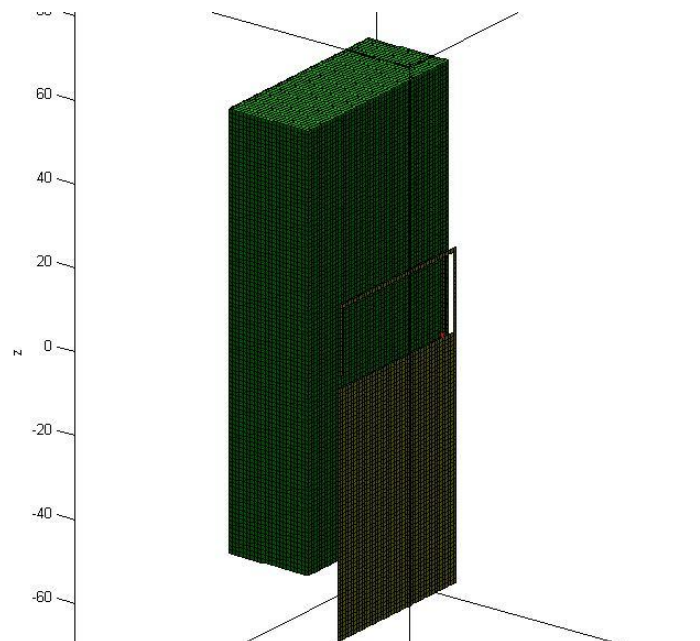


Fig. 90 The brick design of an IFA

The comparative S11 graphs:

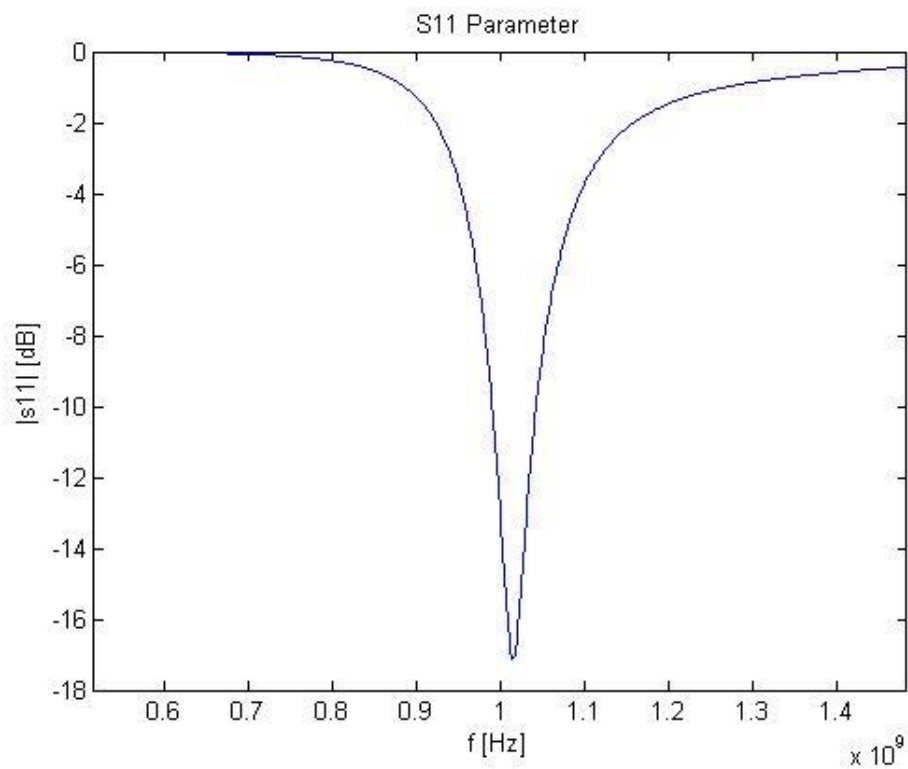


Fig. 91 S11 of an IFA in free space

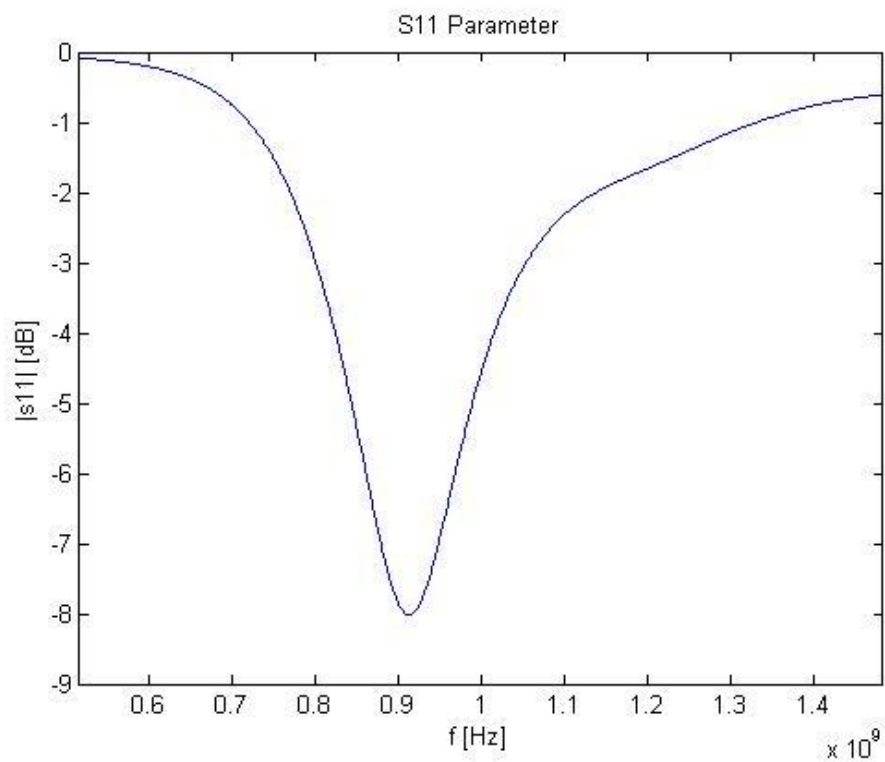


Fig. 92 Brick S11 of an IFA

Imaginary parts of the IFA:

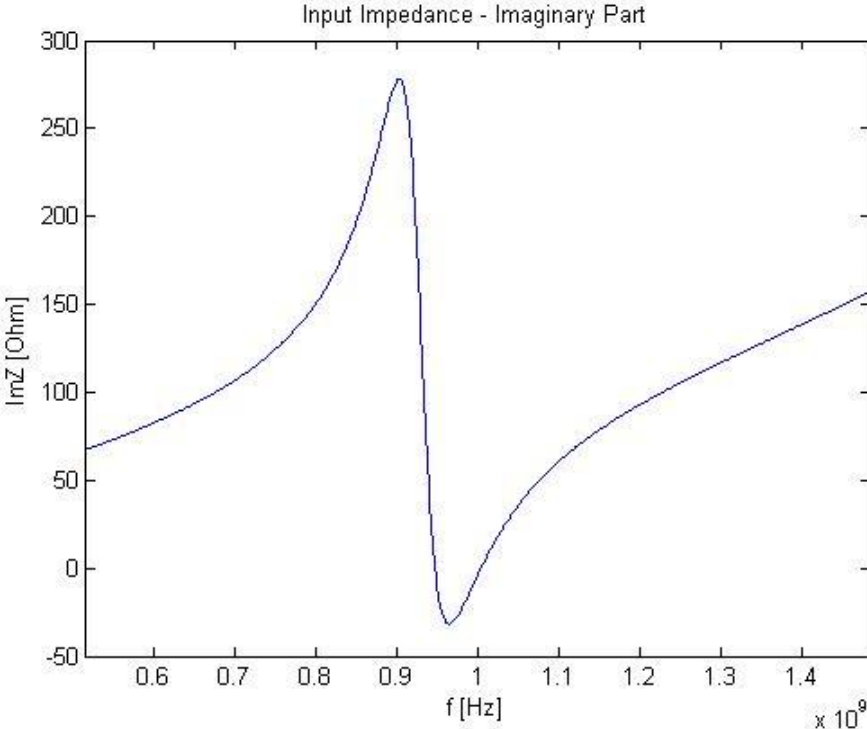


Fig. 93 Imaginary part of a free space IFA

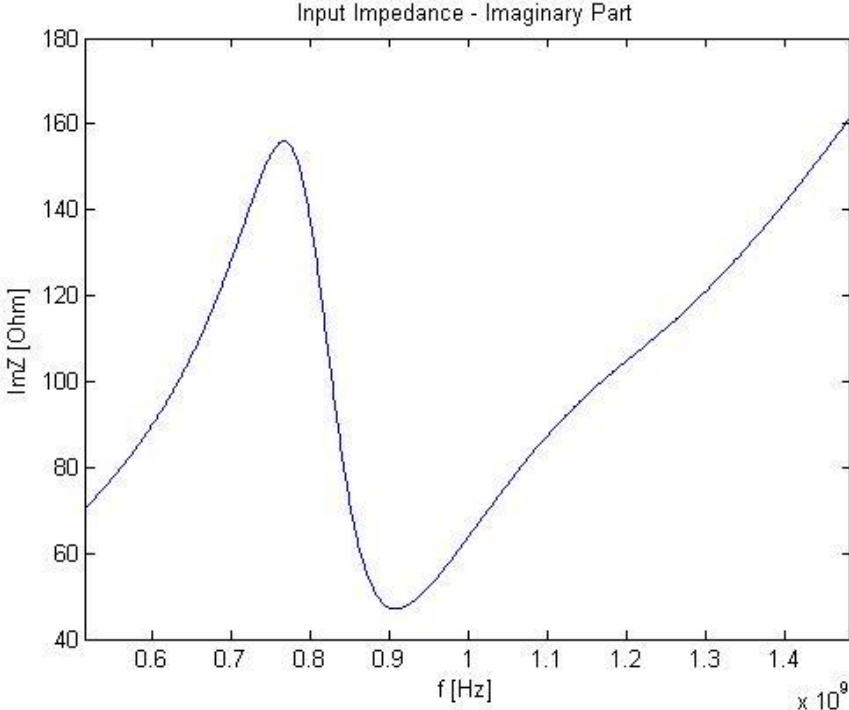


Fig. 94 Brick imaginary part of an IFA

Smith Charts:

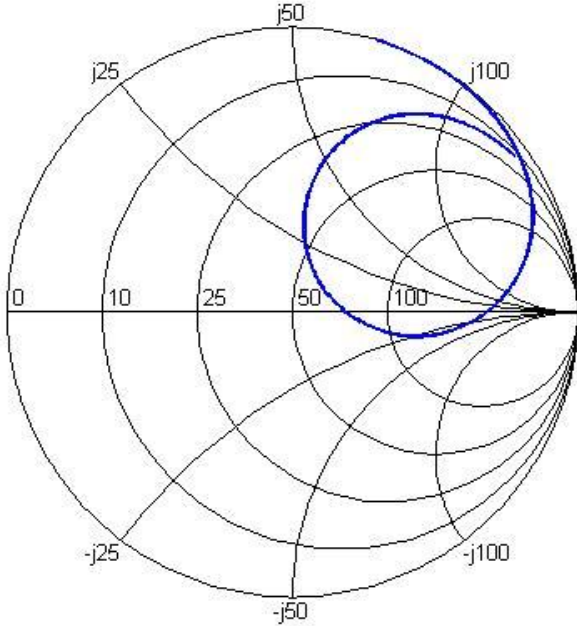


Fig. 95 Smith Chart for a free space IFA

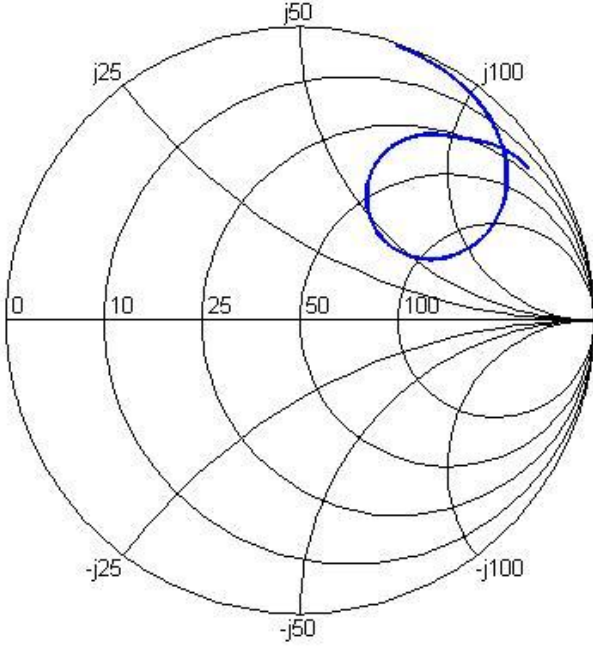


Fig. 96 Brick Smith Chart for an IFA

### Power dissipation along x:

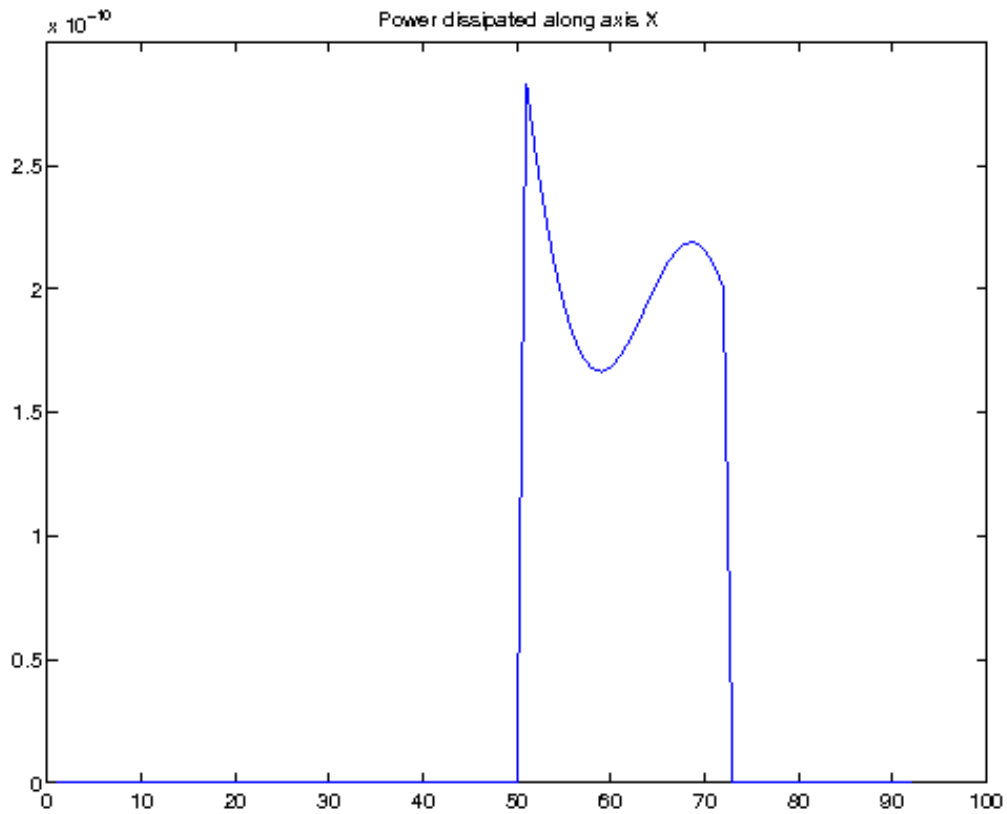


Fig. 97 Power dissipation along x for an IFA

### Numerical indicators:

- 3D Correlation coefficient	8.9221447e-01
- Total power dissipated	4.4539315e-09
- Power dissipated in the first 1.1cm	2.3802706e-09
- In percentage of total power dissipated	53.442012%
- Antenna efficiency without brick	0.9834
- Antenna efficiency with brick	0.12459

# IX – Loop

The actual design of the antenna:

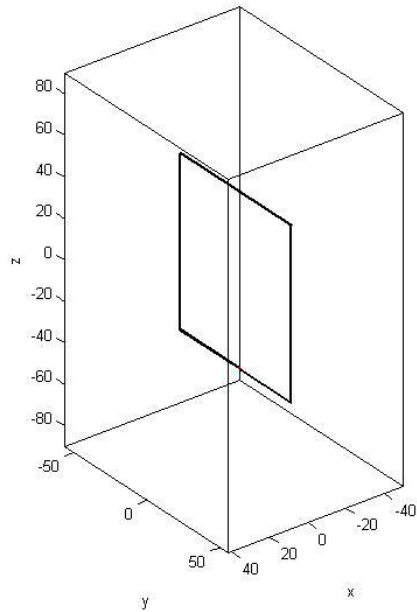


Fig. 98 The free space design of a loop

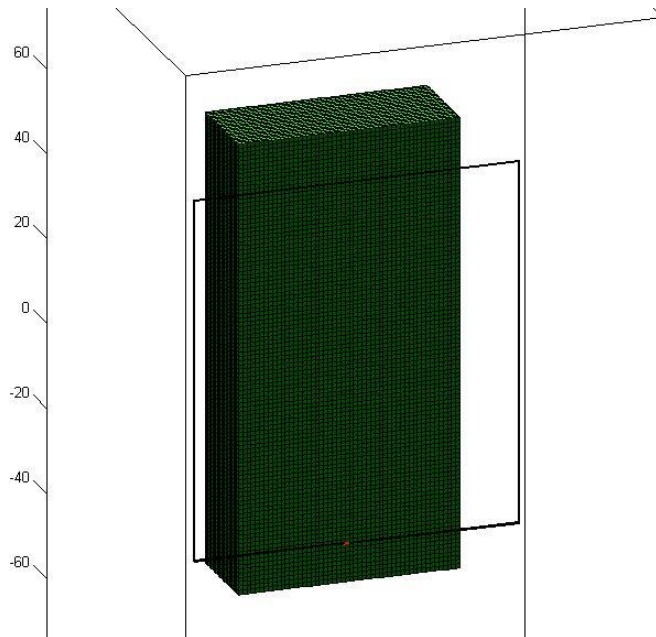


Fig. 99 The brick design of a loop

The comparative S11 graphs:

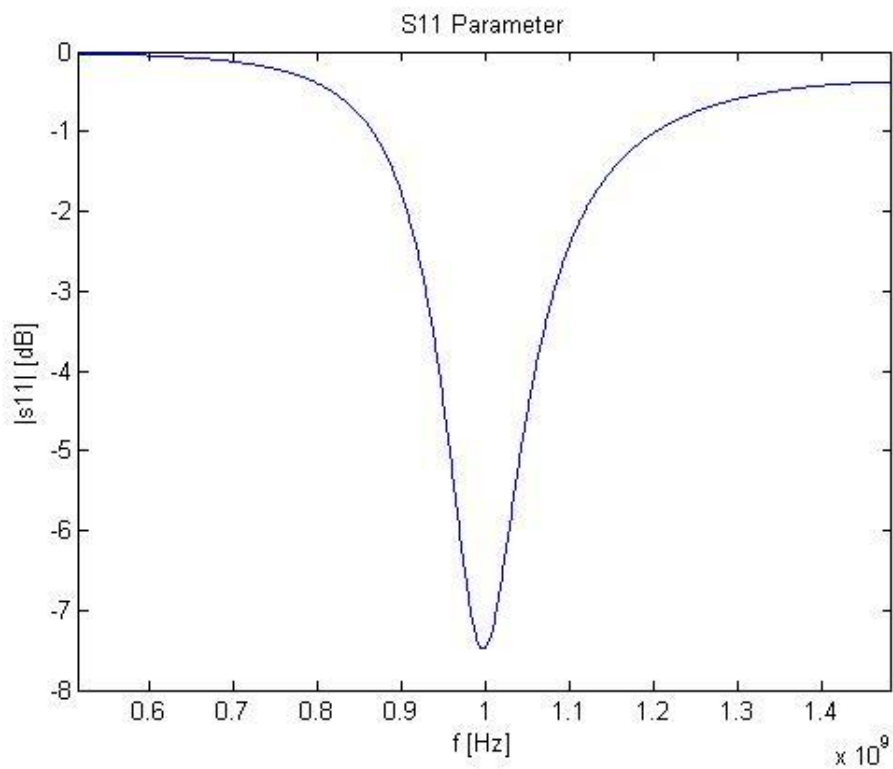


Fig. 100 S11 of a loop in free space

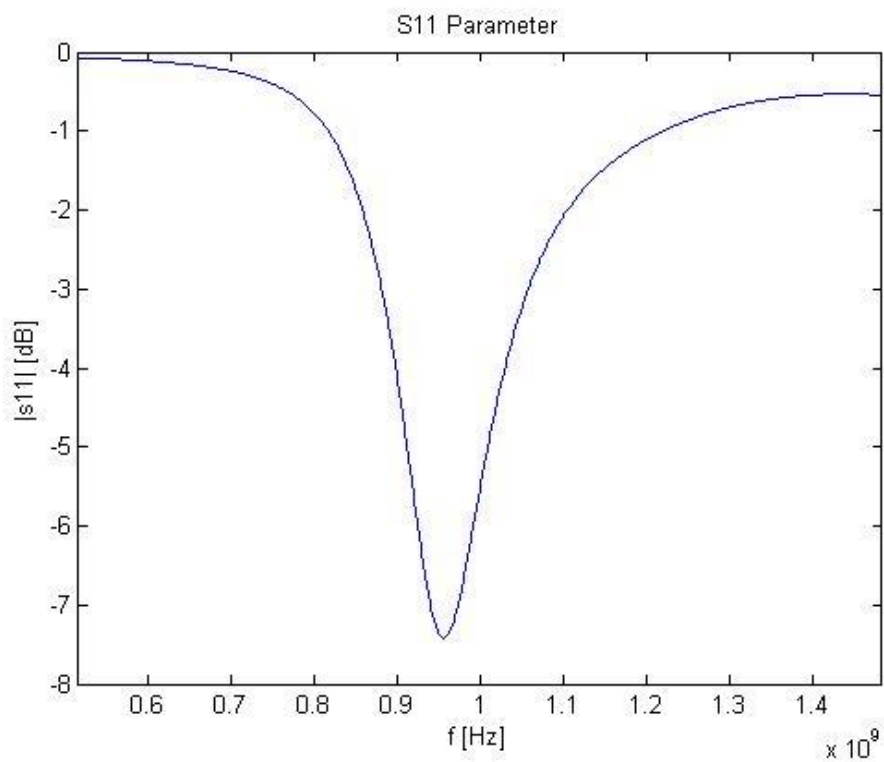


Fig. 101 Brick S11 of a loop

Imaginary parts of the loop:

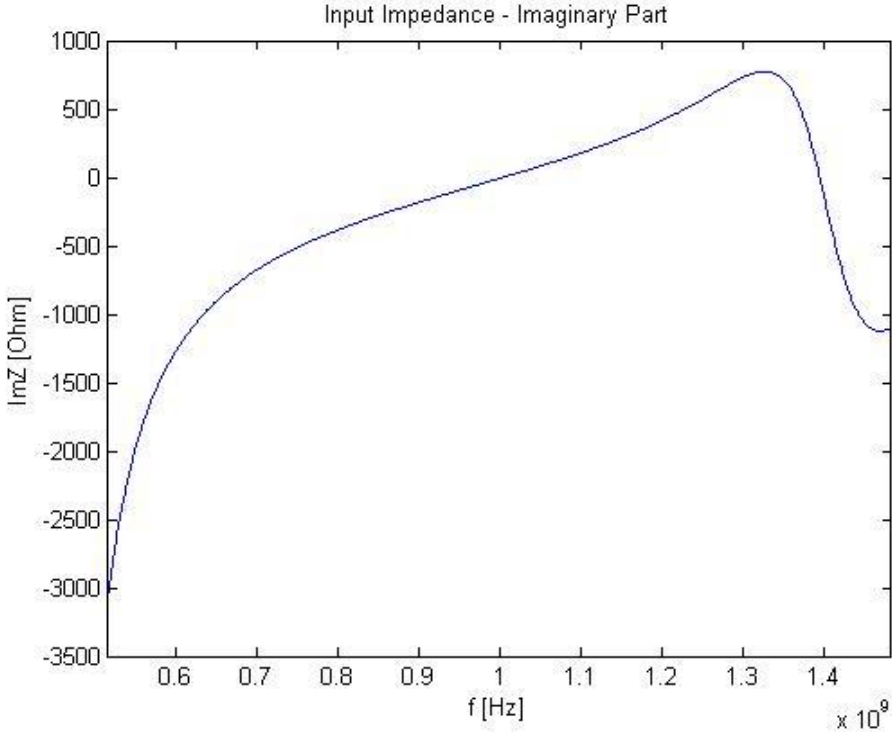


Fig. 102 Imaginary part of a free space loop

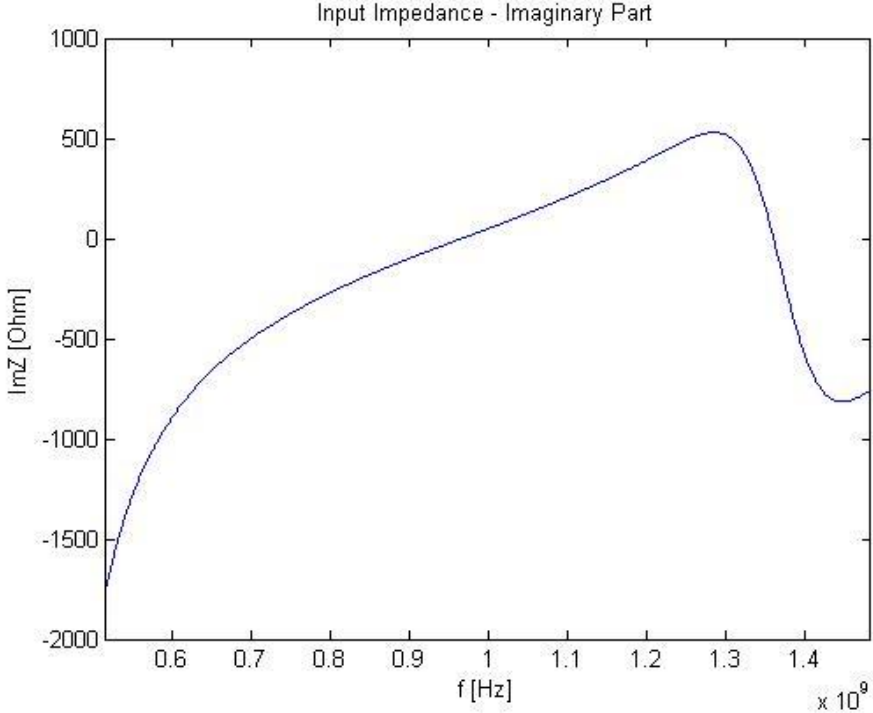


Fig. 103 Brick imaginary part of a loop

Smith Charts:

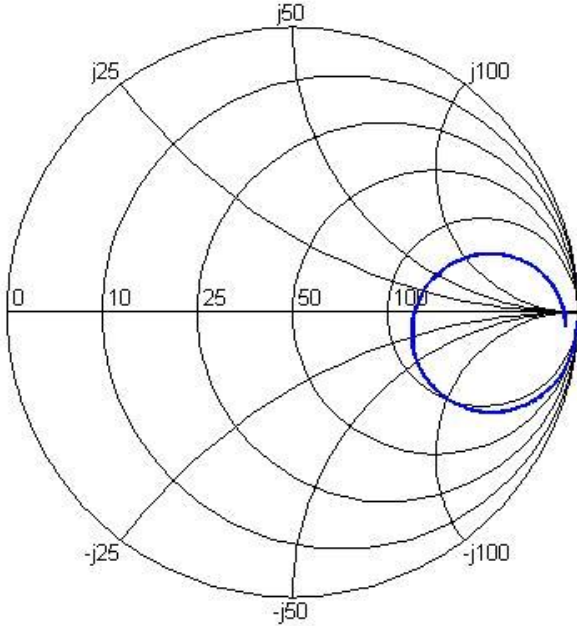


Fig. 104 Smith Chart for a free space loop

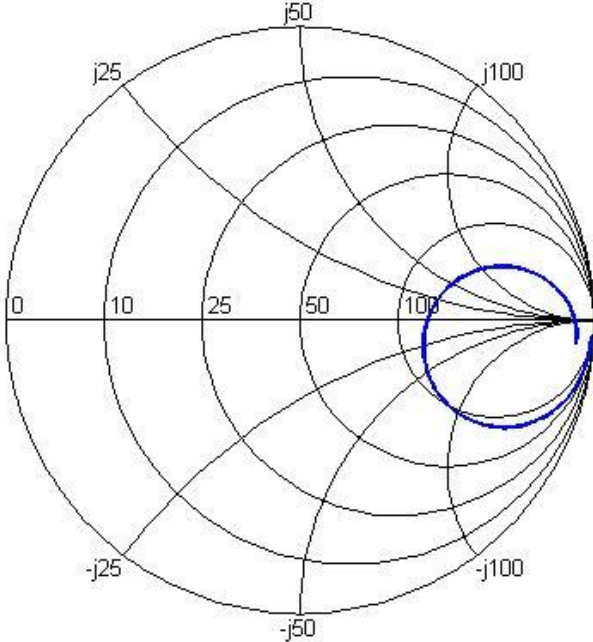


Fig. 105 Brick Smith Chart for a loop

Power dissipation along x:

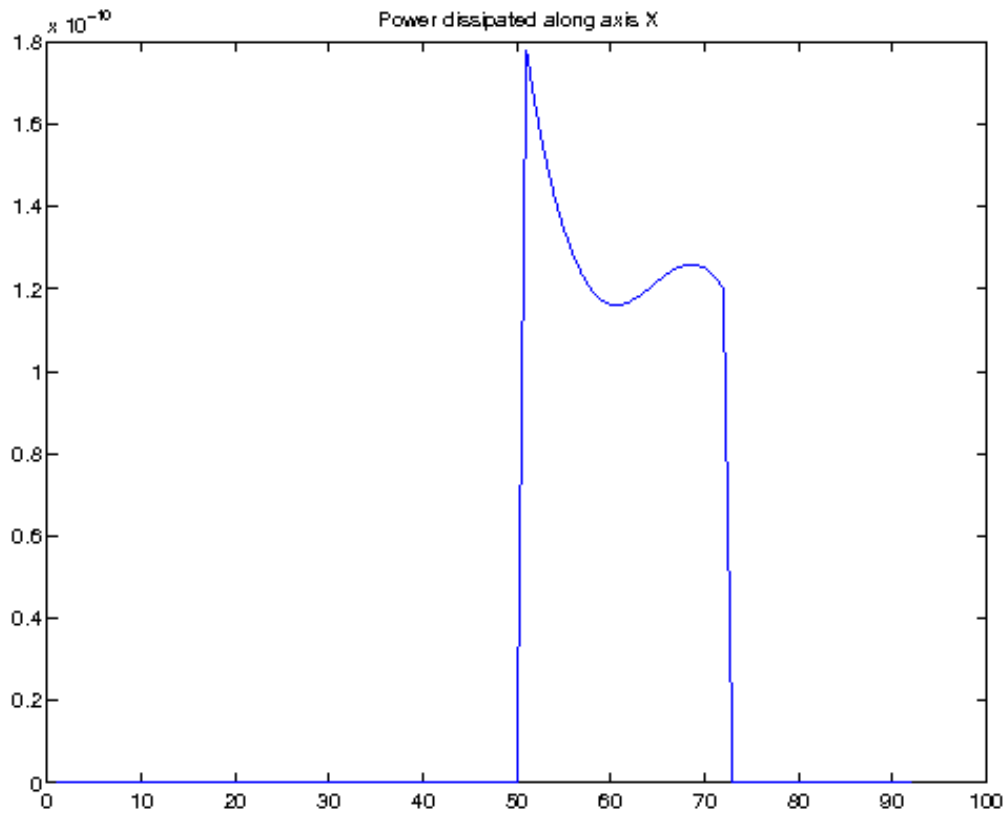


Fig. 106 Power dissipation along x for a loop antenna

Numerical indicators:

- 3D Correlation coefficient	9.7498478e-01
- Total power dissipated	2.8384263e-09
- Power dissipated in the first 1.1cm	1.6093313e-09
- In percentage of total power dissipated	56.698011%
- Antenna efficiency without brick	0.92281
- Antenna efficiency with brick	0.45792

# X – Folded loop

The actual design of the antenna:

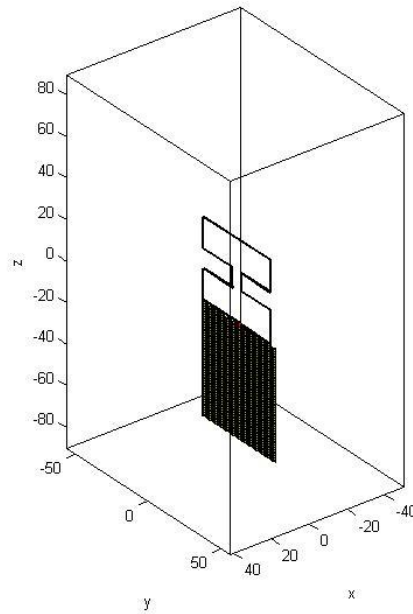


Fig. 107 The free space design of a folded loop

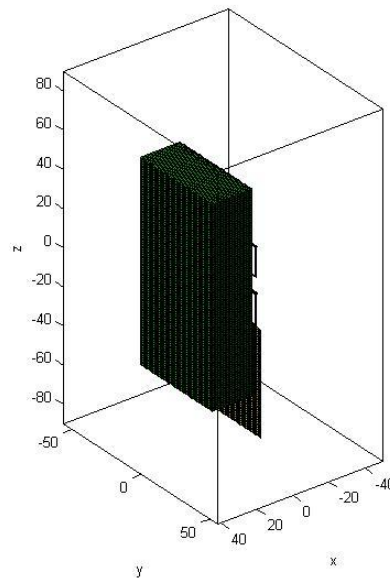


Fig. 108 The brick design of a folded loop

The comparative S11 graphs:

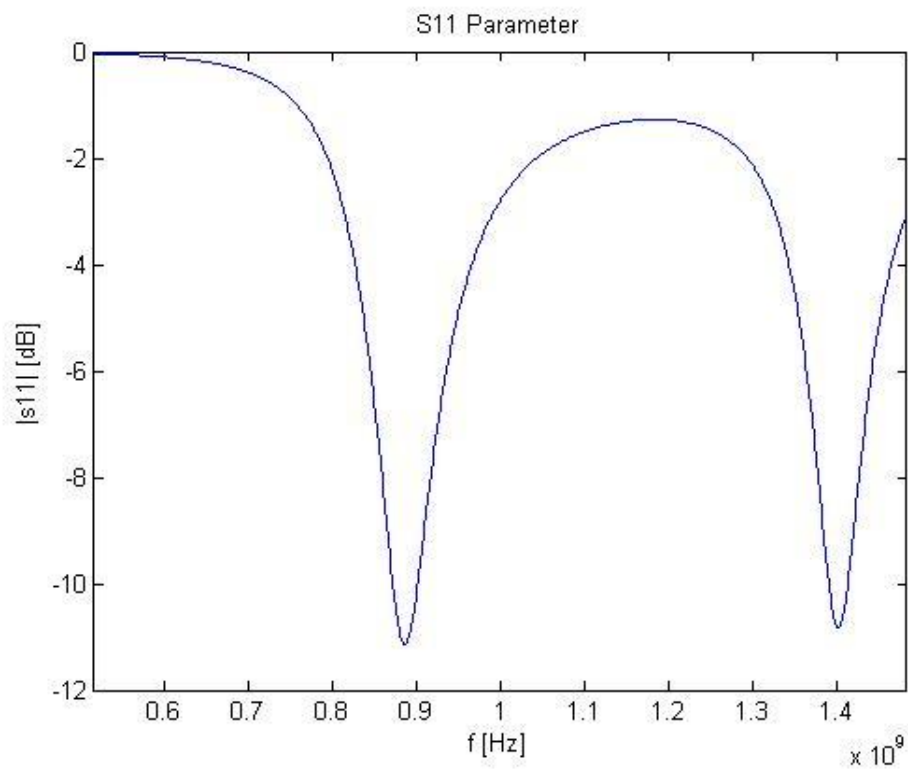


Fig. 109 S11 of a folded loop in free space

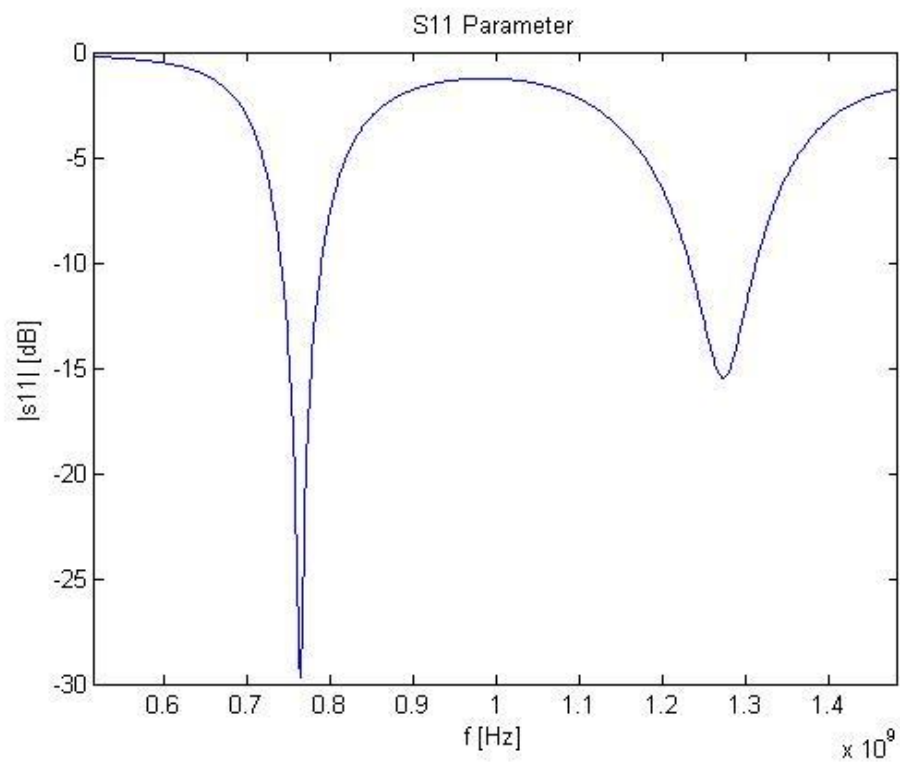


Fig. 110 Brick S11 of a folded loop

Imaginary parts of the folded loop:

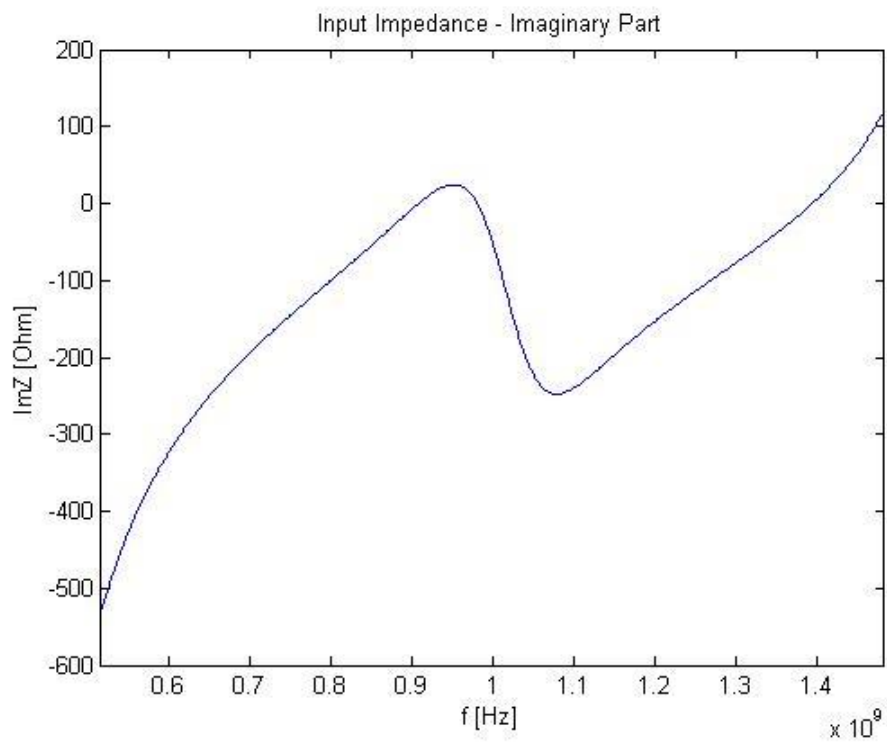


Fig. 111 Imaginary part of a free space folded loop

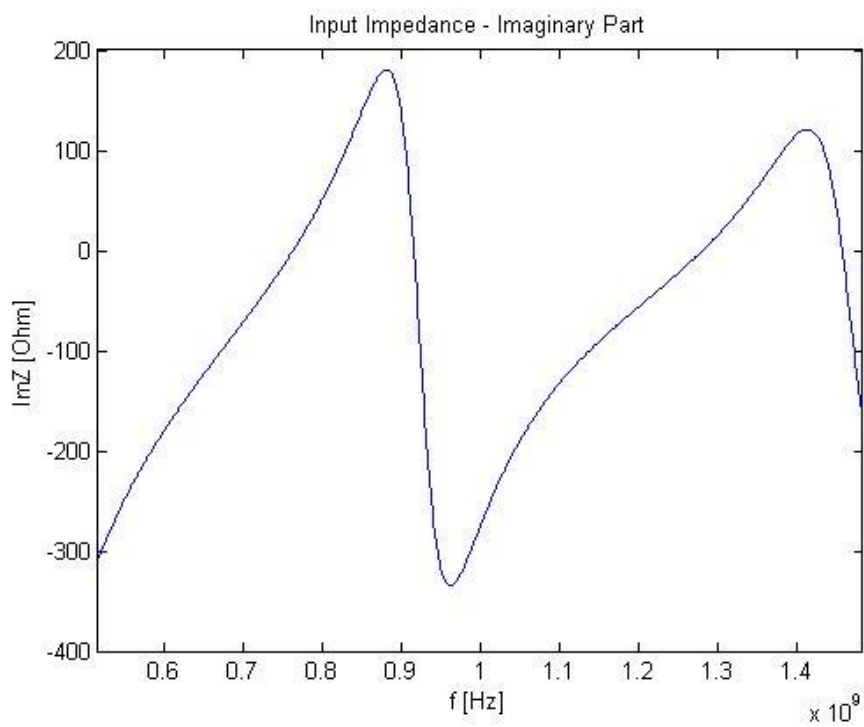


Fig. 112 Brick imaginary part of a folded loop

Smith Charts:

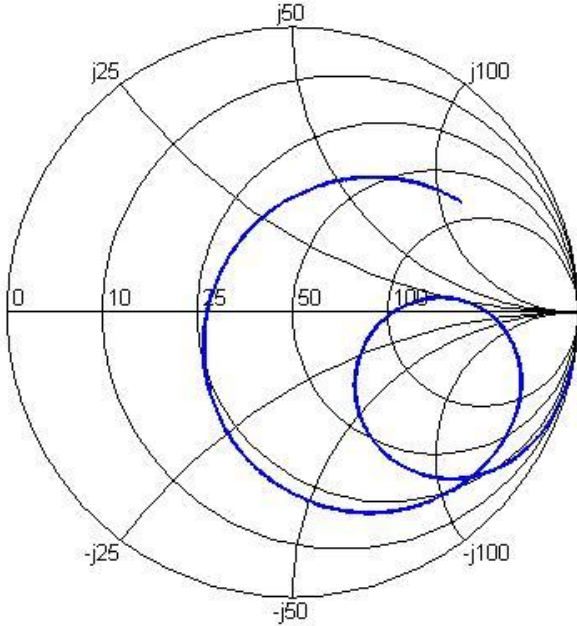


Fig. 113 Smith Chart for a free space folded loop

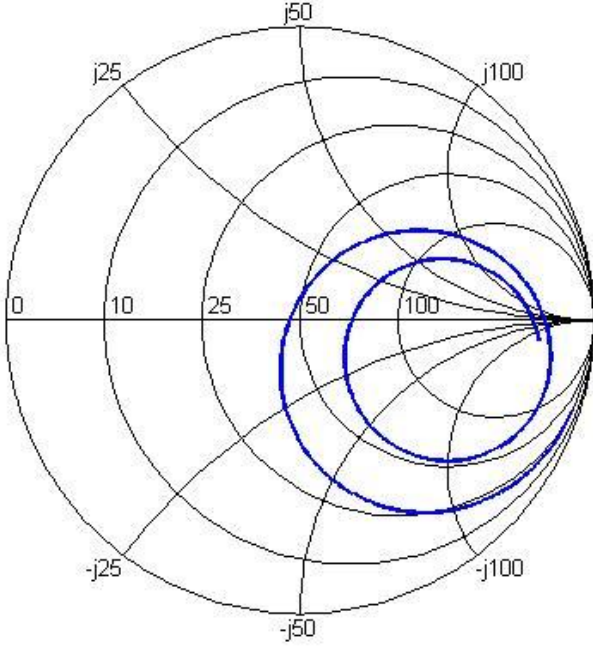


Fig. 114 Brick Smith Chart for a folded loop

Power dissipation along x:

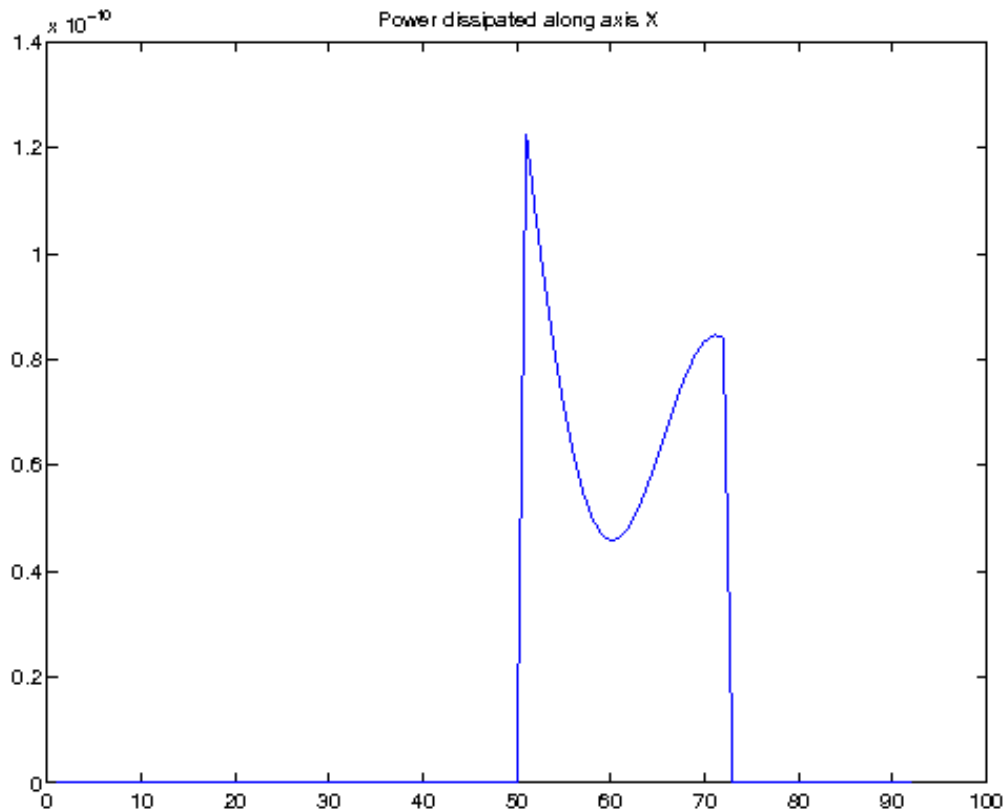


Fig. 115 Power dissipation along x for a folded loop antenna

Numerical indicators:

- 3D Correlation coefficient	8.5352060e-01
- Total power dissipated	1.5518543e-09
- Power dissipated in the first 1.1cm	8.3166922e-10
- In percentage of total power dissipated	53.591967%
- Antenna efficiency without brick	0.99661
- Antenna efficiency with brick	0.21347

# CHAPTER FIVE: PARAMETERISATION AND ROBUSTNESS CRITERION

In this chapter, we will present the results of our different calculations and the antenna ranking in term of robustness established from them.

## I – Percentage of power dissipated

Using a Matlab script, we have determined the quantity of power which has been dissipated in the “test brick”. We have then made a ratio of this quantity over the input power to classify the antennas regarding the fact that they lose the less power as possible inside the brick.

Here is a sum-up table of the results:

	Dissipated power (W)	Input Power (W)	Dissipated power (%)
<b>Loop</b>	2,84E-09	5,63E-09	50,38%
<b>PIFA</b>	1,93E-09	3,73E-09	51,63%
<b>PIFA with substrate</b>	1,75E-09	3,33E-09	52,43%
<b>Slotted PIFA</b>	9,25E-10	1,57E-09	58,80%
<b>Dipole</b>	4,83E-09	7,18E-09	67,21%
<b>Monopole</b>	5,21E-09	7,56E-09	68,84%
<b>Narrowband PIFA</b>	1,66E-09	2,29E-09	72,51%
<b>Folded loop</b>	1,55E-09	1,97E-09	78,59%
<b>IFA</b>	4,45E-09	5,09E-09	87,46%

Table 6 Power dissipated for the different antennas

According to this method, the best antenna is the loop antenna.

## II – 3D Correlation of E-fields

This method consists of a normalized cross correlation in three dimensions between the electric fields of the simulation of the antenna in free space and the electric fields obtained from the simulation of the antenna with the test brick. This way, we measure how much the fields are altered by the brick.

We have based the Matlab script on the function "normxcorr3" developed by Daniel Eaton, initially made for some medical imaging purposes and which is derived from the Matlab "normxcorr2" function.

The following table sums up the results obtained:

	<b>3D-Correlation</b>
<b>Loop</b>	97,50%
<b>Dipole</b>	93,82%
<b>Narrowband PIFA</b>	93,44%
<b>IFA</b>	89,22%
<b>Monopole</b>	88,78%
<b>Folded loop</b>	85,35%
<b>Slotted PIFA</b>	82,94%
<b>PIFA with substrate</b>	78,21%
<b>PIFA</b>	77,95%

Table 7 3D-correlation coefficients

According to this method, the antenna which produces electric fields the least affected by the brick is the loop antenna.

## III – General shape evaluation

In order to classify the antenna based on the graphical representation of the S11 parameters, we firstly decided to make a cross correlation between the data of the s11 obtained in free space and the ones from the s11 obtained with the test brick.

The results we have obtained are listed on the following table:

	Cross-correlation
Slotted PIFA	0,996
Narrowband PIFA	0,987
Monopole	0,978
Folded loop	0,966
Loop	0,947
Dipole	0,658
PIFA	0,521
PIFA with substrate	-0,266
IFA	-0,464

Table 8 Cross-correlation coefficients of S11 curves

Unfortunately, these results didn't appear to be really accurate. This is why we have decided to proceed to a visual comparison of the different graphs and then establish a ranking based on the impact on the shape.

The following figures represent the comparison of the S11 in free space and with the brick for every antenna:

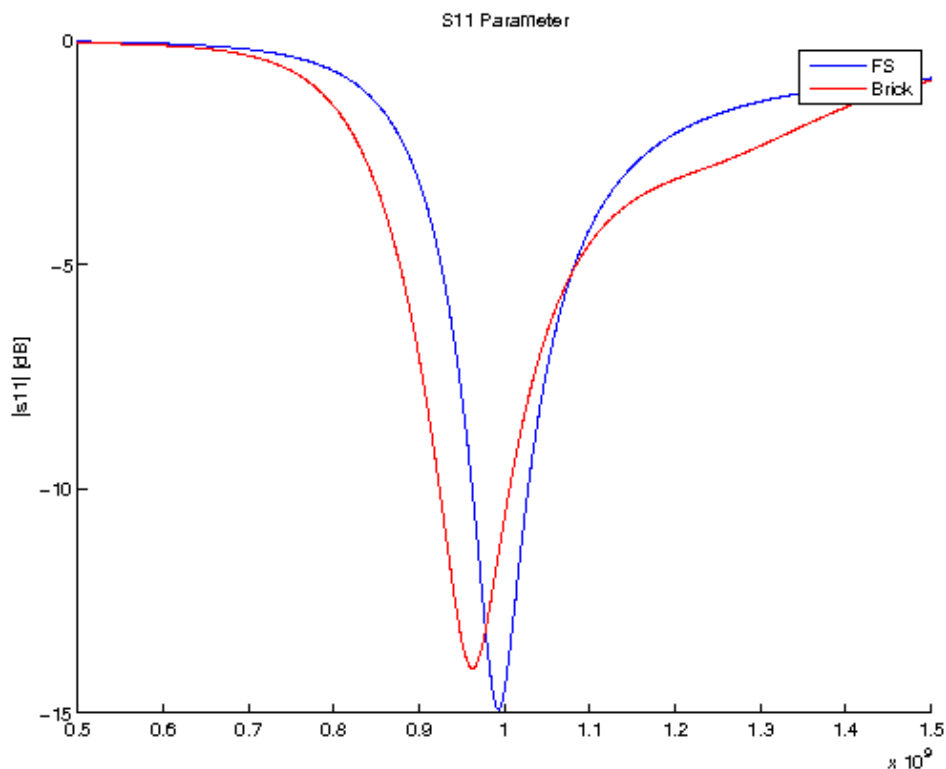


Fig. 116 Comparison of the S11 parameters for the dipole antenna

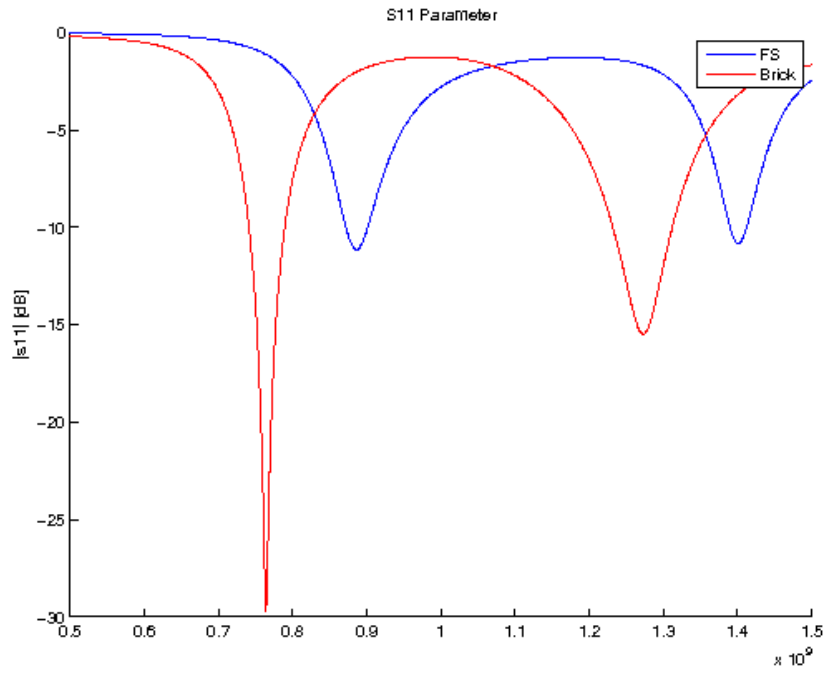


Fig. 117 Comparison of the S11 parameters for the folded loop antenna

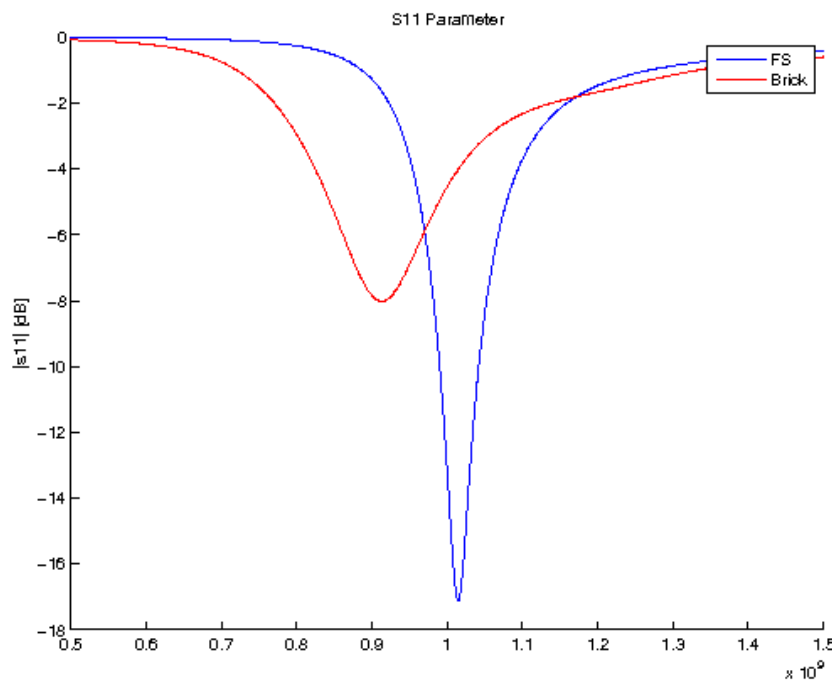


Fig. 118 Comparison of the S11 parameters for the IFA antenna

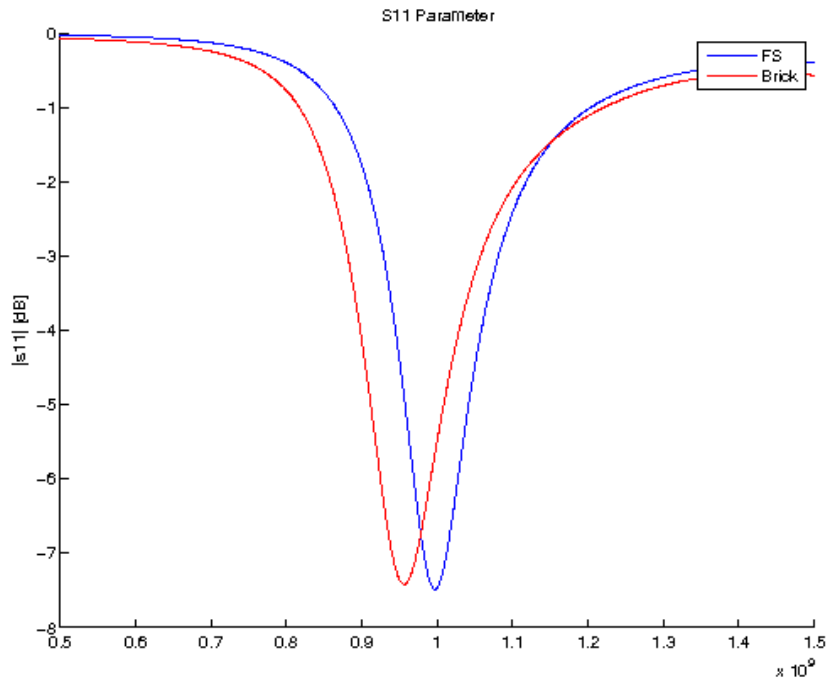


Fig. 119 Comparison of the S11 parameters for the loop antenna

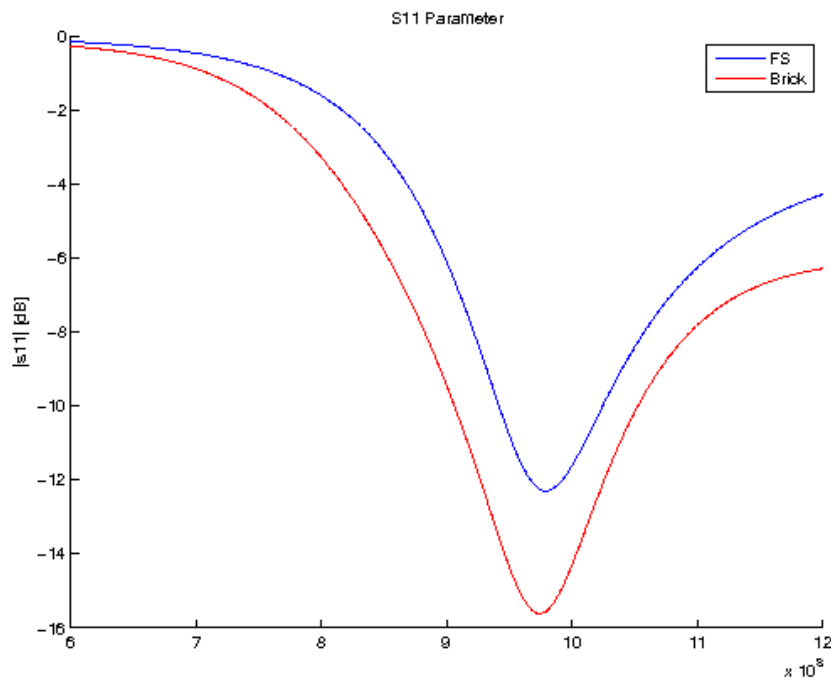


Fig. 120 Comparison of the S11 parameters for the monopole antenna

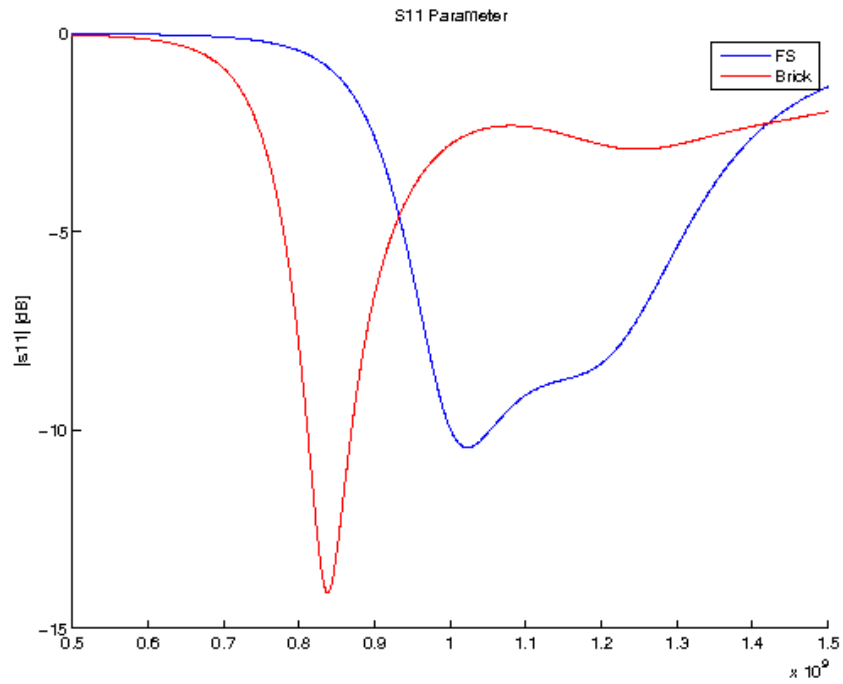


Fig. 121 Comparison of the S11 parameters for the PIFA antenna

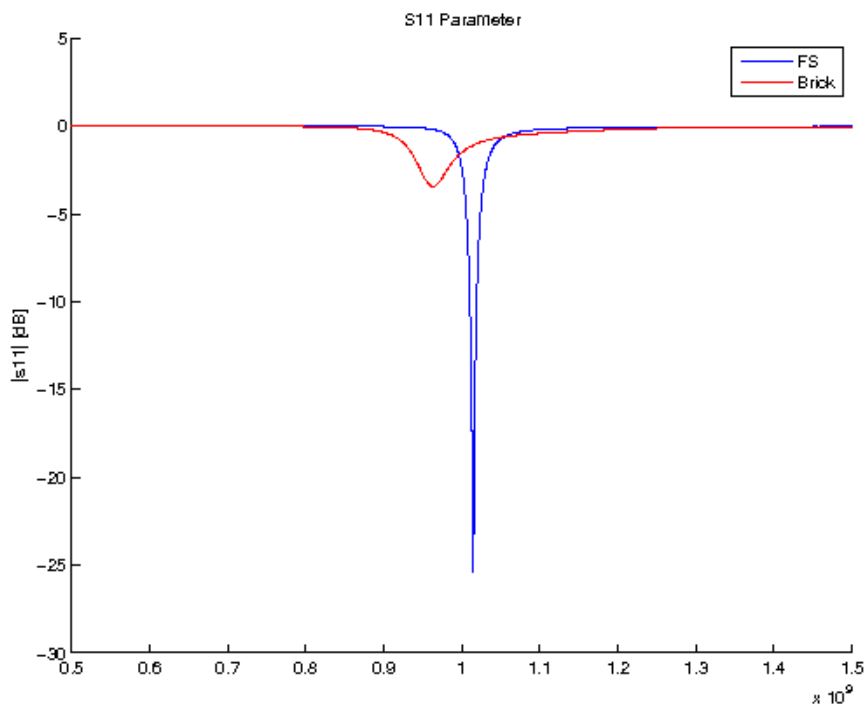


Fig. 122 Comparison of the S11 parameters for the narrowband PIFA antenna

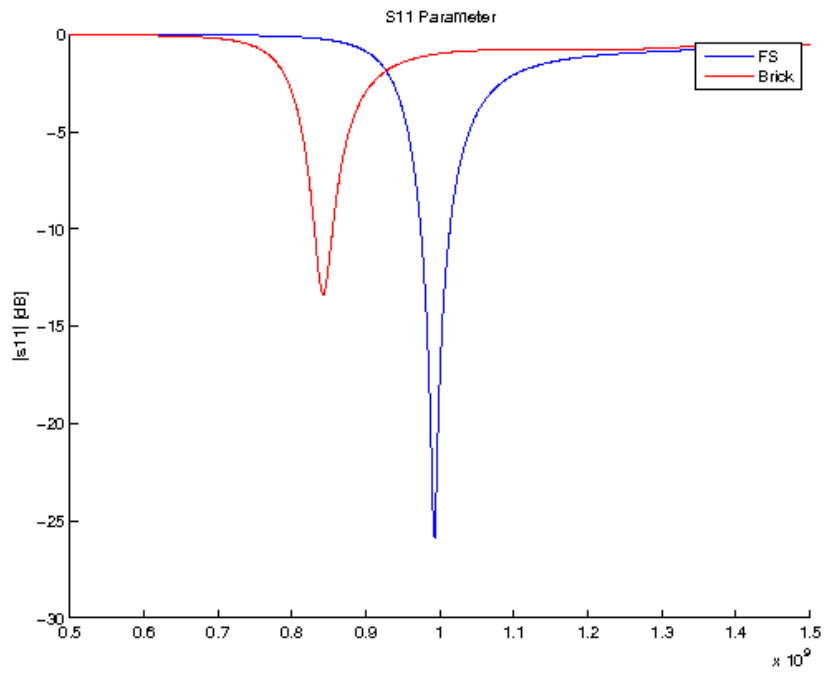


Fig. 123 Comparison of the S11 parameters for the slotted PIFA antenna

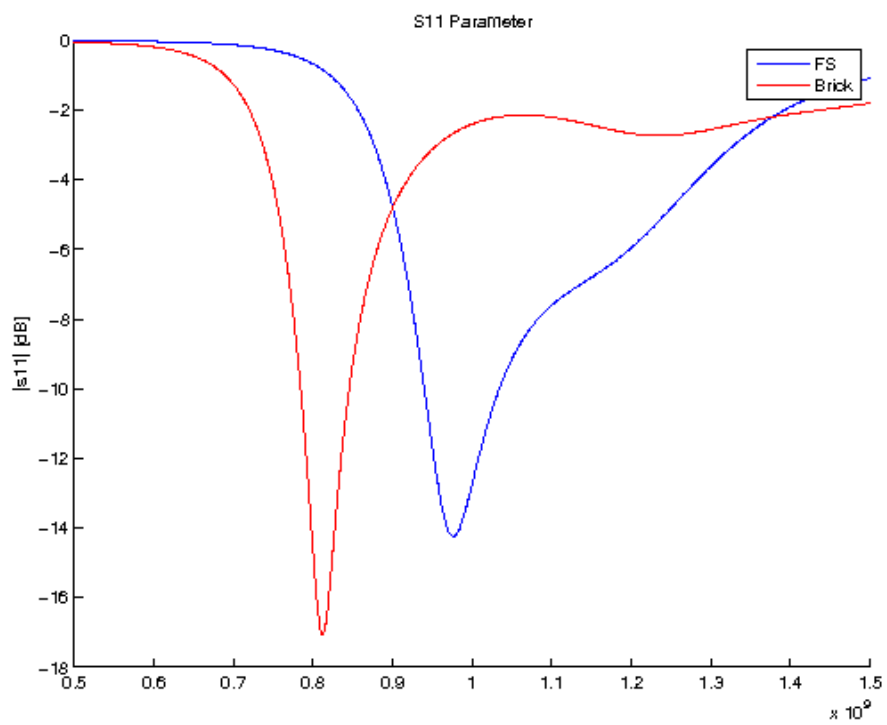


Fig. 124 Comparison of the S11 parameters for the PIFA with substrate antenna

For this visual method, the ranking is now as follows (from the best to the worst antenna):

Monopole
Dipole
Loop
Slotted PIFA
IFA
Folded loop
PIFA with substrate
PIFA
Narrowband PIFA

Table 9 Visual ranking

## IV – Variation of the resonant frequency and the associated S11 parameter

Firstly, we have decided to evaluate the variation of the resonant frequency calculated by the AAU3 software between the free space simulations and the simulations with a brick.

The following table sums up the results:

	Free space freq. (Hz)	Brick freq. (Hz)	Variation (Hz)
<b>Monopole</b>	9,80E+08	9,85E+08	5,00E+06
<b>Dipole</b>	9,94E+08	9,63E+08	3,10E+07
<b>Loop</b>	9,97E+08	9,56E+08	4,10E+07
<b>Narrowband PIFA</b>	1,02E+09	9,63E+08	5,20E+07
<b>IFA</b>	1,02E+09	9,13E+08	1,02E+08
<b>Folded loop</b>	8,86E+08	7,64E+08	1,22E+08
<b>Slotted PIFA</b>	9,93E+08	8,42E+08	1,51E+08
<b>PIFA with substrate</b>	9,85E+08	8,12E+08	1,73E+08
<b>PIFA</b>	1,02E+09	8,38E+08	1,85E+08

Table 10 Resonant frequencies for the different antennas

We have then evaluated the variation of the S11 at the resonant frequency:

	<b>S11 FS (dB)</b>	<b>S11 brick (dB)</b>	<b>Variation (dB)</b>
<b>Loop</b>	-7,49	-7,42	0,07
<b>Dipole</b>	-14,92	-14,00	0,92
<b>Monopole</b>	-12,30	-15,35	3,05
<b>PIFA with substrate</b>	-13,97	-17,07	3,10
<b>PIFA</b>	-10,45	-14,11	3,66
<b>IFA</b>	-17,13	-8,02	9,12
<b>Slotted PIFA</b>	-25,88	-13,37	12,51
<b>Folded loop</b>	-11,14	-29,69	18,55
<b>Narrowband PIFA</b>	-25,37	-3,44	21,93

Table 11 S11 variations

The loop antenna is the antenna which his having the smallest variation of the s11.

## V – Evolution of the Efficiency

Here are the results compiled from AU3 and showing the evolution of the efficiency in case of a free space simulation or with the brick. The antennas have been ranked according to the variation of this efficiency (the smaller, the better):

	<b>Efficiency FS</b>	<b>Efficiency brick</b>	<b>Variation</b>
<b>Loop</b>	0,9228	0,4579	50,38%
<b>PIFA</b>	0,9940	0,4834	51,37%
<b>PIFA with substrate</b>	0,9597	0,4610	51,96%
<b>Slotted PIFA</b>	0,9866	0,3974	59,71%
<b>Dipole</b>	0,9866	0,3293	66,62%
<b>Monopole</b>	0,9876	0,3122	68,39%
<b>Narrowband PIFA</b>	0,9933	0,2721	72,61%
<b>Folded loop</b>	0,9966	0,2135	78,58%
<b>IFA</b>	0,9992	0,1246	87,53%

Table 12 Antennas efficiencies

As seen in the previous table, and for this criterion, the loop antenna is the most robust one.

## VI – Global view of the rankings

The following table is summing up the rankings of the antennas according to the methods we used previously.

	Power dissipated	3D correlation	Visual	Resonant freq.	S11	Efficiency
<b>Loop</b>	1	1	3	3	1	1
<b>Dipole</b>	5	2	2	2	2	5
<b>Monopole</b>	6	5	1	1	4	6
<b>Slotted PIFA</b>	4	7	4	7	6	4
<b>PIFA with substrate</b>	3	8	7	8	3	3
<b>PIFA</b>	2	9	8	9	5	2
<b>Narrowband PIFA</b>	7	3	9	4	8	7
<b>IFA</b>	9	4	5	5	7	9
<b>Folded loop</b>	8	6	6	6	9	8

Table 13 Antennas final rankings

# CONCLUSION

When we started this project, it was with the firm knowledge that we were venturing into the unknown. There was little if not almost no theory concerning the topic we chose and thin leads on the proper way to follow. It was for us the occasion to see what pure research on uncharted territories of science looked like, and for four month we dealt with experimentation – some of it pertinent for what we looked for – but unfortunately some of it of no use. All these experiments were, however, a great leap of experience for all of us.

The main objective of this thesis was to find a brick to define properly the human hand and a criterion for the robustness of antennas. Defining the brick has come to be a success, allowing future research to simulate the hand with an easier model to simulate the interactions of the antenna with it. However, there was never one, but a great number of criterions for the robustness. According to the main focus of the antenna (the S11, the efficiency, the power dissipated...), the most robust antenna changed.

In the end, just like for the design of an antenna, there is mostly simulation and experimentation that can really define the robustness of an antenna, and not really a theoretical criterion.

# References

- [1] User's Influence Mitigation for Small Terminal Antenna Systems, Mauro Pelosi
- [2] Computational Electrodynamics: The Finite Difference Time Domain Method, Allen Taflove
- [3] Antenna Theory Analysis and Design, Constantine A. Balanis
- [4] <http://mathbits.com/mathbits/tisection/statistics2/correlation.htm>
- [5] <http://www.experiment-resources.com/pearson-product-moment-correlation.html>
- [6] Les Antennes : Théories, conceptions et applications, Odile Picon
- [7] <http://www.antenna-theory.com/basics/impedance.php>
- [8] <http://www.antenna-theory.com/antennas/smallLoop.php>
- [9] <http://www.allenhollister.com/allen/files/scatteringparameters.pdf>
- [10] Lectures on microwaves Part 4- Smith Chart, Xavier Le Polozec, ECE Paris 2010
- [11] <http://www.antenna-theory.com/tutorial/smith/chart.php#smithchart>
- [12] <http://f5zv.pagesperso-orange.fr/RADIO/RM/RM23/RM23p/RM23p01.html>
- [13] Interaction between mobile terminal antenna and user, Juho Poutanen
- [14] On the general energy absorption mechanism in the human tissue, Outi Kivakäs, Tuukka Lehtiniemi, Pertti Vainikainen
- [15] AAU3 User Manual